SPECIALIZATION PROJECT 2010

TKP 45

PROJECT TITLE:

Stabilization of two-phase flow in risers from reservoirs
Comparison of alternative simple models

By

Knut Åge Meland

In this project a new and improved Miniloop experiment was build. A few components did not arrive before the project deadline, and the experiment was therefore not completely finished.

The NewModel by Esmaeil Jahanshahi was compared with the DiMeglio model. Mainly the non-linear effect was investigated. The analysis shows some deviations from linearity when changing the valve opening. Otherwise, both models did behave very similar, and did not have any significant differences.

Controlling the riser system using the bottom pressure as a controlled variable was also investigated. It was found that using a cascade control structure with a flow controller in the inner loop performed better than a single pressure controller.

Supervisor for the project: Sigurd Skogestad
Date: 15.12.2010

Stabilization of two-phase flow in risers from reservoirs(anti-slug control) (in cooperation with Siemens) Comparison of alternative simple models

Knut Aage Meland

knutage@stud.ntnu.no

December 15, 2010

Contents

Nomenclature

$m_{g,eg}$ Mass of gas in the gas bubble

$m_{g,r}$ Mass of gas in the riser

m_{G1} Mass of gas in the pipeline

m_{G2} Mass of gas in the riser

$m_{l,r}$ Mass of liquid in the riser

m_{L1} Mass of liquid in the pipeline

m_{L2} Mass of liquid in the riser

$P1$ The low point pressure in the riser

$P2$ The topside pressure in the riser

$w_{G,in}$ Mass flow of gas in the pipeline

$w_{L,in}$ Mass flow rate of liquid in the pipeline

Q   The volumetric flow rate

z   The choke valve opening

List of Figures

List of Tables

Chapter 1

Introduction

This project is written as a part of the final year master program at the Norwegian University of Science and Technology(NTNU). Apart from the master thesis, this project is the largest hand in during the master program. The project is suppose to be the final preparation for the master thesis. The work for this project has been carried out at the Department of Chemical Engineering with financial support by Siemens. The project has been supervised by professor Sigurd Skogestad with assistance of Ph.D student Esmaeil Jahanshahi.

1.1 Objective

The main objective for this project was to analyze the dynamic behavior for the newly developed simple model, named New Model, for riser slugging systems. A secondary objective was to build an experimental setup of the riser system to generate experimental data. Originally, the New Model was to be compared with experimental data and other simple models. Due to unforeseen complications during the build of the experimental setup, the objective was shifted during the work period. The new objective became to analyze the New Model dynamics with simulations, and to compare the New Model with the simple DiMeglio model. Other objectives was to compare different control structures, and figure out which that could be used most efficiently for controlling the riser system. Main focus was on using the bottom pressure measurement as the controlled variable.

1.2 Background

Pipelines carrying multiphase flow are a common in the North Sea[7]. Offshore pipelines consists of two main pipeline types, infield pipelines and export pipelines. Export pipelines transports oil-water or gas-condensate flows to shore for further processing. Infield pipelines transports wellstreams to the platforms.[6] The pressure drop from the wells to the platforms are very large, and will create gas-condensate multiphase flow for gas fields and oil-gas-water multiphase flow for oilfields. The latter leading to one of the biggest challenges in offshore operations, control of disturbances in the feed to the separation process. Control and transport of multiphase flow entering the separation process is often referred to as flow assurance. Flow assureance are of high importance to the oil industry and will probably only increase in the future, since even more pipelines containing multiphase flow most likely will be laid.[7]

Chapter 2

Theory

2.1 Definition of slug flow

When oil, gas and water flows inside a pipeline simultaneously, the three phases can distribute in many configurations due to density difference. How the phases are distributed in the pipeline are depended of the operating conditions, such as phase velocities and pipeline angle. The possible configurations are called flow regimes, and the main categories are: stratified flow, annular flow, bubble flow, slug flow and churn flow. In this report slug flow has been the main concern. Slug flow can also be divided into multiple categories[15][11][6]:

- **Hydrodynamic slugging**, develops in the horizontal parts of the pipeline. Liquid waves grows on the liquid-gas interface and creates slugs when they get large enough to close the cross-section.

- **Riser slugging**, occurs when liquid blocks the low-point of a down-sloping pipeline which is connected to a riser. The liquid slug will grow until the pressure build up upstream gets large enough to blow the slug out of the riser.

- **Terrain slugging**, develops in pipelines at rough seafloor terrain, where liquid accumulates in the inclined sections.

- **Transient slugging** is caused by increased liquid flow rates at pipeline exit to processing facilities in response to changes in operating conditions. Typical examples of changes in operating conditions are change in flow rates and pressure. During startup and shutdown, transient slugging is a typical problem

2.2 Definition of a riser

Risers are long pipes connection the reservoirs to surface facilities for oil production. There are essentially two kinds of risers, flexible and rigid risers. The risers comes in different shapes and configurations, such as free hanging catenary(J-shaped) risers, S and wave risers(S-shaped), see figure 2.1.
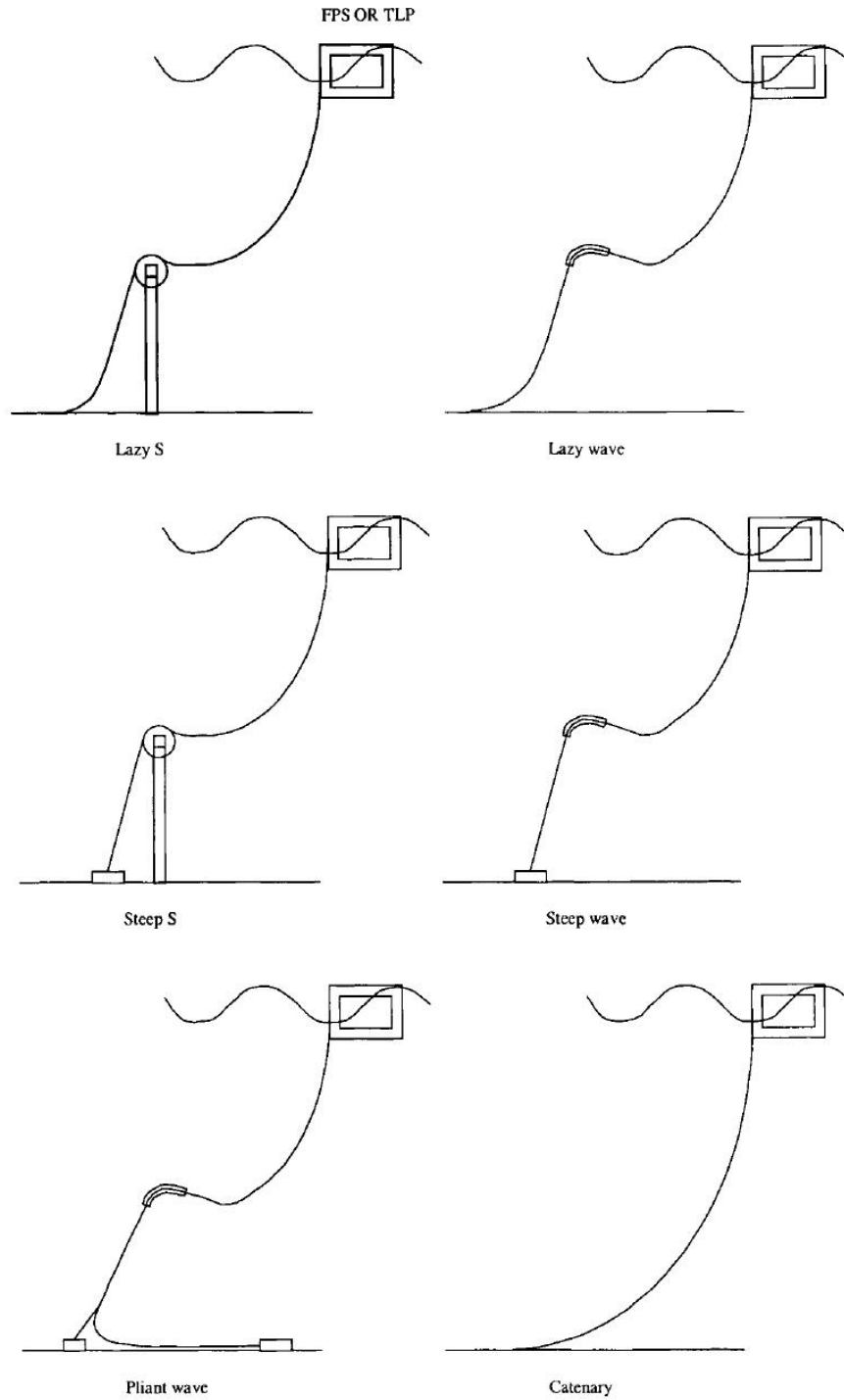
Figure 2.1: The figures shows the most common riser configurations used in the oil and gas industry [3]

2.3 Riser slugging

2.3.1 Problems caused by slugging

The most serious type of slugging for oil/water systems are riser slugging, possibly combined with or initiated by terrain slugging. The riser slugs can be several hundred meters long, and could fill up the entire riser. The inlet separator on receiving downstream facilities are not large enough to receive slugs of this magnitude, and could cause overfilling which could trip the production. Small slugs are also problematic, as it could lead to poor separation, varying compressor load and wear and tear on the equipment.[15] As a consequence this results in unwanted flaring and reduced operating capacity for separation and compression units, due to the need for larger operating margins. The larger disturbances requires a larger backoff from the optimal operation point, and thus reducing the throughput.[7] Another solution could be to install slug-catchers. This are large tanks installed on the platform to receive the slugs. Installing such large devices are often not economically viable offshore, where space is limited.[17]

2.3.2 Mechanism of riser slugging

The cyclic behavior of riser slugging can be broken down into four parts. These steps are illustrated in the figure 2.2. Gravity causes the liquid to collect in the low point, and causes pipe blockage (step 1). Liquid will only collect in the low point if the gas and liquid flow rates are low. The liquid slug will continue to grow as long as the hydrostatic head of the liquid in the riser increases faster than the pressure drop (step 2). When the pressure build up overcomes the liquid head in the riser, the liquid slug is pushed upwards by the pressure difference (step 3). Gas starts to penetrate the liquid slug, and eventually the driving force is to low to push the remaining liquid out of the riser (step 4). The remaining of the liquid slug is again accumulated in the low point.
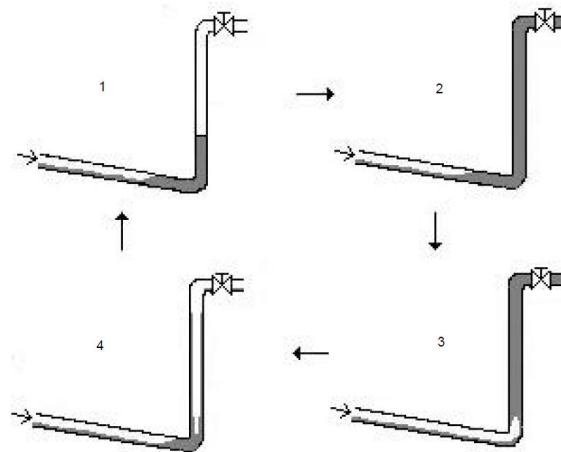
Figure 2.2: Cyclic behavior of riser slugging. [15]

2.4 Anti-slug control

Usually pipelines are designed such that slugging are prevented in some extent. Due to changes in the operation conditions, slugging often becomes a larger issue towards the

end of the well lifetime. Redesigning the riser/pipeline system is often not economical, and other measures should be used. In this section, the most commonly used methods for stabilizing and preventing slugging are described shortly.

2.4.1   Choking

It is well known that riser slugging may be avoided by choking of the valve at the riser top. This phenomenon can be explained by considering a pipeline-riser system which initially is non oscillatory. Increasing the liquid flow will cause the liquid to collect in the low point of the riser. Resulting in an increased pressure drop over the riser, due to compression of the gas upstream and decreased cross-section due to liquid blockage. The increased pressure drop results in less gas going through to the riser. The gas in the riser will expand, and result in reduced pressure in the top of the riser. The increased pressure upstream the low point will push the liquid slug to the top of the riser. If the choke valve opening is larger than a critical value, the liquid outflow rate will be larger than the liquid flow to the riser. This leads to a negative deviation in the liquid holdup, larger than the positive perturbation, and will result in growing oscillations and unstable slug flow. Valve opening lower than the critical value will result in less liquid leaving the system, and a liquid holdup deviation smaller than the perturbation resulting in a stable non-slugging system. [15]

2.4.2   Active control

Use of active control by controlling the topside choke valve could be done for preventing slugging. The valve position could be controlled using a simple feed back loop, measuring either the upstream pressure at the low point of the riser or the top pressure before the choke valve. The latter have been proved difficult in practice.

2.4.3   Gas lift

An other commonly used method is the use of gas lift. Slugging is prevented by continuously removing liquid from the riser by injecting gas into the riser, and thereby preventing pipe blockage.[1]

2.5   Short presentation of simple models

2.5.1   DiMeglio model

The DiMeglio model uses a simple one dimensional model to represent the two phase flow of liquid and compressible gaseous flow. A virtual valve located at the bottom of the riser represented by a elongated gas bubble is used to decide the gas flow trough the riser low point. Using a three-state set of ordinary differential equations, the model is fairly simple. The states used to represent the system are the mass of liquid in the riser $(m_{l,r})$, the mass of gas in the riser $(m_{g,r})$ and the mass of gas in the elongated gas bubble $(m_{g,eb})$. The figure 2.3 shows the main states used by the DiMeglio model. It must be noted that the DiMeglio model uses an assumption of constant gas and liquid inflow. Also the mass of gas in the riser is assumed to be negligible compared to the liquid mass in the riser. Five tuning parameters are necessary to decide to fit the model.
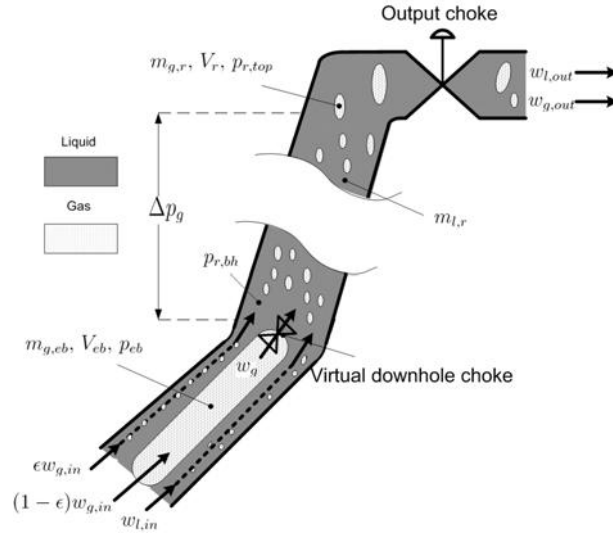
Figure 2.3: Overview of the DiMeglio model[4]

2.5.2 New model

The New Model developed by Esmaeil Jahanshahi is a simple model based on a four-state set of ordinary differential equations. Mass of liquid (m_{L1}) and gas (m_{G1}) in the pipeline, and mass of liquid (m_{L2}) and gas (m_{G2}) in the riser are the states used in the model, see figure 2.4. Four tuning parameters are needed to fit the model. All tuning parameters are completely independent of the physical property of the system. A valve equation is used to describe the gas flow trough the low point. When the liquid reaches a critical height, the liquid blocks the pipeline and no gas is transfered from the pipeline to the riser, resulting in pressure buildup. When the pressure force overcomes the liquid gravity force, the liquid slug is forced up to the choke valve. Slugging will occur if the choke valve opening is larger than a critical value.[8]
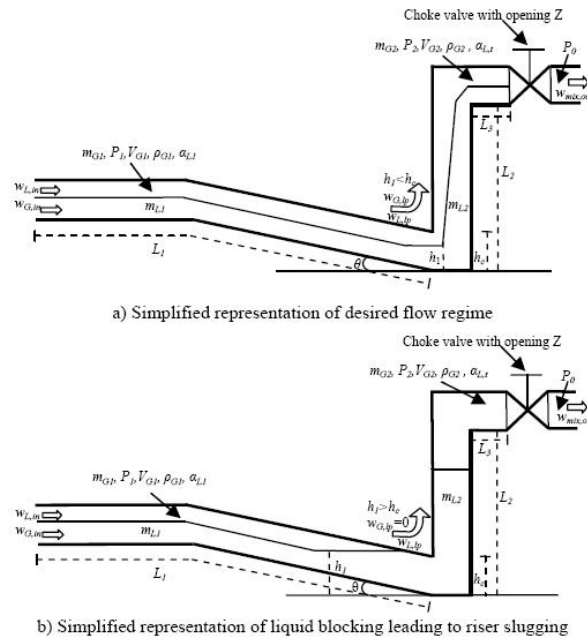
Figure 2.4: Overview of the New Model[8]

Chapter 3

Experimental

A part of this project consisted of building an experimental setup for studying the dynamic of the riser slugging phenomena caused by two phase flow. The experimental rig is supposed to be used to create experimental results to be compared with the simple models for finding the best model. Trying different control structures are also part of the usage. It's especially interesting to investigate if control using different configurations of topside measurements would be possible.

The main parts for the the experimental setup was started during the summer 2010 by Weiwei Qui. Some parts however, was missing or errorously ordered, and needed to be replaced. Fitting and building the rig was done with good help of Ph.D student Esmaeil Jahanshahi. It was decided to include all the datasheets and specifications in the appendix for the different components used in this setup. The idea was that it would be nice to have everything together for others going to be working with this experiment in the future. A list of the equipment cost is also included in appendix H.

3.1   Experimental setup

As a part of this project a small scale riser setup should be constructed. Previously, a similar system had been constructed by Baardsen[2]. This system differs from the original setup by using newer sensors and equipment.

In figure 3.1 an illustration of the setup is shown. Water from the water storage tank is pumped by the water pump through the mass flow meter to the mixing point, where the water is mixed with pressurized air. Pressurized air is supplied from the air supply in the laboratory. The air supply is connected to a pressure regulator and a flow meter before the air enters the air buffer tank. This tank contains a pressure sensor and a safety valve to to decrease the possibility of bursting the buffer tank. From the air buffer tank, pressurized air is supplied to the mixing point, where the pressure is recorded again. The two phase flow flows up the riser, through the choke valve and separates in the separator on top. The water is recycled back to the water storage tank. Slugging can occur in the riser if the gas and water flow rates are within the slugging flow regime. All sensors are connected to a computer through an I/O module.
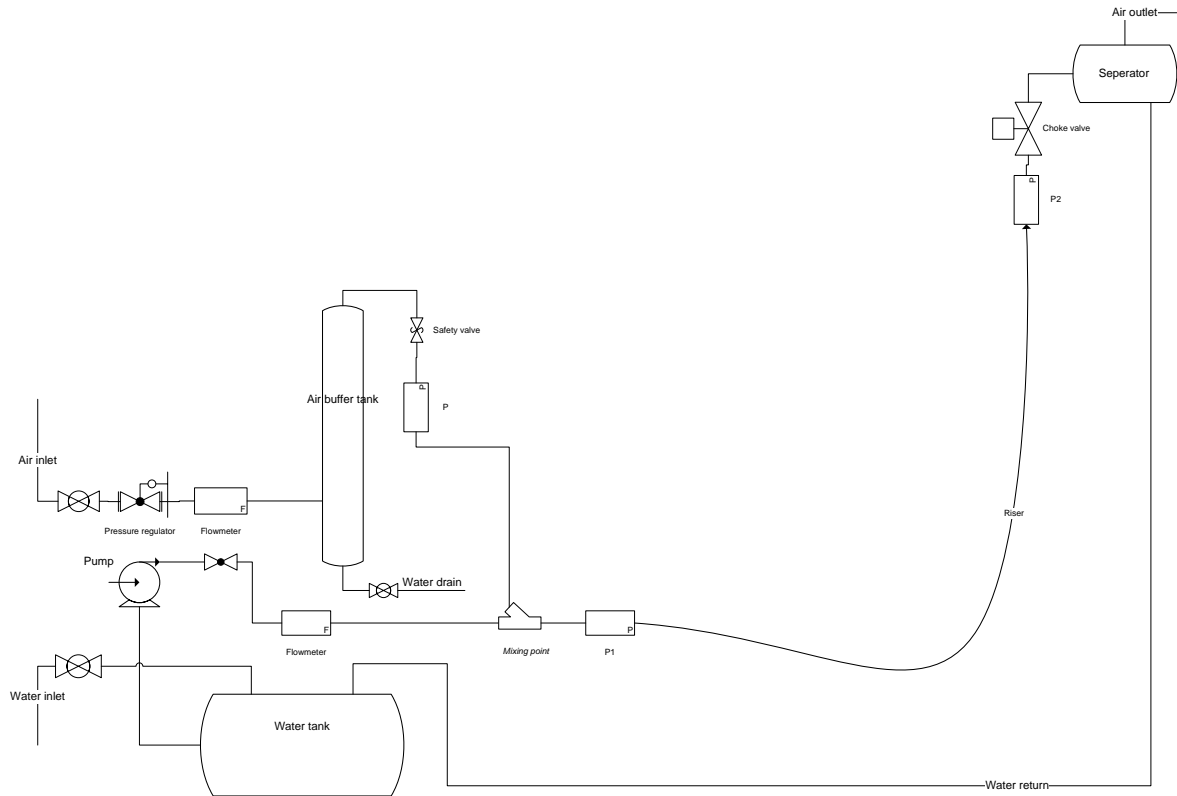
Figure 3.1: Sketch of the experimental setup. Water and air is mixed and forced up the riser using pressure forces. Depending on the choke valve opening, water and gas flow rate slugging could occur.

3.1.1 Components

Water reservoir tank

The water reservoir tank is used to store water to ensure that the water pump gets a continuous feed of water. After going through the riser and into the topside separator, the water is recycled to the water tank. The tank is connected to a water source to make filling the tank easy. The tank is made of transparent plexiglas and have a cylindrical shape. A picture of the tank can be seen in figure 3.2.
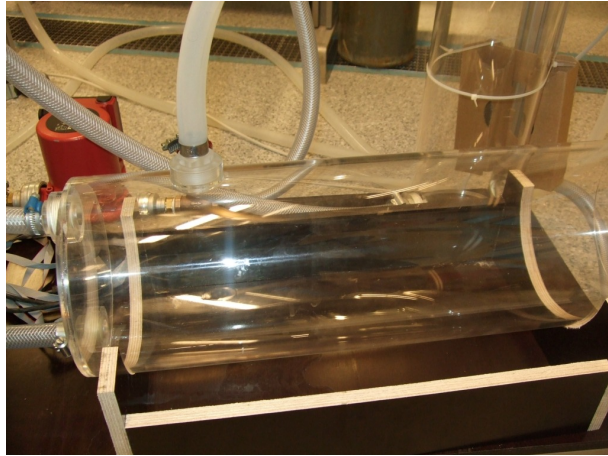
Figure 3.2: The water storage tank.

Air buffer tank

The air buffer tank is made of transparent plexiglas with an cylindrical shape. A picture of the tank can be seen in figure 3.3. To make slugging possible, a large pipevolume for pressure buildup is necessary. The buffer tank increases this pipevolume, which can be adjusted by filling the tank partly with water. Maximum pressure the buffertank can withstand, is not so high. For safety, the tank has been equipped with a safety value, to ensure that the pressure not will exceed 1 barg.

Figure 3.3: The air buffer tank.

Separator tank

Just like the air buffer tank and the water reservoir tank, the separator tank is made of transparent plexiglas. The shape is also similar. The separator is situated at the top of the riser, after the choke valve. A picture of the separator is shown underneath in figure 3.4. The outlet on top releases the air from the riser. The bottom outlet is used for the water recycle, returning the water to the water reservoir tank.
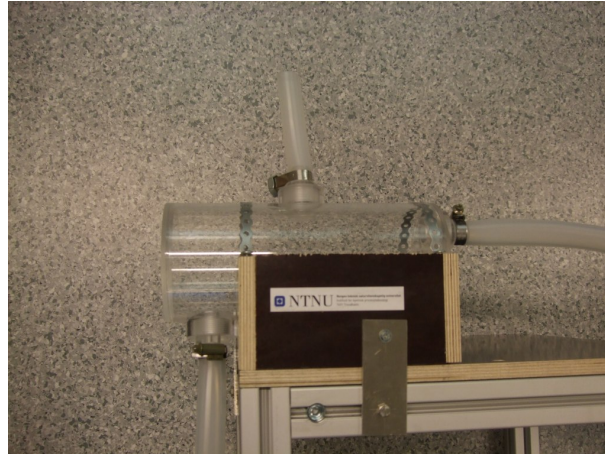
Figure 3.4: Water and air separator.

Water circulation pump

The water circulate pump is used to increase the water pressure before before the mixing point to make it possible for water to go up the riser. The pump is located between the water tank and the mixing point. It is important that the water level in the water tank is above the water outlet to avoid air getting into the pump and damaging the pump. The figure 3.5 shows a picture of the water circulation pump.
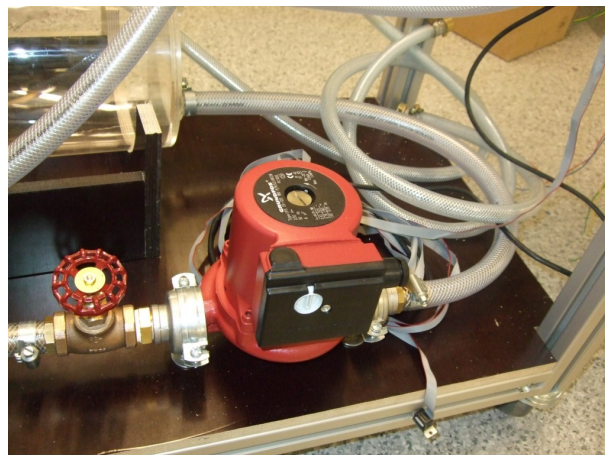
Figure 3.5: Water circulation pump

Tubing

The tubes used in the pipeline and riser sections are made from transparent silicon-rubber hoses with an inner diameter of 20 mm. Figure 3.7(a) shows such a pipe. The hose used

to build the pipe sections upstream the mixing point are made of reinforced rubber to ensure no pipe blockage because of sharp twists and turns, see figure 3.7(b).

Figure 3.6: Tubes used in the setup.
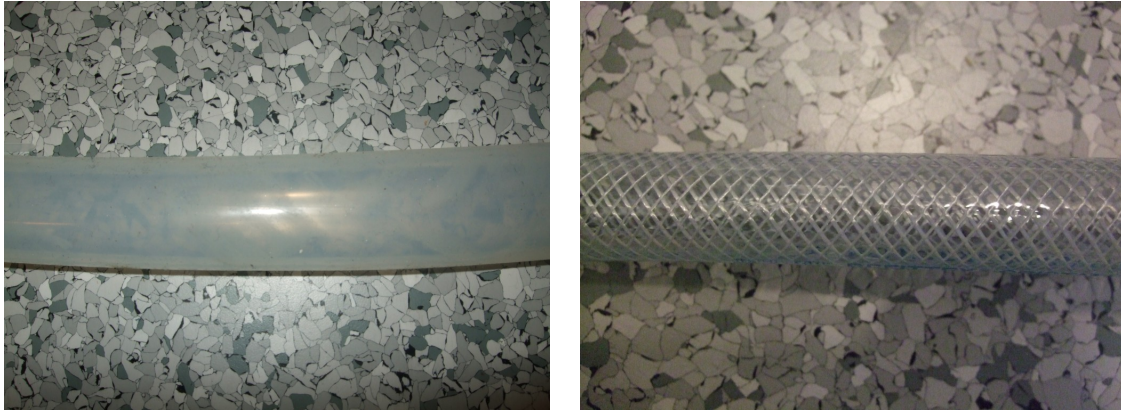
(a) Transparent rubber tube, 20 mm inner diameter

(b) Reinforced tube, 19 mm inner diameter

Air flow meter

The air flow meter, manufactured by M+W Instruments, is located upstream the air buffertank and downstream the pressure regulator. The principle of through-flow measurement is used to measure the mass of air flowing through the device. More information about this principle can be found in the air flow meter datasheet given in appendix I. In addition to measure the mass flow, the flow meter can be used to control the flow rate. Figure 3.7 shows the air flow meter connected in the setup.

Figure 3.7: Air flow meter from M+W Instruments.

Water flow meter

A flow meter is used to measure the water flow in the riser, see figure 3.8. The flow meter, located upstream of the mixing point, is manufactured by Gemü. This liquid flow meter utilizes turbine flow measurements with a low pressure drop to obtain the liquid flow rates. More information about the unit is available in the appendix J.

Figure 3.8: Liquid flow meter

Pressure transmitters

Siemens pressure transmitters are used to measure the pressure for this setup, see figure 3.9. The transmitters uses a piezoresistive measuring cell with a diaphragm, installed in a stainless steel housing for measuring the absolute pressure of the liquid and gas flow. Three pressure transmitters are located at different places in the setup. The pressure before the choke valve on the top of the riser, the pressure at the mixing point and the pressure in the buffertank are measured.

The transmitters can be used with both current output (0-20 mA) and voltage output (0-10 V) depending on the connection configuration used. Current output is the preferred setting in this setup. In the appendix K, the instruction manual for pressure transmitter is attached.

Figure 3.9: Pressure transmitters from Siemens.

Pressure regulator

A manual pressure regulator is used at the air inlet to ensure that the pressure will not exceed the upper limit of the air buffertank, see figure 3.10. The regulator, manufactured by Rexroth, have a working pressure range of 0.1 to 16 barg with a adjustment range of 0.1 to 1 barg. Attached in the Appendix L is a datasheet for this regulator.

Figure 3.10: Manual pressure regulator from Rexroht.

Choke valve

The choke valve is an angle seat valve manufactured by Gemü. Located upstream of the separator on the top of the riser, the valve is operated by pressurized air (4-8 bar) supplied from the pressurized air system in the laboratory. Normally, the valve in open position. It must be noted that this valve only have the option of being either fully open or fully closed. The valve position is therefore decided by the time spent in the open/closed position and will have an oscillating during operation. The choke valve positioner is used to control the valve position. A picture of the choke valve in the figure 3.11 underneath. The datasheet for the choke valve is given in appendix M.
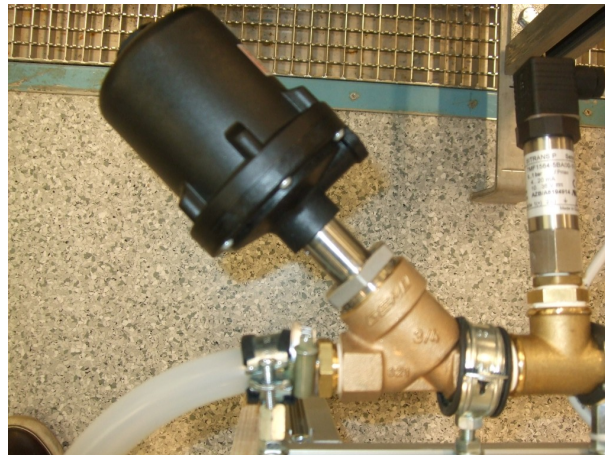
Figure 3.11: The choke valve used before the separator

Choke valve positioner

A valve positioner is used to keep a valve in a given position. The positioner utilizes pressurized air to open and close the valve, and the positioner is mechanically connected to the valve, such that the valve position is always known.

I/O module

The I/O module is used to convert the measured signals into a signal the computer can handle. The I/O module consists of multiple analog or digital modules output and input modules mounted in a cabinet. Due to the delivery delay, no specific information about the modules were available at the time of writing.

Valves

Regular ball valves was used to control water inlet, water drain, and air inlet. The figures 3.12(a),3.12(b) and 3.12(c) shows pictures of these valves. A globe valve was used to control the water flow in the riser. Using a global valve instead of a normal valve ensures good control of the flow rate, because a global valve is linear. The valve is located upstream the water pump and a picture can be seen in figure 3.12(d).

(a) Ball valve at the water inlet.
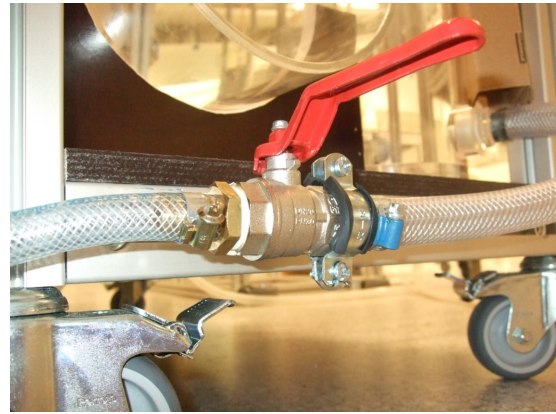
(b) Ball valve at the water drain.

(c) Ball valve at the air inlet.
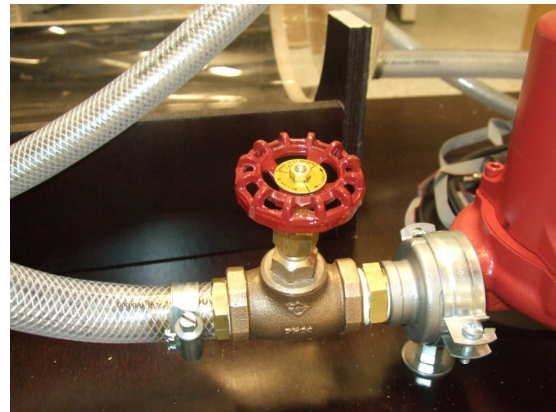
(d) Globe valve for controlling the water flow.

Figure 3.12: Various valves used in the setup.

Chapter 4

Result and discussion

4.1 Building the experimental setup

A part of this project was to build an experimental setup for a small scale riser model. This setup will from now be called a Miniloop. Most of the parts had been ordered by Ph.D student Weiwei Qui during the summer. Everything looked good when starting the build, and it was expected that assembling the setup should be done in a couple of weeks since mostly all the main parts were ordered

Difficulties regarding fitting the parts together in a good secure manner soon became clear. Time was used to investigate and order adapters for fitting the parts. Larger problems concerning missing crucial parts, and unusable parts of the wrong type which had to be replaced and new parts ordered. Some other parts was supposedly ordered, but not received. The parts in question was the I/O modules for handling the signals between the computer and sensors.

As the time went by everyone was expecting the I/O modules to arrive. After a while, it was decided to investigate why the parts had not arrived. The person responsible for handing orders at the department had no record of ever placing and order for the I/O modules, even though it was clearly specified in the papers from Weiwei Qui. Clearly there had been a misunderstanding between them. New modules were ordered, but they had a couple of weeks delivery time.

Since the I/O modules are crucial for operating the Miniloop, it was impossible to do experiments before the deadline for handing in this report.

The choke valve positioner was one of the parts needed to be replaced. The received positioner was unusable, and was actually only a position indicator, not a complete positioner able to control the valve position. It was not noticed that positioner needed to replaced until approximately one month before the project deadline. The supplier was contacted and they agreed to send an offer of a suitable part. Still after one month, no offer had been received, despite contacting them several times and each time promising to send an offer.

For this project, the plan was to to some experiments on the Miniloop, but unfortunately the Miniloop was not completed in time because of the reasons mentioned above. However, the build was not a total waste since the Miniloop also was planed to be used during the master thesis. This project was partly done as a preparation for the master thesis. All the work put into building this experiment is therefor not waisted.

4.2 Changes to New Model during the analysis

. The New Model by Jahanshahi was in a changing state when this analysis started. To make the model fit better to the OLGA model, which was used a reference, the author introduced some new terms. The analysis suffered a little bit because of this, as some parts of the analysis needed to be changed.

4.3 Linear approximation of the non-linear models

Using a linear model instead of a non-linear model would be very favorable. Linearizion of the non-linear models were done by calculating the Jacobian matrix. Since the models consisted of a lot of equations, it would not be favorable to calculate the derivatives for the state equations directly. A better approach would be to calculate the partial derivative for each equations separately. The partial derivatives could then be substituted into the derivative of the state equations to obtain the the Jacobian matrix. The latter approach was used in this report, and a more detailed description is given in appendix A. The derivatives calculations were done analytically using pen and paper, and implemented into the Matlab linearizion models for the DiMeglio model and the New Model, given in the appendix E.

Before using hand calculations to calculate the analytical expressions for the linearized model, an alternative approach using the symbolic toolbox in MATLAB was attempted for the New Model. The method was completed, but eventually scraped because of poor performance and high complexity. As explained before, the New Model did undergo some changes during this analysis, and because of having a working model with acceptable performance, it was not prioritized to keep the symbolic model updated.

The linearized models build by the LinMod Matlab scrips in appendix E was verified by comparing the analytical models with simple numerical models. First order forward difference was used to approximate the derivatives of the state equations. For both models the resulting Jacobian matrices was similar to their analytical equivalent. The MATLAB scripts used to calculate the numerical Jacobians for both the DiMeglio model and New Model can be found in appendix F.

4.4 Comparing the non-linear model to the linear model

A very important part of the comparison of the two simple models are the non-linear effect in the two models. The non-linear effect in the operating region was found using transfer functions. If a linear model representation would be sufficient instead of a non-linear model would make calculations much easier. To check the effect of the non-linear part of the model, the linear model was used to generate transfer functions. Transfer functions for different combinations of inputs and outputs for various steady state input values was generated and plotted in bode plots. The non-linearity effect are small if the curves in the gain plot do not deviate much from each other. Gas flow rate and liquid flow rate inputs are mainly dependent of reservoir characteristics like the nominal pressure, and can not be changed. Only the opening of the choke valve is possible to change. The transfer functions of real interest are therefore the transfer functions between the choke valve opening and the outputs. In this project the main focus has been on using the

bottom pressure measurement to control the flow rate in the riser system. It could also be possible to control using either the flow rate through the choke valve or the top pressure measurement, but this will not be the focus point in this report. However, the flow rate through the choke valve would be of some interest, because a control structure using a flow controller in combination with a pressure controller is proposed later in this report.

Given in the following sections are the bode plots of the transfer functions from the choke valve opening to the outputs low point pressure(P1) and volumetric flow rate out of the riser(Q) for various steady state choke valve openings, gas flow rates and liquid flow rates. Rest of the bodeplots are given in the appendix C for completeness. Both DiMeglio model and New Model bodeplot are shown side-by-side for comparison. In the following sections, the differences will be discussed in more detail.

4.4.1 Transfer functions from the choke valve opening(z) to the bottom pressure(P1)

Both New Model and DiMeglio model have extensive non-linear effects when changing the steady state valve opening, seen in the figure 4.1. Especially at low frequencies the non-linear effect is large. The distinctive peak in the figures are called a resonance peak, and are common in underdamped systems with complex poles. The peak are only visible for a damping factor between 0 and 0.707[10].

(a) New Model bode plot   (b) DiMeglio model bode plot
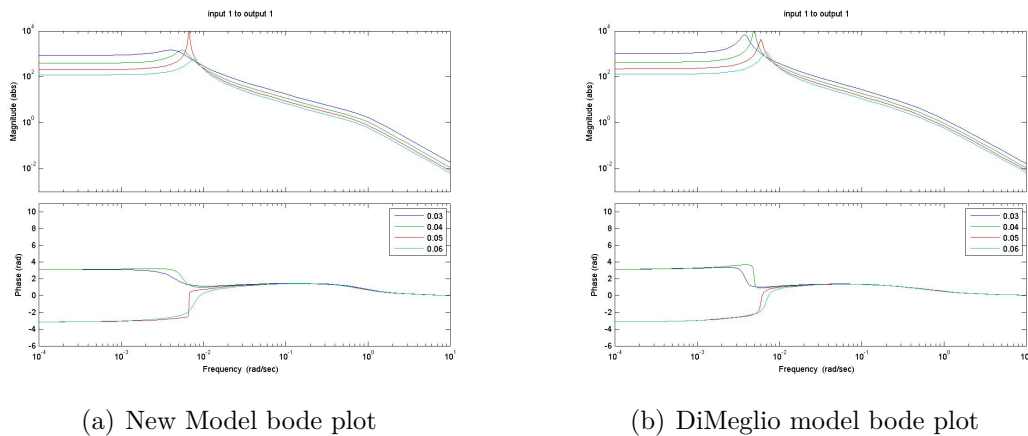
Figure 4.1: Bode plot of the transfer function to the bottom pressure(P1) from the choke valve opening(z) for various steady state choke valve openings.
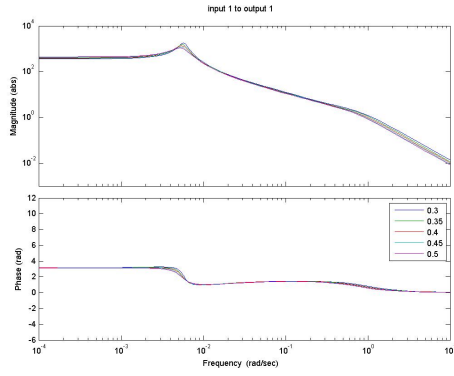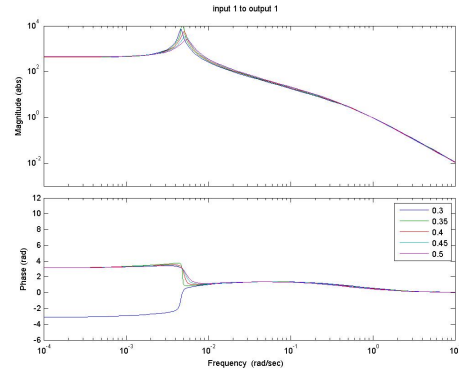
(a) New Model bode plot (b) DiMeglio model bode plot

Figure 4.2: Bode plot of the transfer function to the bottom pressure(P1) from the choke valve opening(z) for various steady state gas flow rates.
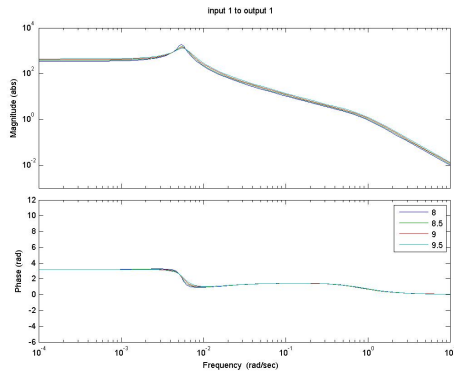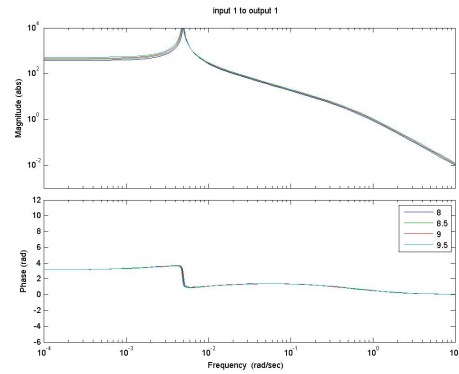
(a) New Model bode plot (b) DiMeglio model bode plot

Figure 4.3: Bode plot of the transfer function to the bottom pressure (P1) from the choke valve opening (z) for various steady state liquid flow rates.

In the phase plots, the differences are probably caused by a jump from a stable system, where the poles have negative real parts, to a unstable system with positive real parts.

The relationship between the valve opening(z) and bottom pressure(P1) are according to the figures 4.2 and 4.3 close to linear when changing the gas and liquid flow rates. Controlling a non-linear system using tuning parameters obtain from a linear model could cause problems. A large large divination from the non-linear model would give non-ideal tuning parameter if the condition changes. To prevent this a solution could be to use a flow controller to linearize the choke valve. Introducing this controller would potentially increase the non-linearity the pressures (P1 and P2), but could help reduce the non-linearity in the flowrate. The flow rate non-linearity effect have been investigated in the following section.

26

4.4.2 Transfer functions from choke valve opening(z) to the volumetric flow rate(Q).

The figure 4.4 shows both models have flow rates that are largely non-linear with respect to the valve position. However, both models does not seem be very sensitive for changes in gas and liquid inputs, figures 4.5 and 4.6.

Using a cascade control structure could seem to be a good idea to reduce the non-linearity effect when changing the valve position. In the next section the performance of this control structure is compared with the performance of a single pressure controller.

(a) New Model bode plot   (b) DiMeglio model bode plot
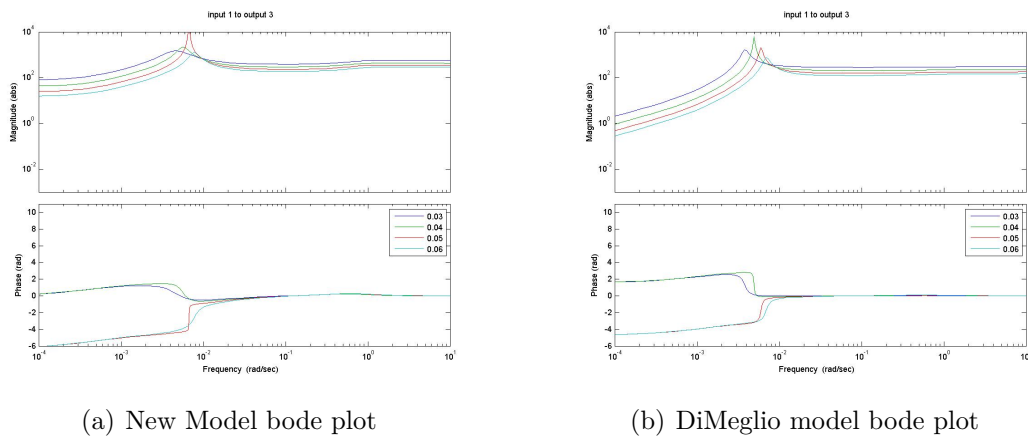
Figure 4.4: Bode plot of the transfer function to the flow out of the system (Q) from the choke valve opening (z) for various steady state choke valve openings.

(a) New Model bode plot   (b) DiMeglio model bode plot
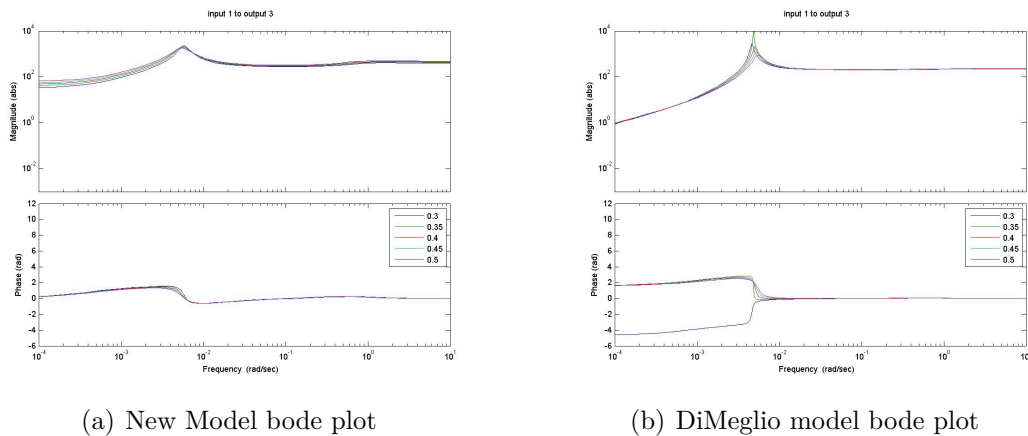
Figure 4.5: Bode plot of the transfer function to the flow out of the system (Q) from the choke valve opening (z) for various steady state gas flow rates.

(a) New Model bode plot   (b) DiMeglio model bode plot
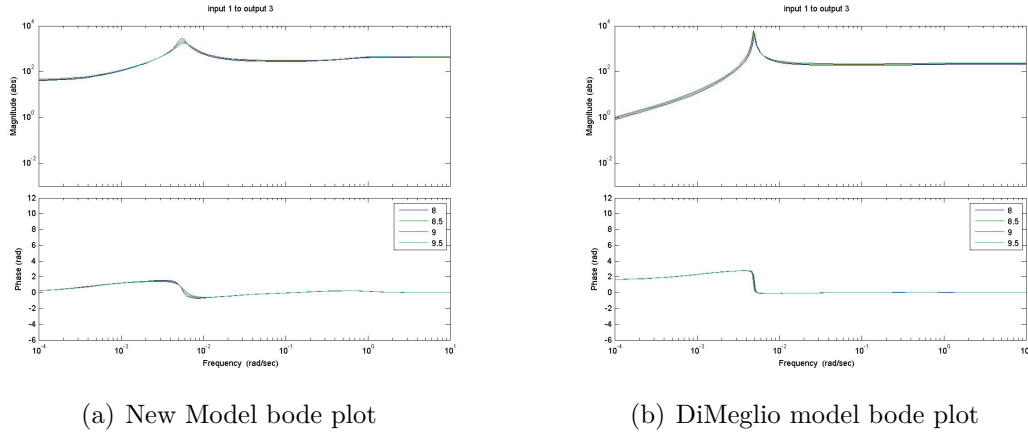
Figure 4.6: Bode plot of the transfer function to the flow out of the system (Q) from the choke valve opening (z) for various steady state liquid flow rates.

4.5 Simulating slug flow

As explained before the experimental rig was not completed because of delivery problems. It was therefore decided to do some simulations instead. The simulations were done using Simulink. The main objective of these simulations were to compare the effect of using a cascade control structure.

In the previous section it was proposed to use a flow controller for linearizing the choke valve. Comparing the performance of the cascade control structure with a single pressure controller was evaluated in this section. Because of similar bodeplots it was decided to only do the simulations for one of the simple models. The DiMeglio model used shorter time to converge, and was therefore chosen.

4.5.1 The Simulink model

The Simulink modeling tool bundled with Matlab was used to build the model for testing the proposed control structures. A flow sheet can be found in the appendix G. To represent the riser model a S-function block was used. This S-function block is requiring a S-function which is containing the system model. In the model there is a manual switch to make it possible to easily change between the single pressure controller structure and the cascade controller structure.

Model basis

Input steady state values are shown in the table 4.1 below together with steady state setpoints for top pressure (P1) and flow rate (Q). Setpoints was found by running a initialization script which calculated steady state output values. To represent noise and disturbances, band limited white noise blocks was used. Approximate 10% changes in the steady state inputs was assumed and 1 unit for the messurement errors. A small measurment delay was added for the flow measurment such that the desired respons for the flow controller used when tuning could be obtained. Table 4.5.1 showns all the model parameters.

28

Table 4.1: Steady state values for inputs and setpoints for the controllers

Parameter	Magnitude	Unit
Steady state choke valve position	0.1	-
Steady state gas mass flow	0.36	$\frac{kg}{s}$
Steady state liquid mass flow	8.64	$\frac{kg}{s}$
Setpoint for pressure controllers	70.6668	bar
Setpoint for flow controller	9	$\frac{kg}{s}$

Table 4.2: Disturbance, measurement noise and delay

Parameter	Magnitude	Unit	Frequency$[s^{-1}]$
Disturbance valve position	0.01	-	10
Disturbance gas input flow rate	0.036	$\frac{kg}{s}$	10
Disturbance liquid input flow rate	0.86	$\frac{kg}{s}$	10
Noise top pressure measurement	1	bar	10
Noise mass flow rate measurement	1	$\frac{kg}{s}$	10
Time delay for measuring mass flow	0.01	s	-

4.5.2 Tuning the controllers

Finding good tuning parameters proved to be challenging because the SIMC[14] tuning rules by Skogestad are not good for unstable systems with complex poles. Some research have been done in that area by Manum[9] in a project report. A better solution would be to use the 'Setpoint overshoot method' by Shamsuzzoha, Skogestad and Halvorsen[12]. It was reported that this method could handle oscillating unstable systems. Using this approach, step responses for the different controllers were obtained, and the tuning parameters calculated. A more detailed explanation of the tuning method is given in appendix D. Listed in table 4.5.2 is the parameter used for tuning the single PI controller and the controllers in the cascade control structure. When tuning a cascade, it is very important to ensure that the controllers operate in different timescales to avoid interactions. A reasonable timescale separation would typically be of a factor 5 in terms of closed loop response time.[13]. Using timescale separations ensures the controller in the inner layer to be unaffected by the presence of the controller in the outer layer, and vice versa. For this particular case, time scale separation was of no concern. The response time for the flow controller was instantaneous, and a small time delay was needed to get the desired oscillating response. Nevertheless, a higher detuning factor was used on the pressure controllers to make sure the time scale separation was adequate. Tuning of the inner controller was done before the outer controller, and while tuning the outer controller the inner controller was closed and tuned with correct tuning parameters.

As expected, the inner controller was close to an integrate controller, while in the pressure controller the proportional part was dominating.

Table 4.3: Controller tuning parameters for the two control structures

Controller	P	I	D	detuning factor
Pressure controller for the single controller configuration	$-0.0281[bar^{-1}]$	$-6e-5[s^{-1}bar^{-1}]$	$0[sbar^{-1}]$	50
Flow controller in the inner loop in the cascade configuration	$2e-4[\frac{s}{kg}]$	$0.2023[kg]$	$0[\frac{s^2}{kg}]$	5
Pressure controller in the outer loop in the cascade configuration	$-2.11[bar^{-1}]$	$-0.0048[s^{-1}bar^{-1}]$	$0[sbar^{-1}]$	50

4.5.3   Comparing control structures

Running the simulation with the described conditions and tuning parameters for both control structures gives a system response for the DiMeglio model shown in the figures 4.7,4.8 and 4.9. The cascade control structure had some effect on the bottom pressure variations compared to the single controller structure. However, the difference was not very large. Variations in the top pressure was significant less using the cascade controllers compared to the single pressure controller. One of the reasons for wanting to remove slugging is because the fluctuations could effect the downstream process. Thus having a small variation the top pressure is very important. Variations in the bottom pressure don't have any effect later in the process, but will probably have some effect on the stabilization region. It could look like the cascade control structure would have a larger stability region than the single controller because of sightly less pressure fluctuations, but this is merely speculations and needs to be investigated further.

Variations in the flow rate through the choke valve is also very important with respect to downstream processing. The figure 4.9 shows slightly less variations in the flow rate through the choke valve for the cascade control structure control structure. Fluctuations in the flow rate are easier to handle than fluctuations in the pressure. Small fluctuations could be reduced using a buffer tank. Large fluctuations, on the other hand could be critical to the downstream process.
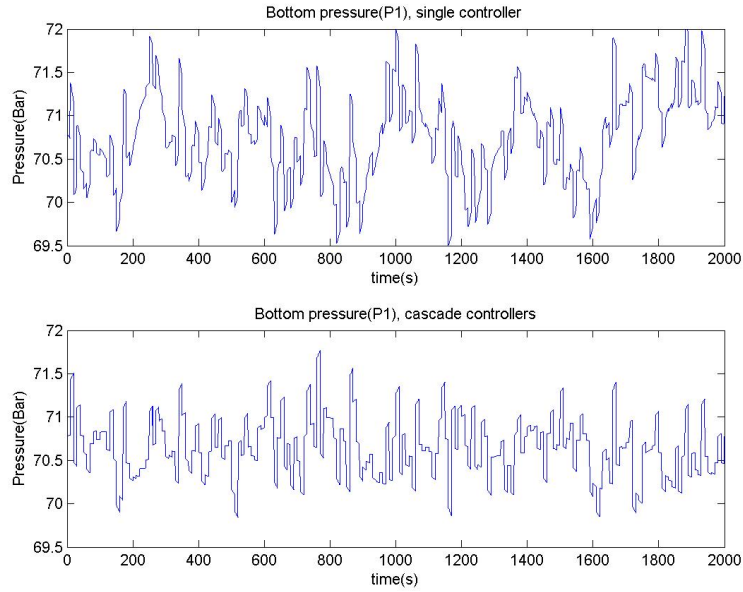
Figure 4.7: Bottom pressure response for the DiMeglio system when applying disturbances and noise. Using the cascade control structure makes the pressure variations a little less compared to the single pressure controller.
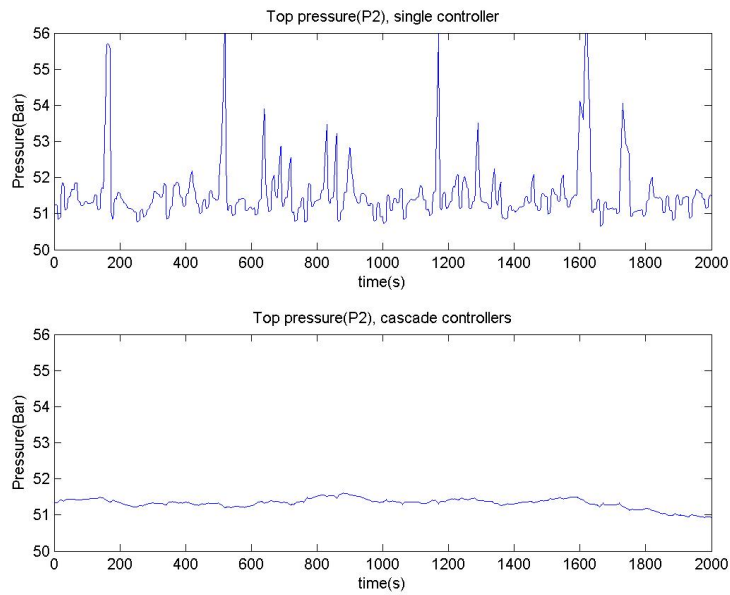
Figure 4.8: Top pressure response for the DiMeglio system when applying disturbances and noise. Using the cascade control structure insted of the single pressure controller makes a huge difference for the pressure variations at the top of the riser system.
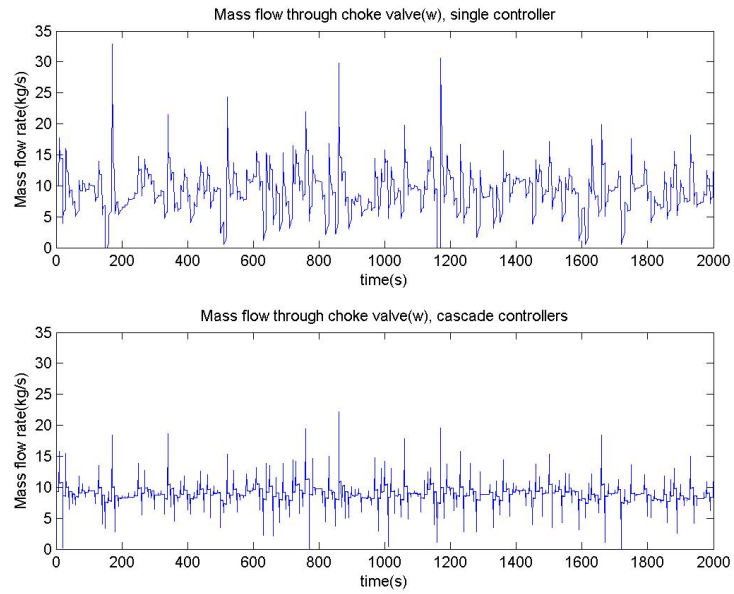
Figure 4.9: Mass flow rate through the choke valve for the DiMeglio system when applying disturbances and noise. Using the cascade control structure makes less variations in flow rate compared to the single pressure controller.

Chapter 5

Conclusion and further work

5.1 Conclusion

The building of the experimental setup was almost complete. The main components are installed, only missing the valve positioner and the I/O module.

The DiMeglio model and NewModel had very similar frequency responses when the bode plots for the two linearized models was compared. The models seems to be equally good in describing the riser system. NewModel has a slight advantage of having fewer tuning parameters, and tuning parameters which are independent of the physical property of the system.

It proved effective to use a cascade control structure for controlling riser system, even when the disturbances were large. Especially the top pressure fluctuations were much less for the cascade structure compared to the single pressure controller case.

5.2 Further work

The valve positioner needs to be ordered and installed. The same goes for the I/O module. After everything is installed a safety evaluation needs to be done before the experiment can be used. The system can then be tested for leaks before doing test runs.

When getting the experiment running, experimental data needs to be created to compare with the simple models. Will the simple models be valid?

Testing the different control structures to see if the simulation results can be recreated and verified. Further testing of control structures will be done in the following master thesis next semester.

Bibliography

[1] ABB, (14.12.2004), *Transient/slugging*, `https://www.abb.com/cawp/seitp161/2cfdabece457886841256f500041089e.aspx`, [downloaded 12.12.2010].

[2] Baardsen, I. (2003), *Slug regulering i tofase strømning, Eksperimentell verifikasjon*, Master Thesis at Department of Chemical Engineering NTNU, Trondheim, 90.

[3] Bai, Y. (2001), *Pipelines and Risers*, Elsevier, Nederlands, 498.

[4] Di Meglio, F., Kaasa, G.O, Petit, N. (2009), *A first principle model for multiphase slugging flow in vertical risers.*, Joint 48th IEEE Conference on Decision and Control and 28th Chinese Control Conference,8244 - 8251.

[5] Fahadi, J. (2007), *Anti-slug control, an experimental approach*, Project at Department of Chemical Engineering NTNU, Trondheim,50.

[6] Guo, B., Song, S., Chacko, J., Ghalambor, A. (2005), *Offshore Pipelines*, Elsevier, United States of America, 281.

[7] Havre, K. Stornes, K.O, Stray, H.(2000), *Taming slug flow in pipelines*, ABB review 4, 55-63.

[8] Jahanshahi, E., Skogestad, S. (2010), *Simplified Dynamical Models for Control of Severe Slugging in Multiphase Risers*, 18th IFAC World Congress, xxx-xxx.

[9] Manum, H. (2005), *Extensions of Skogestad's SIMC tuning rules to oscillatory and unstable processes*, Project at Department of Chemical Engineering NTNU, Trondheim, 60.

[10] Ogata, K. (2002), *Modern Control Enginering*, Prentice-Hall, New Jersey, 976.

[11] Ringereide Hyllestad, E.L. (2010), *Stabilization of two-phase flow in risers from reservoirs (anti-slug control).*, Master Thesis at Department of Chemical Engineering NTNU, Trondheim, 85.

[12] Shamsuzzoha, M., Skogestad, S. (2010), *The setpoint overshoot method: A simple and fast method for closed-loop PID tuning*, Journal of Process Control, 20, xxx-xxx.

[13] Skogestad, S., Postlethwaite, I. (2005), *Multivariable Feedback control*, 2nd ed., John-Wiley & Sons, 595.

[14] Skogestad, S. (2003), *Simple analytic rules for model reduction and PID controller design*, Journal of Process Control, Vol. 13, 291-309.

[15] Storkaas, E.(2005), *Stabilizing control and controllability: Control solutions to avoid slug flow in pipeline.riser systems*, Department of Chemical Engineering NTNU,Trondheim, 148.

[16] Søndrol, M (2005), *Anti-slug control. Experimental testing and verification*, Master Thesis at Department of Chemical Engineering NTNU, Trondheim, 112.

[17] Trudvang, C.F. (2003), *Modellbasert stabiliserende regulering av gravitasjonsindusert slugging i pipeline-riser systemer*, Master Thesis at Department of Chemical Engineering NTNU, Trondheim, 57.

Appendix A

Linearization

Linearized models of the New Model and the DiMeglio model was created by linearizing the model equations described in the appendix B.

$$\dot{\underline{x}} = \underline{A}\underline{x} + \underline{B}\underline{u}$$

$$y = \underline{C}\underline{x} + \underline{D}\underline{u} \tag{A.1}$$

By the use of Taylor's formula and neglecting higher order terms, a linearized system around the steady state point can be represented according to the equation A.1,where x is the state vector, u is the i input vector, and y is the output vector. The matrices A, B, C and D can be expressed using the Jacobian matrix shown in equation A.2.

$$J = \begin{bmatrix} \frac{\partial f_1}{\partial x_1} & \cdots & \frac{\partial f_1}{\partial x_n} \\ \vdots & \ddots & \vdots \\ \frac{\partial f_n}{\partial x_1} & \cdots & \frac{\partial f_n}{\partial x_n} \end{bmatrix} \tag{A.2}$$

The model equations derivatives can be calculated using the rules of total derivative, given in equation A.3. Here the function, f, is linearized with respect to the variable x_1. The other function variables, x_2, x_3, ..., x_n, are depended on x_1. The Jacobian's can then be found by substitution.

$$\frac{df}{dx_1}(x_1, x_2, x_3...x_n) = \frac{\partial f}{\partial x_1} + \frac{\partial f}{\partial x_2}\frac{dx_2}{dx_1} + \frac{\partial f}{\partial x_3}\frac{dx_3}{dx_1} + ... + \frac{\partial f}{\partial x_n}\frac{dx_n}{dx_1} \tag{A.3}$$

All derivatives was calculated by hand, and transfered into Matlab where the Jacobian's, and thus the linearized model, was calculated. The Matlab script is given in appendix E.

Appendix B

Models

In this appendix the model equations for the two model, NewModel and DiMeglio model, are shown.

B.1 Newmodel

B.1.1 State equations

$$\dot{m}_{G1} = w_{G,in} - w_{G,lp} \tag{B.1}$$
$$\dot{m}_{L1} = w_{L,in} - w_{L,lp} \tag{B.2}$$
$$\dot{m}_{G2} = w_{G,lp} - w_{G,out} \tag{B.3}$$
$$\dot{m}_{L2} = w_{L,lp} - w_{L,out} \tag{B.4}$$
$$\tag{B.5}$$

B.1.2 Model equations

Inflow conditions

$$\overline{\alpha}_{L1} = \frac{\rho_{G1} w_{L,in}}{\overline{\rho}_{G1} w_{L,in} + \rho_L w_{G,in}} \tag{B.6}$$
$$\overline{\rho}_{G1} = \frac{P_{1,nom} M_G}{R T_1} \tag{B.7}$$

Outflow conditions

$$w_{mix,out} = K_{pc} f(z) \sqrt{\rho_t (P_{2,t} - P_0)} \tag{B.8}$$
$$w_{L,out} = \alpha_{lm,t} w_{mix,out} \tag{B.9}$$
$$w_{G,out} = (1 - \alpha_{lm,t}) w_{mix,out} \tag{B.10}$$

Pipeline model

$$h_1 = h_c \overline{\alpha}_{L1} + (\frac{m_{L1} - \rho_L V_1 \overline{\alpha}_{L1}}{\pi r_1^2 (1 - \overline{\alpha}_{L1}) \rho_L}) sin(\theta) \tag{B.11}$$

$$V_{G1} = V_1 - \frac{m_{L1}}{\rho_L} \tag{B.12}$$

$$\rho_{G1} = \frac{m_{G1}}{V_{G1}} \tag{B.13}$$

$$P_1 = \frac{\rho_{G1} R T_1}{M_G} \tag{B.14}$$

$$\Delta P_{fp} = \frac{\overline{\alpha}_{L1} \lambda_p \rho_L \overline{U}_{sl,in}^2 L_1}{4 r_1} \tag{B.15}$$

$$\lambda_p = 0.0056 + 0.5 Re_p^{-0.32} \tag{B.16}$$

$$Re_p = \frac{2 \rho_L \overline{U}_{sl,in} r_1}{\mu} \tag{B.17}$$

$$\overline{U}_{sl,in} = \frac{w_{L,in}}{2 \pi r_1^2 \rho_L} \tag{B.18}$$

Riser model

$$V_2 = A_2 (L_2 + L3) \tag{B.19}$$

$$V_{G2} = V_2 - \frac{m_{L2}}{\rho_L} \tag{B.20}$$

$$\rho_{G2} = \frac{m_{G2}}{V_{G2}} \tag{B.21}$$

$$P_{2,t} = \frac{\rho_{G2} R T_2}{M_G} \tag{B.22}$$

$$\overline{\alpha}_{L2} = \frac{m_{L2}}{V_2 \rho_L} \tag{B.23}$$

$$\overline{\rho}_2 = \frac{m_{G2} + m_{L2}}{V_2} \tag{B.24}$$

$$\Delta P_f r = \frac{\overline{\alpha}_{L2} lambda_r \overline{\rho}_m \overline{U}_m^2 (L_2 + L_3)}{4 r_2} \tag{B.25}$$

$$\lambda_r = 0.0056 + 0.5 Re_r^{-0.32} \tag{B.26}$$

$$Re_p = \frac{2 \overline{\rho}_m \overline{U}_m r_2}{\mu} \tag{B.27}$$

$$\overline{U}_m = \overline{U}_{sl2} + \overline{U}_{sg2} \tag{B.28}$$

$$\overline{U}_{sl2} = \frac{w_{L,in}}{\rho_L \pi r_2^2} \tag{B.29}$$

$$\overline{U}_{sg2} = \frac{w_{G,in}}{\rho_{G2} \pi r_2^2} \tag{B.30}$$

Gas flow at low point

$$w_{G,lp} = 0, \ h \geq h_c \tag{B.31}$$

$$w_{G,lp} = K_G A_G \sqrt{\rho_{G1} \Delta P_G}, \ h < h_c \tag{B.32}$$

$$\Delta P_G = P_1 - P_{2,t} - \overline{\rho}_2 g L_2 - \Delta P_{fp} - \Delta P_{fr} \tag{B.33}$$

$$\tag{B.34}$$

Liquid flow at low point

$$w_{L,lp} = K_L A_L \sqrt{\rho_L \Delta P_L} \tag{B.35}$$

$$\Delta P_L = P_1 + \rho_L g h_1 - P_{2,t} - \overline{\rho}_2 g L_2 - \Delta P_{fp} - \Delta P_{fr} \tag{B.36}$$

$$A_G = \pi r_1^2 \left(\frac{h_c - h_1}{h_c}\right)^2 \tag{B.37}$$

$$A_L = \pi r_1^2 - A_G \tag{B.38}$$

Phase distribution model at outlet choke valve

$$\alpha_{Lm,t} = \frac{\alpha_{L,t} \rho_L}{\alpha_{L,t} \rho_L + (1 - \alpha_{L,t}) \rho_{G2}} \tag{B.39}$$

$$\rho_t = \alpha_{L,t} \rho_L + (1 - \alpha_{L,t}) \rho_{G2} \tag{B.40}$$

$$\alpha_{L,lp} = \frac{A_L}{\pi r_1^2} \tag{B.41}$$

$$\alpha_{L,t} = 2\overline{\alpha}_{L2} - \alpha_{L,lp}$$
$$= \frac{2 m_{L2}}{V_2 \rho_l} - \frac{A_L}{\pi r_1^2} \tag{B.42}$$

B.2   Di Meglio model

B.2.1   State equations

$$\dot{m}_{G1} = (1 - \varepsilon) w_{G,in} - w_{G,lp} \tag{B.43}$$

$$\dot{m}_{G2} = \varepsilon w_{G,in} + w_{G,lp} - w_{G,out} \tag{B.44}$$

$$\dot{m}_{L2} = w_{L,in} - w_{L,out} \tag{B.45}$$

B.2.2   Calculation of state-dependent internal variables

$$w_{G,lp} = K_G \max(0, P_1 - P_{2,b}) \tag{B.46}$$

$$w_{mix,out} = z K_{pc} \sqrt{P_{2,t} - P_0} \tag{B.47}$$

$$w_{L,out} = \frac{m_{L2}}{m_{L2} + m_{G2}} w_{mix,out} \approx w_{mix,out} \tag{B.48}$$

$$w_{G,out} = \frac{m_{G2}}{m_{L2} + m_{G2}} w_{mix,out} \approx \frac{m_{G2}}{m_{L2}} w_{mix,out} \tag{B.49}$$

$$V_{G2} = V_2 - \frac{m_{L2} + m_{L,still}}{\rho_L} \tag{B.50}$$

$$P_1 = \frac{RT_1}{M_G V_{G1}} m_{G1} \tag{B.51}$$

$$P_{2,b} = P_{2,t} + \frac{g \sin(\theta)}{A}(m_{L2} + m_{L,still}) \tag{B.52}$$

$$P_{2,t} = \frac{RT_2}{M_G V_{G2}} m_{G2} \tag{B.53}$$

Appendix C

Comparing New Model and DiMeglio models

C.1   Bode plots for various steady state inputs

In the following sections bode plots for various steady state input values are shown for the DiMeglio model and The New Model. The sections denote which steady state values that are changing. The undersections denotes which inputs are belonging to the plotted transfer functions.

C.1.1   Changing steady state choke valve position

Transfer function from choke valve position (z)

(a) New Model bode plot   (b) DiMeglio model bode plot
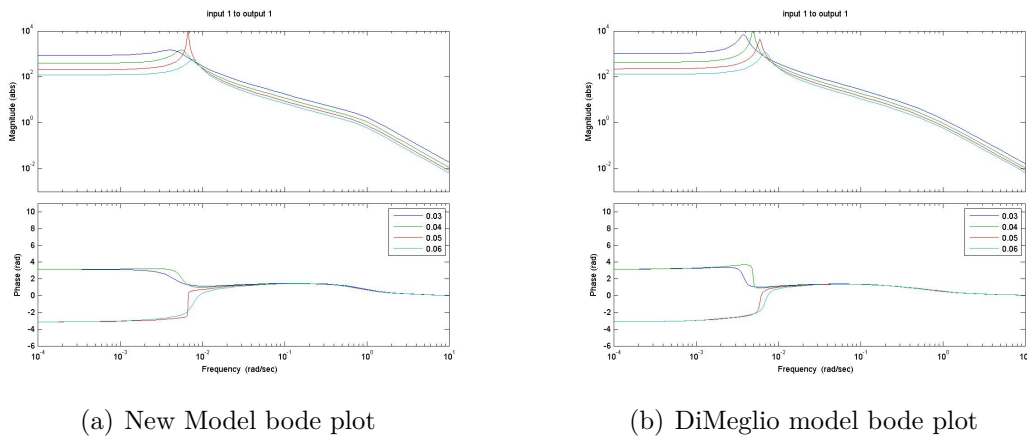
Figure C.1: Bode plot of the transfer function to the bottom pressure (P1) from the choke valve opening (z) for various steady state choke valve openings.
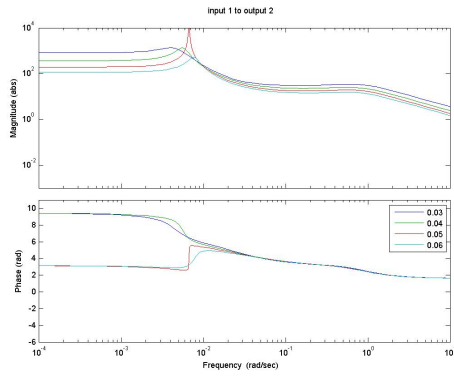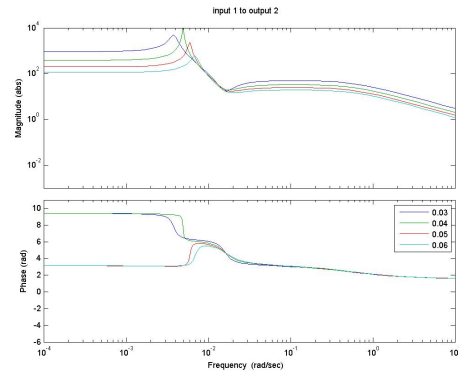
(a) New Model bode plot   (b) DiMeglio model bode plot

Figure C.2: Bode plot of the transfer function to the top pressure (P2) from the choke valve opening (z) for various steady state choke valve openings.
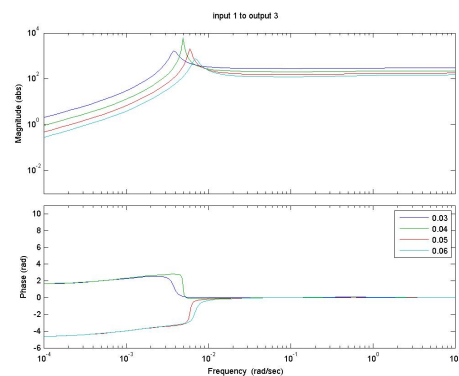
(a) New Model bode plot   (b) DiMeglio model bode plot

Figure C.3: Bode plot of the transfer function to the flow out of the system (q_{out}) from the choke valve opening (z) for various steady state choke valve openings.

Transfer function from gas flow rate ($w_{G,in}$)

(a) New Model bode plot

(b) DiMeglio model bode plot

Figure C.4: Bode plot of the transfer function to the bottom pressure (P1) from the gas flow rate ($w_{G,in}$) for various steady state choke valve openings.

(a) New Model bode plot
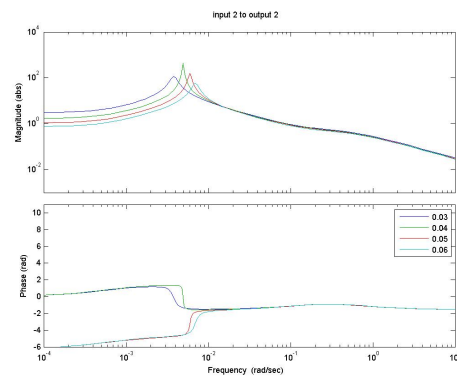
(b) DiMeglio model bode plot

Figure C.5: Bode plot of the transfer function to the top pressure (P2) from the gas flow rate ($w_{G,in}$) for various steady state choke valve openings.
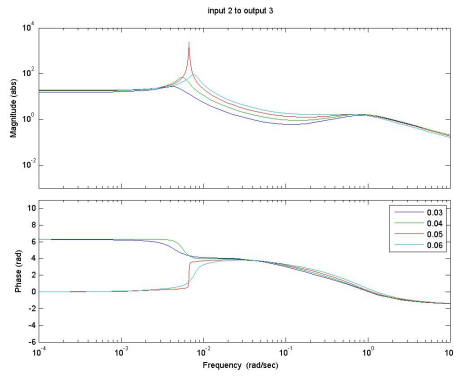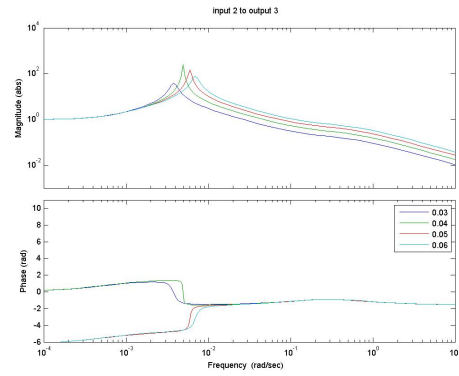
(a) New Model bode plot (b) DiMeglio model bode plot

Figure C.6: Bode plot of the transfer function to the flow out of the system (q_{out}) from the liquid flow rate ($w_{L,in}$) for various steady state choke valve openings.

Transfer function from liquid flow rate ($w_{L,in}$)
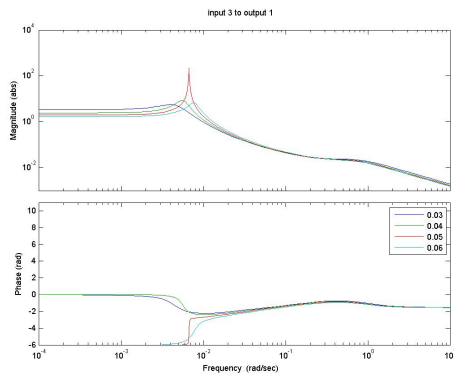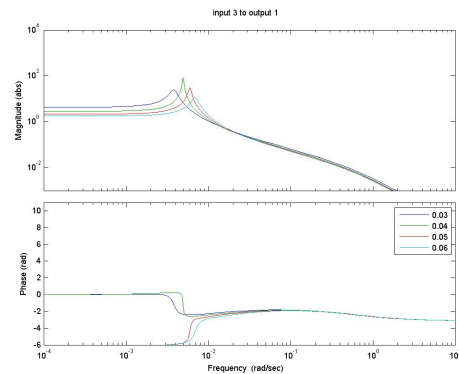
(a) New Model bode plot (b) DiMeglio model bode plot

Figure C.7: Bode plot of the transfer function to the bottom pressure (P1) from the liquid flow rate ($w_{L,in}$) for various steady state choke valve openings.
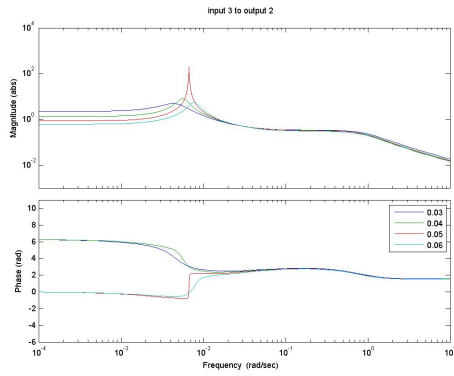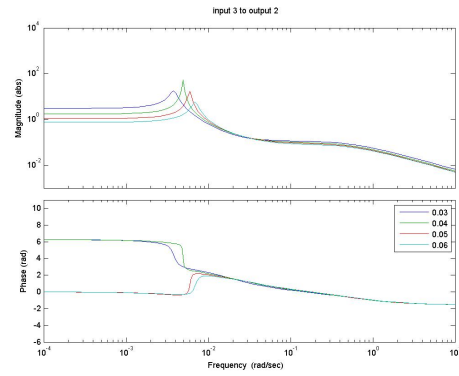
(a) New Model bode plot   (b) DiMeglio model bode plot

Figure C.8: Bode plot of the transfer function to the top pressure (P2) from the liquid flow rate ($w_{L,in}$) for various steady state choke valve openings.
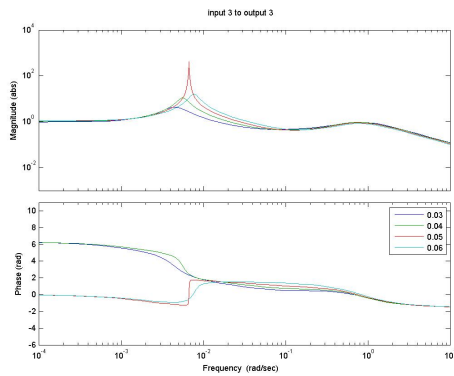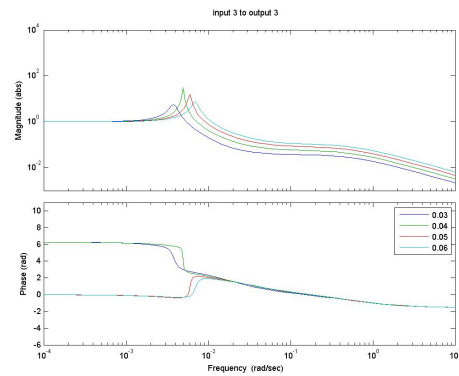
(a) New Model bode plot   (b) DiMeglio model bode plot

Figure C.9: Bode plot of the transfer function to the flow out of the system (q_{out}) from the gas flow rate ($w_{G,in}$) for various steady state choke valve openings.

C.1.2 Changing the gas flow rate

Transfer function from choke valve position (z)
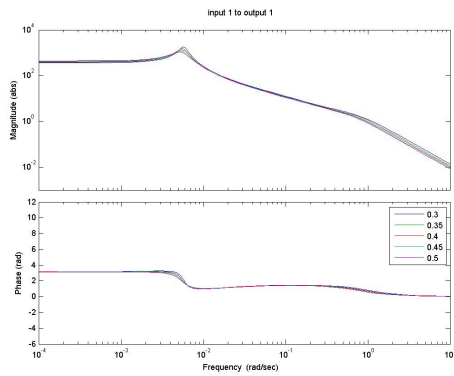
(a) New Model bode plot
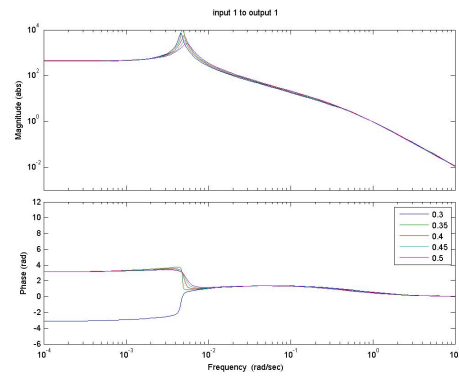
(b) DiMeglio model bode plot

Figure C.10: Bode plot of the transfer function to the bottom pressure (P1) from the choke valve opening (z) for various steady state gas flow rates.
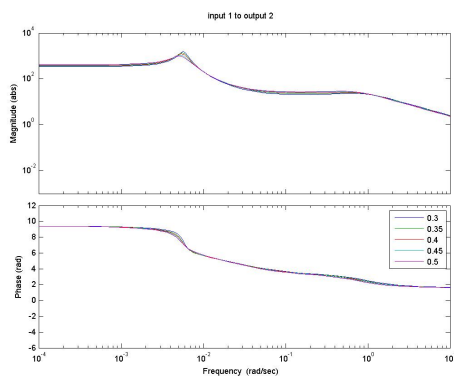
(a) New Model bode plot
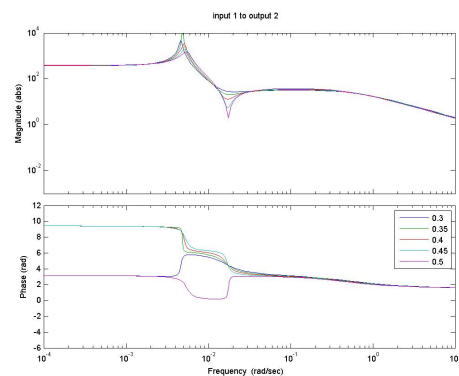
(b) DiMeglio model bode plot

Figure C.11: Bode plot of the transfer function to the top pressure (P2) from the choke valve opening (z) for various steady state gas flow rates.
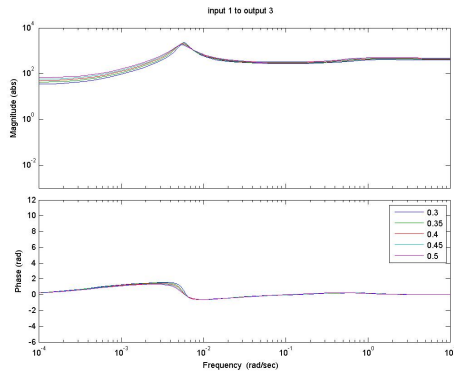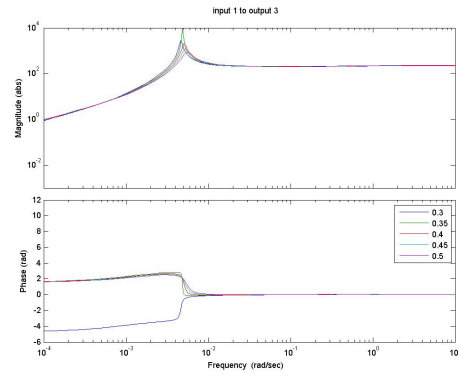
(a) New Model bode plot   (b) DiMeglio model bode plot

Figure C.12: Bode plot of the transfer function to the flow out of the system (q_{out}) from the choke valve opening (z) for various steady state gas flow rates.

Transfer function from gas flow rate ($w_{G,in}$)
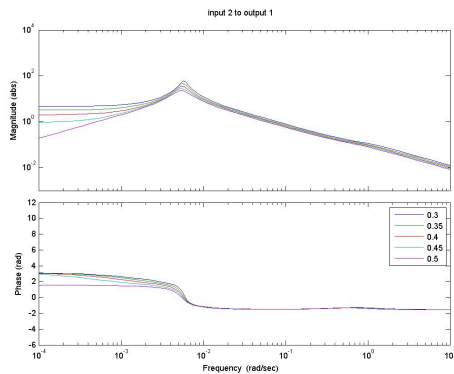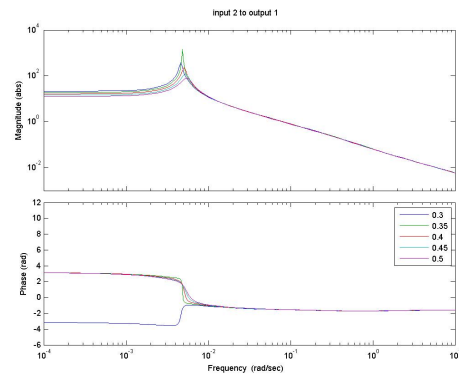
(a) New Model bode plot   (b) DiMeglio model bode plot

Figure C.13: Bode plot of the transfer function to the bottom pressure (P1) from the gas flow rate ($w_{G,in}$) for various steady state gas flow rates.
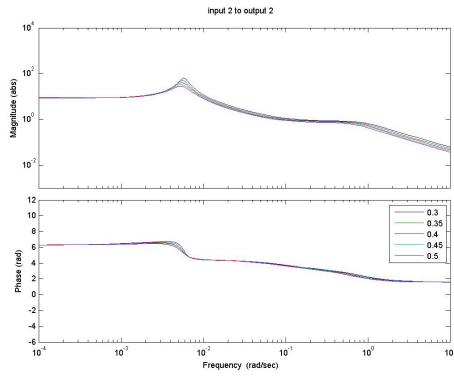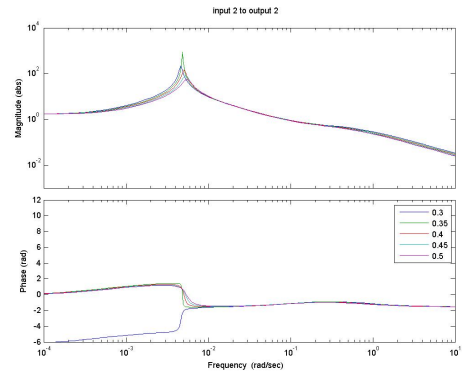
(a) New Model bode plot (b) DiMeglio model bode plot

Figure C.14: Bode plot of the transfer function to the top pressure (P2) from the gas flow rate ($w_{G,in}$) for various steady state gas flow rates.
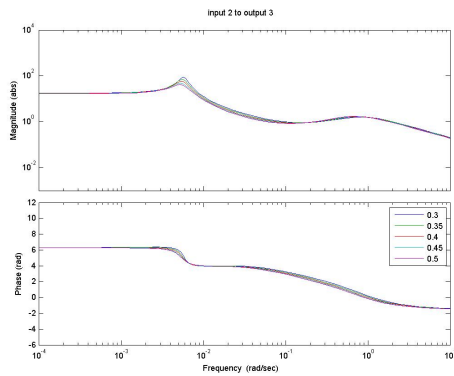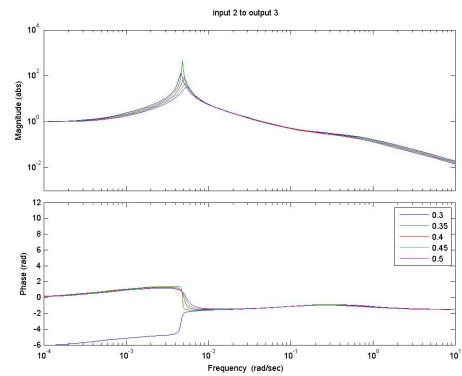
(a) New Model bode plot (b) DiMeglio model bode plot

Figure C.15: Bode plot of the transfer function to the flow out of the system (q_{out}) from the gas flow rate ($w_{G,in}$) for various steady state gas flow rates.

Transfer function from liquid flow rate ($w_{L,in}$)
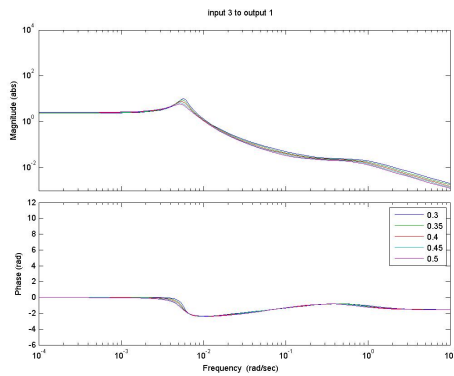
(a) New Model bode plot
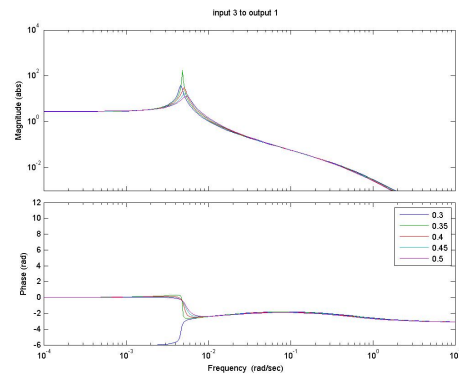
(b) DiMeglio model bode plot

Figure C.16: Bode plot of the transfer function to the bottom pressure (P1) from the liquid flow rate ($w_{L,in}$) for various steady state gas flow rates.
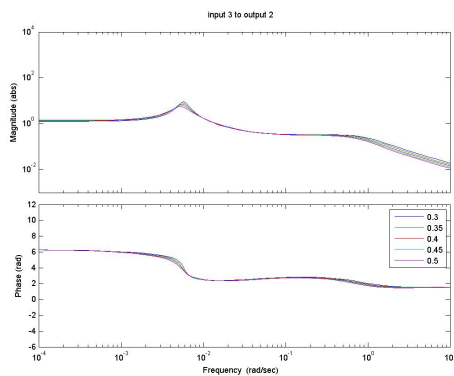
(a) New Model bode plot
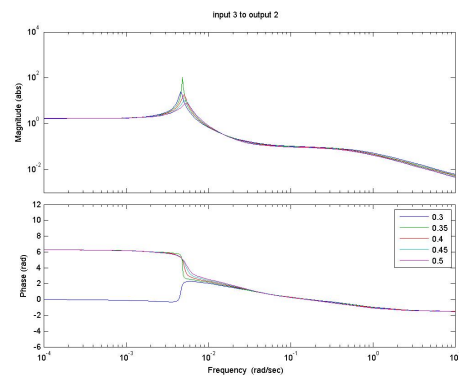
(b) DiMeglio model bode plot

Figure C.17: Bode plot of the transfer function to the top pressure (P2) from the liquid flow rate ($w_{L,in}$) for various steady state gas flow rates.
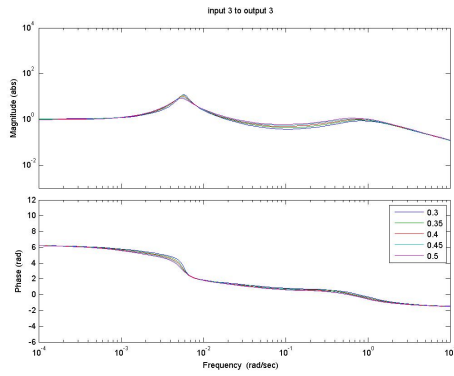
(a) New Model bode plot
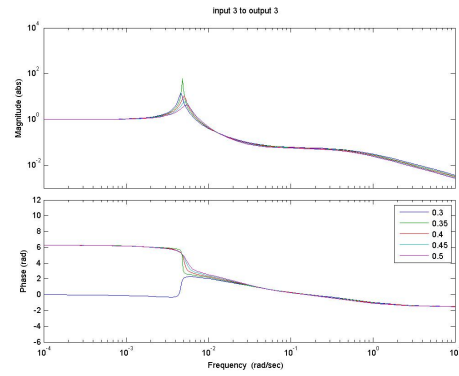
(b) DiMeglio model bode plot

Figure C.18: Bode plot of the transfer function to the flow out of the system (q_{out}) from the liquid flow rate ($w_{L,in}$) for various steady state gas flow rates.

C.1.3 Changing the liquid flow rate

Transfer function to choke valve position (z)
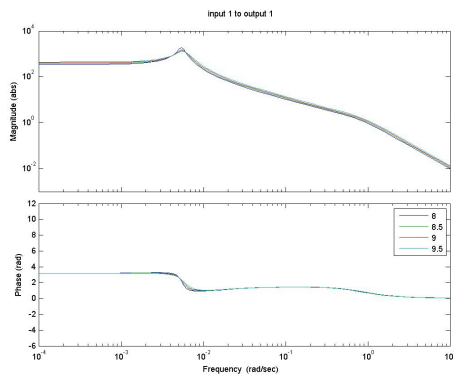
(a) New Model bode plot
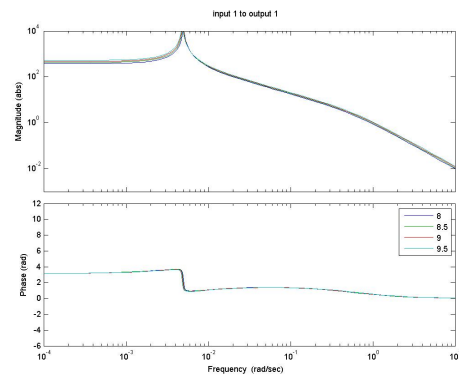
(b) DiMeglio model bode plot

Figure C.19: Bode plot of the transfer function to the bottom pressure (P1) from the choke valve opening (z) for various steady state liquid flow rates.
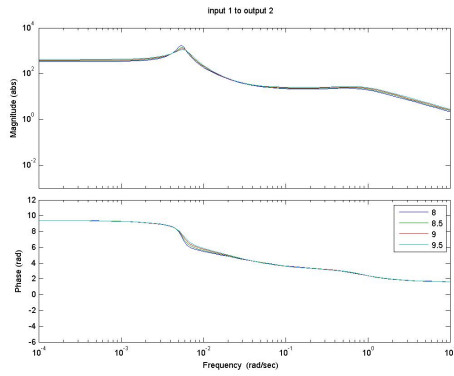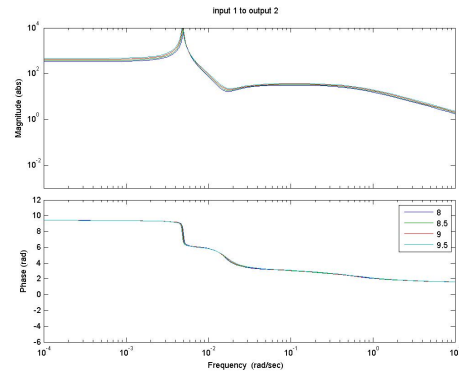
(a) New Model bode plot   (b) DiMeglio model bode plot

Figure C.20: Bode plot of the transfer function to the top pressure (P2) from the choke valve opening (z) for various steady state liquid flow rates.
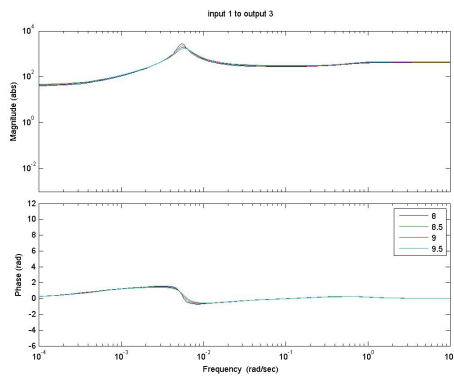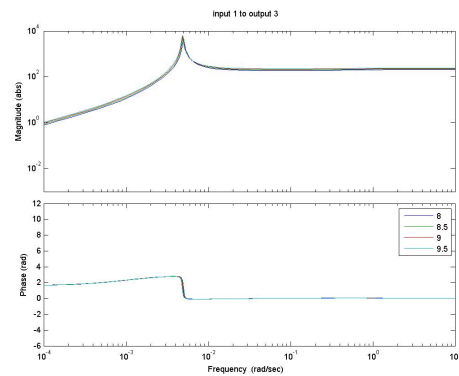
(a) New Model bode plot   (b) DiMeglio model bode plot

Figure C.21: Bode plot of the transfer function to the flow out of the system (q_{out}) from the choke valve opening (z) for various steady state liquid flow rates.

Transfer function from gas flow rate ($w_{G,in}$)
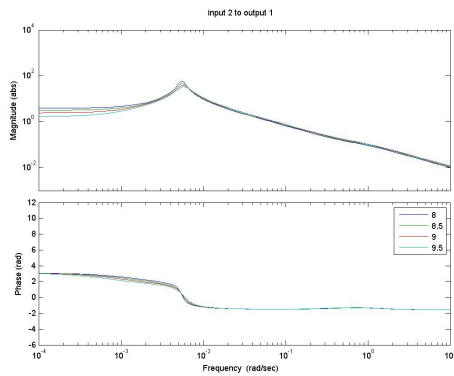
(a) New Model bode plot
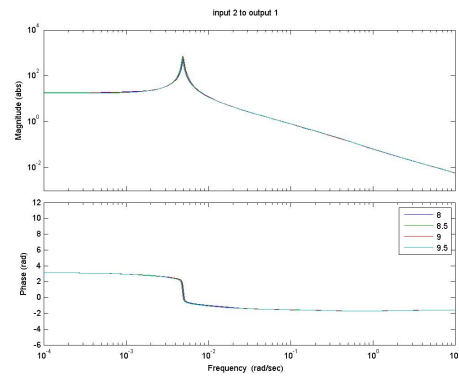
(b) DiMeglio model bode plot

Figure C.22: Bode plot of the transfer function to the bottom pressure (P1) from the gas flow rate ($w_{G,in}$) for various steady state liquid flow rates.
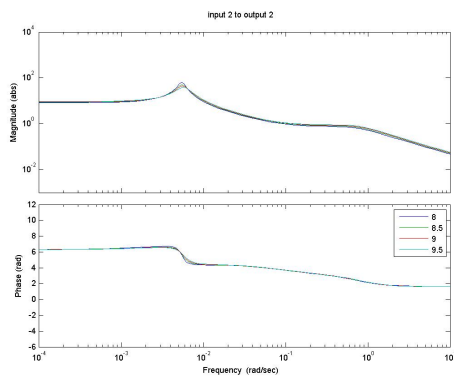
(a) New Model bode plot
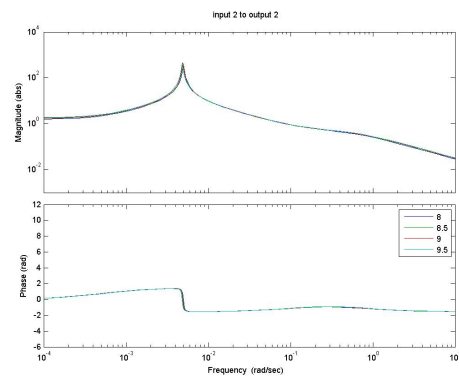
(b) DiMeglio model bode plot

Figure C.23: Bode plot of the transfer function to the top pressure (P2) from the gas flow rate ($w_{G,in}$) for various steady state liquid flow rates.
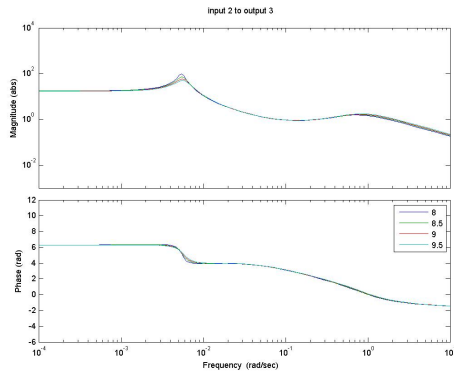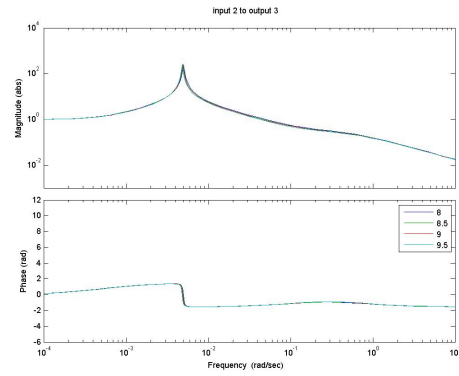
(a) New Model bode plot   (b) DiMeglio model bode plot

Figure C.24: Bode plot of the transfer function to the flow out of the system (q_{out}) from the gas flow rate $(w_{G,in})$ for various steady state liquid flow rates.

Transfer function from liquid flow rate $(w_{L,in})$
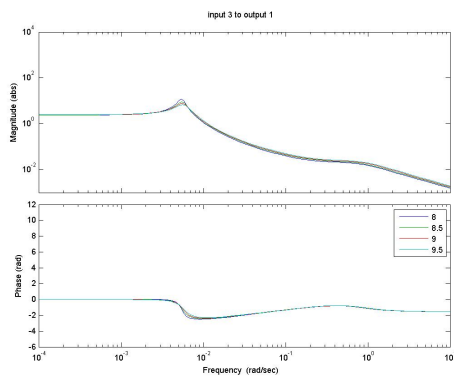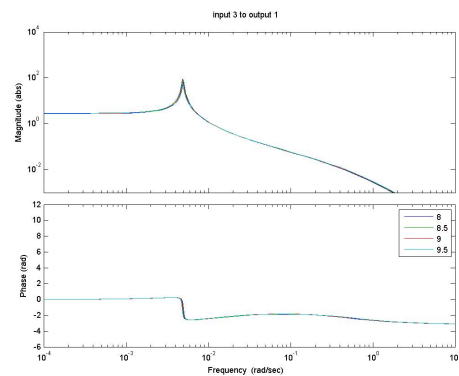
(a) New Model bode plot   (b) DiMeglio model bode plot

Figure C.25: Bode plot of the transfer function to the bottom pressure (P1) from the liquid flow rate $(w_{L,in})$ for various steady state liquid flow rates.
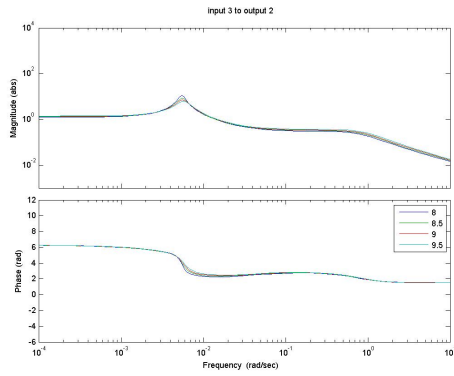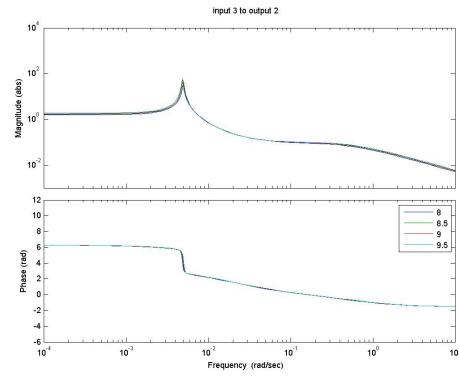
(a) New Model bode plot   (b) DiMeglio model bode plot

Figure C.26: Bode plot of the transfer function to the top pressure (P2) from the liquid flow rate ($w_{L,in}$) for various steady state liquid flow rates.
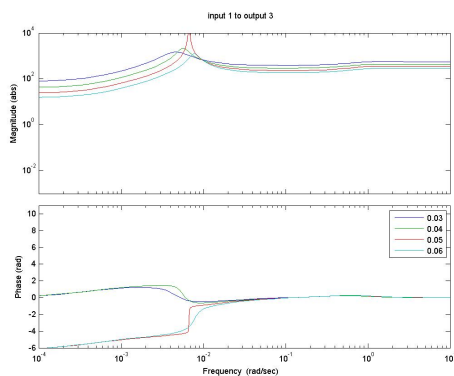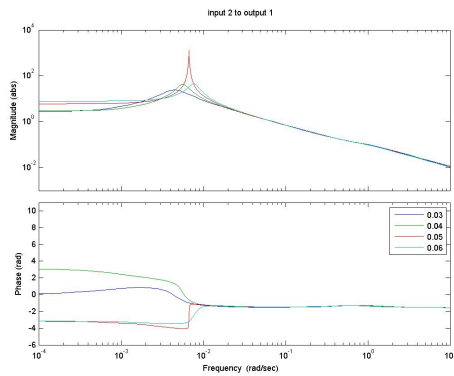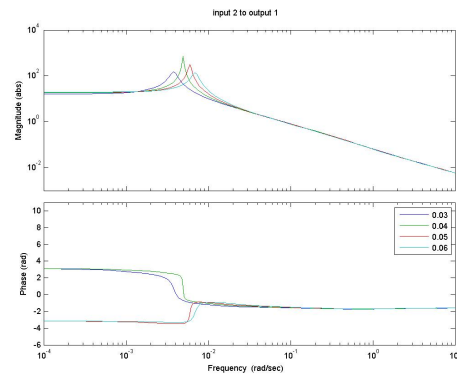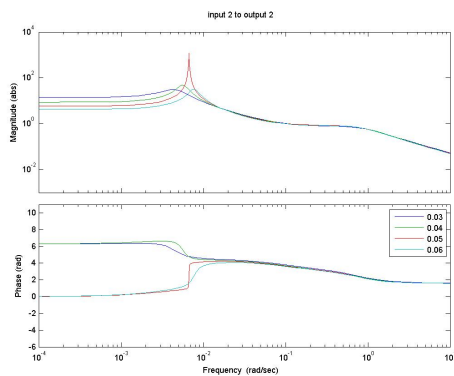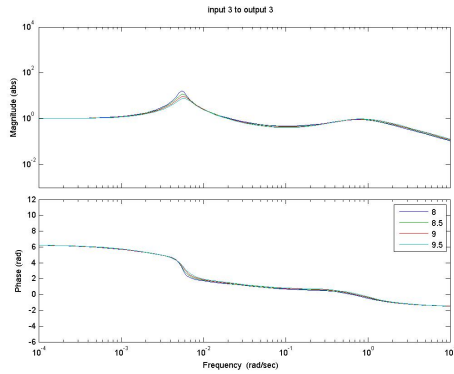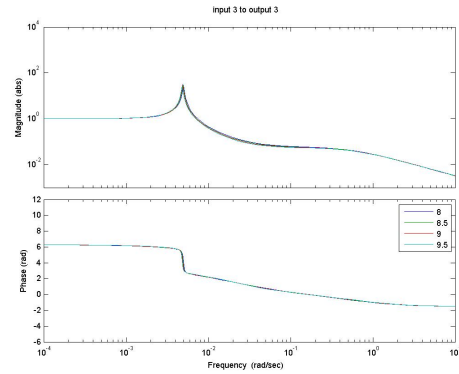

(a) New Model bode plot   (b) DiMeglio model bode plot

Figure C.27: Bode plot of the transfer function to the flow out of the system (q_{out}) from the liquid flow rate ($w_{L,in}$) for various steady state liquid flow rates.

Appendix D

Tuning the PI controllers

There are many stable self regulating open-loop process, unfortunately the riser slugging system are not one. This processes have proven impossible to control without using feedback control. A feedback controller is stable if the roots are negative, or have negative real parts.

The Simulink model shown in appendix G was controlled in two ways, a single pressure PI controller or a pressure PI controller in cascade configuration with a flow controller in the inner loop. The definition of a PI controller is shown in the equation D.1 where u(t) is the output of the controller, u(0) is the steady state output, e(t) is the error between the measurement and the desired setpoint, Kc is the gain constant and τ_I is the integral tuning parameter.

$$u(t) = u(0) + K_c \left(e(t) + \frac{1}{\tau_I} \int_0^t e(\tau)d\tau \right) \tag{D.1}$$

Finding the tuning parameters Kc and τ_I can be difficult if not a systematic approach is used. Tuning this case is even more difficult than normal, since the model is unstable and non-linear. The natural first choice for finding the tuning parameters would normally be to use the SMIC method[14]. Since the SIMC method, only can be used on stable system an other method has to be used for this problem. A newly developed method by Shamsuzzoha et.al [12] was chosen. This promising method is similar to the Ziegler-Nichols tuning, and supports closed-loop tuning. The main steps are given underneath:

1. In a closed-loop configuration, find a P value (Kc0) that gives approximate 30% overshoot.

2. Record overshoot = $\left(\frac{\Delta y_p - \Delta y_\infty}{\Delta y_\infty} \right)$

3. Record τ_p

4. Record steady state value, b= $\frac{\Delta y_\infty}{\Delta y_s}$

The figure D.4 shows graphically the definition of the different parameters recorded above. The tuning parameters can then be calculated according to the equations D.2, D.3 and D.4.

$$Kc = \frac{K_{c0}A}{F} \tag{D.2}$$

$$A = 1.152(overshoot^2) - 1.607(overshoot) + 1.0 \tag{D.3}$$

$$\tau_I = min\left(0.86A \left|\frac{b}{1-b}\right| \tau_p, 2.44t_pF\right) \tag{D.4}$$

$$\tag{D.5}$$
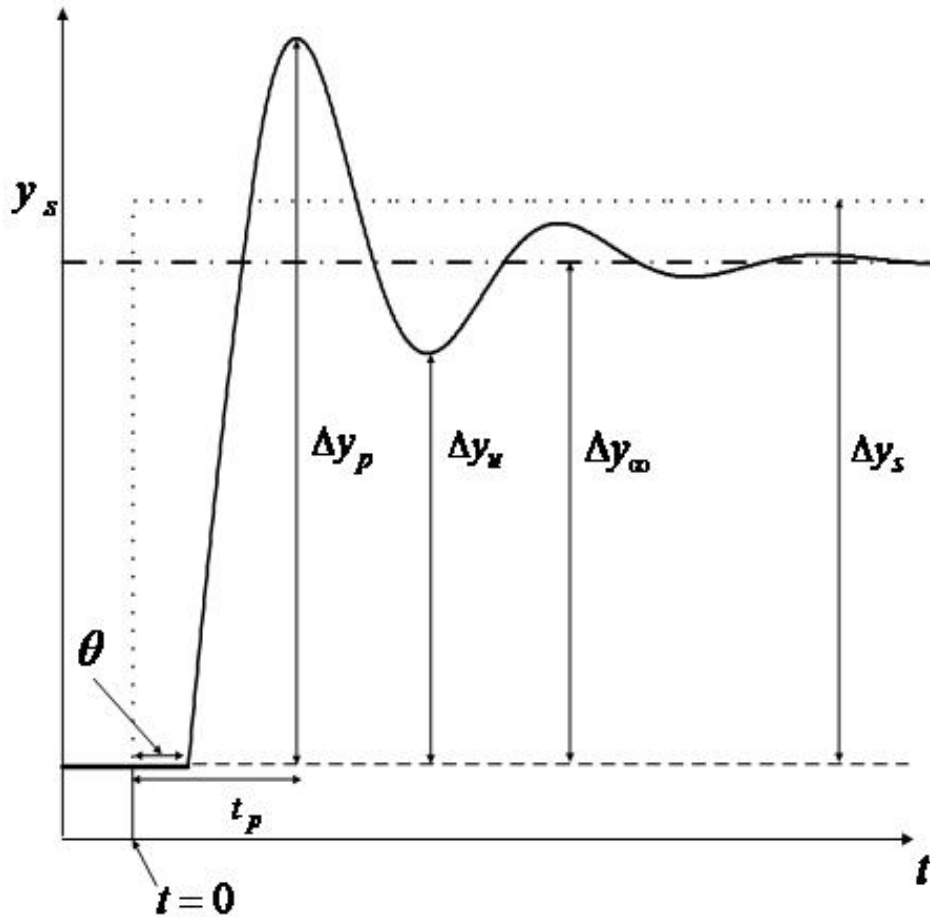
Figure D.1: Example of closed loop setpoint response with only P control [12]

Tuning parameters for the simulation was then found using a small step in the setpoint for the different controllers. For the cascade case, the inner-loop was first tuned, and kept closed while tuning the outer-loop. The recorded parameters can be seen in the table D.1.

Table D.1: Parameters for tuning the controllers in the Simulink model

Parameter	Single pressure controller	Inner loop for cascade case	Outer loop for cascade case
K_{c0}	-2	0.002	-200
Δy_p	0.0122	0.045	0.0142
Δy_∞	0.01	0.0315^1	0.01
$\tau_p[\text{s}]$	3.9	0.005	3.6
Δy_s	0.01	0.1	0.01
b	1	0.315	1
overshoot	0.220	0.4286	0.420
Kc	-0.0281	2.00e-4	-2.11
A	0.7022	0.5229	0.5283
τ_I	0.00100	476	439
F	5	5	50

Since the PI module in Simulink is in the form: P+I/s+Ds. The τ_I needs to be converted to I. The final tuning parameters are given in the table underneath.

Table D.2: Controller tuning parameters for the two control structures

Controller	P	I	D
Pressure controller for the single controller configuration	$-0.0281[bar^{-1}]$	$-6.00\text{e-}5[s^{-1}bar^{-1}]$	$0[sbar^{-1}]$
Flow controller in the inner loop in the cascade configuration	$2.00\text{e-}4[\frac{s}{kg}]$	$0.202[\text{kg}]$	$0[\frac{s^2}{kg}]$
Pressure controller in the outer loop in the cascade configuration	$-2.11[bar^{-1}]$	$-0.00480[s^{-1}bar^{-1}]$	$0[sbar^{-1}]$

---

[1]This value was calculated using the approximation formula: $\Delta y_\infty = 0.45(\Delta y_p + \Delta y_u)$

Appendix E

Linearized model-Matlab (analytical)

This appendix shows the Matlab code for the linearized models.

E.1 NewModel

```
% %%%%%%%%%%%%%%%%%%%%%%%%%%%%%%%%%%%%%%%%%%%%%%%%%%%%%%%%%%%%%%%%%%%%%%%%%%%
%
% Linerized model of final version New model. Function version.
%
% x1=mg1
% x2=ml1
% x3=mg2
% x4=ml2
% u1=z
% u2=w_G_in
% u3=w_L_in
%
% %%%%%%%%%%%%%%%%%%%%%%%%%%%%%%%%%%%%%%%%%%%%%%%%%%%%%%%%%%%%%%%%%%%%%%%%%%%
%
% Written by:  Knut Åge Meland
% Date:          27.10.2010
%
% %%%%%%%%%%%%%%%%%%%%%%%%%%%%%%%%%%%%%%%%%%%%%%%%%%%%%%%%%%%%%%%%%%%%%%%%%%%

%%
function [A,B,C,D]= v4_new_4d_linmod_knut(x0,y0,u,par)

%%
u1 = u(1);
u2 = u(2);
u3 = u(3);


x1 = x0(1);
x2 = x0(2);
x3 = x0(3);
x4 = x0(4);
```

```
P1_nom=y0(1)*10^5;

%%
g=par.g;
R=par.R;
rho_L=par.rho_L;
theta=par.theta;
r1=par.r1;
r2=par.r2;
hc=par.hc;
A1=par.A1;
A2=par.A2;
L1=par.L1;
L2=par.L2;
L3=par.L3;
T1=par.T1;
T2=par.T2;
M_G=par.M_G;
P0=par.P0;
V2=par.V2;
V1=par.V1;


K_pc =par.K_pc;
K_g =par.K_g;
K_L=par.K_o;

K_h=par.k_h; %correction factor to finetune model
my=par.visl; %friction factor




%%
%%%%%%%%%%%%%%%%%%%%%%%%%%%%%%%%%%%%%%%%%%%%%%%%%%%%%%%%%%%%%%%%%%%%%%%%%%%%%%%%
% Calculating differensials:
%%%%%%%%%%%%%%%%%%%%%%%%%%%%%%%%%%%%%%%%%%%%%%%%%%%%%%%%%%%%%%%%%%%%%%%%%%%%%%%%
%%
rho_G1_av=P1_nom*M_G/(R*T1);

%%
a_L1_av=(rho_G1_av*u3)/(rho_G1_av*u3 + rho_L*u2);

da_L1_av__dx1 = 0;
da_L1_av__dx2 = 0;
da_L1_av__dx3 = 0;
da_L1_av__dx4 = 0;
da_L1_av__du1 = 0;
da_L1_av__du2 = 0;%-(rho_L*rho_G1_av*u3)/(rho_G1_av*u3 +rho_L*u2)^2;
```

```
da_L1_av__du3 = 0;%(rho_G1_av*rho_L*u2)/(rho_G1_av*u3 +rho_L*u2)^2;
%%
h1_av = K_h*hc*a_L1_av;

dh1_av__dx1 = 0;
dh1_av__dx2 = 0;
dh1_av__dx3 = 0;
dh1_av__dx4 = 0;
dh1_av__du1 = 0;
dh1_av__du2 = K_h*hc*da_L1_av__du2;
dh1_av__du3 = K_h*hc*da_L1_av__du3;
%%
h1 = h1_av + sin(theta)*(x2 - V1*rho_L*a_L1_av)/(A1*(1-a_L1_av)*rho_L);

dh1__dx1 = 0;
dh1__dx2 = sin(theta)/(A1*(1-a_L1_av)*par.rho_L);
dh1__dx3 = 0;
dh1__dx4 = 0;
dh1__du1 = 0;
dh1__du2 = dh1_av__du2 ...
    +sin(theta)*x2*da_L1_av__du2/(A1*rho_L*(1-a_L1_av)^2)...
    -(V1*sin(theta)/A1)*da_L1_av__du2/(1-a_L1_av)^2;
dh1__du3 = dh1_av__du3 ...
    +sin(theta)*x2*da_L1_av__du3/(A1*rho_L*(1-a_L1_av)^2)...
    -(V1*sin(theta)/A1)*da_L1_av__du3/(1-a_L1_av)^2;

%%
V_G1 = V1 -x2/rho_L;

dV_G1__dx1 = 0;
dV_G1__dx2 = -1/rho_L;
dV_G1__dx3 = 0;
dV_G1__dx4 = 0;
dV_G1__du1 = 0;
dV_G1__du2 = 0;
dV_G1__du3 = 0;

%%
rho_G1 = x1/V_G1;

drho_G1__dx1 = 1/V_G1;
drho_G1__dx2 = -x1*dV_G1__dx2/V_G1^2;
drho_G1__dx3 = 0;
drho_G1__dx4 = 0;
drho_G1__du1 = 0;
drho_G1__du2 = 0;
drho_G1__du3 = 0;
```

```
%%
P1 = rho_G1*R*T1/M_G;

dP1__dx1 = R*T1*drho_G1__dx1 / M_G;
dP1__dx2 = R*T1*drho_G1__dx2 / M_G;
dP1__dx3 = 0;
dP1__dx4 = 0;
dP1__du1 = 0;
dP1__du2 = 0;
dP1__du3 = 0;

%%
U_slin_av = u3/(pi*r1^2*rho_L);

dU_slin_av__dx1 = 0;
dU_slin_av__dx2 = 0;
dU_slin_av__dx3 = 0;
dU_slin_av__dx4 = 0;
dU_slin_av__du1 = 0;
dU_slin_av__du2 = 0;
dU_slin_av__du3 = 1 / (pi*r1^2*rho_L );

%%
Re_p = 2*rho_L*U_slin_av*r1 / my ;

dRe_p__dx1 = 0;
dRe_p__dx2 = 0;
dRe_p__dx3 = 0;
dRe_p__dx4 = 0;
dRe_p__du1 = 0;
dRe_p__du2 = 0;
dRe_p__du3 = 2*rho_L*r1* dU_slin_av__du3 / my;

%%
L_p = 0.0056 +0.5*Re_p^(-0.32);

dL_p__dx1 = 0;
dL_p__dx2 = 0;
dL_p__dx3 = 0;
dL_p__dx4 = 0;
dL_p__du1 = 0;
dL_p__du2 = 0;
dL_p__du3 = -0.5*0.32*Re_p^(-1.32)*dRe_p__du3;

%%
DP_fp = a_L1_av*L_p*rho_L*U_slin_av^2*L1/(4*r1);

dDP_fp__dx1 = 0;
```

```
dDP_fp__dx2 = 0;
dDP_fp__dx3 = 0;
dDP_fp__dx4 = 0;
dDP_fp__du1 = 0;
dDP_fp__du2 = L_p*rho_L*U_slin_av^2*L1*da_L1_av__du2 / (4*r1);
dDP_fp__du3 = ( L_p*rho_L*U_slin_av^2*L1*da_L1_av__du3  ...
    +a_L1_av*rho_L*U_slin_av^2*L1*dL_p__du3 ...
    +2*a_L1_av*rho_L*L_p*U_slin_av*L1*dU_slin_av__du3 ) / (4*r1);

%%
V_G2 = V2 - x4 / rho_L ;

dV_G2__dx1 = 0;
dV_G2__dx2 = 0;
dV_G2__dx3 = 0;
dV_G2__dx4 = -1/rho_L ;
dV_G2__du1 = 0;
dV_G2__du2 = 0;
dV_G2__du3 = 0;

%%
rho_G2 = x3 / V_G2 ;

drho_G2__dx1 = 0;
drho_G2__dx2 = 0;
drho_G2__dx3 = 1/V_G2;
drho_G2__dx4 = -x3*dV_G2__dx4 / V_G2^2;
drho_G2__du1 = 0;
drho_G2__du2 = 0;
drho_G2__du3 = 0;

%%
P2 = rho_G2*R*T2 / M_G;

dP2__dx1 = 0;
dP2__dx2 = 0;
dP2__dx3 = R*T2*drho_G2__dx3/M_G;
dP2__dx4 = R*T2*drho_G2__dx4/M_G;
dP2__du1 = 0;
dP2__du2 = 0;
dP2__du3 = 0;

%%
Alpha_L2_av = x4/(rho_L*V2);

dAlpha_L2__dx1 = 0;
dAlpha_L2__dx2 = 0;
dAlpha_L2__dx3 = 0;
```

```
dAlpha_L2__dx4 = 1/(rho_L*V2);
dAlpha_L2__du1 = 0;
dAlpha_L2__du2 = 0;
dAlpha_L2__du3 = 0;

%%
rho_m_av = (x3+x4)/V2;

drho_m_av__dx1 = 0;
drho_m_av__dx2 = 0;
drho_m_av__dx3 = 1/V2;
drho_m_av__dx4 = 1/V2;
drho_m_av__du1 = 0;
drho_m_av__du2 = 0;
drho_m_av__du3 = 0;

%%
U_sl2_av=u3/(rho_L*pi*r2^2);
U_sg2_av=u2 /(rho_G2*pi*r2^2);

%%
U_m_av = U_sl2_av +U_sg2_av;

dU_m_av__dx1 = 0;
dU_m_av__dx2 = 0;
dU_m_av__dx3 = -U_sg2_av * drho_G2__dx3 / rho_G2;
dU_m_av__dx4 = -U_sg2_av * drho_G2__dx4 / rho_G2;
dU_m_av__du1 = 0;
dU_m_av__du2 = U_sg2_av / u2 ;
dU_m_av__du3 = U_sl2_av / u3 ;

%%
Re_r= 2*rho_m_av *U_m_av* r2 / my;

dRe_r__dx1 = 0;
dRe_r__dx2 = 0;
dRe_r__dx3 = 2*rho_m_av * r2* dU_m_av__dx3 / my  ...
    + 2 *U_m_av* r2* drho_m_av__dx3 / my;
dRe_r__dx4 = 2*rho_m_av * r2* dU_m_av__dx4 / my  ...
    + 2 *U_m_av* r2* drho_m_av__dx4 / my;
dRe_r__du1 = 0;
dRe_r__du2 = 2*rho_m_av * r2* dU_m_av__du2 / my;
dRe_r__du3 = 2*rho_m_av * r2* dU_m_av__du3 / my;

%%
L_r = 0.0056 + 0.5*Re_r^(-0.32);

dL_r__dx1 = 0;
```

```
dL_r__dx2 = 0;
dL_r__dx3 = -0.5*0.32*Re_r^(-1.32)*dRe_r__dx3;
dL_r__dx4 = -0.5*0.32*Re_r^(-1.32)*dRe_r__dx4;
dL_r__du1 = 0;
dL_r__du2 = -0.5*0.32*Re_r^(-1.32)*dRe_r__du2;
dL_r__du3 = -0.5*0.32*Re_r^(-1.32)*dRe_r__du3;


%%
DP_fr = Alpha_L2_av * L_r *rho_m_av *U_m_av^2 * (L2 + L3) / (4*r2);

dDP_fr__dx1 = 0;
dDP_fr__dx2 = 0;
dDP_fr__dx3 = ( 2*Alpha_L2_av * L_r *rho_m_av *U_m_av * (L2 + L3)*dU_m_av__dx3 ...
    + Alpha_L2_av * L_r *U_m_av^2 * (L2 + L3) * drho_m_av__dx3 ...
    +Alpha_L2_av *rho_m_av *U_m_av^2 * (L2 + L3) *dL_r__dx3 ) / (4*r2);
dDP_fr__dx4 = ( 2*Alpha_L2_av * L_r *rho_m_av *U_m_av * (L2 + L3)*dU_m_av__dx4 ...
    + Alpha_L2_av * L_r *U_m_av^2 * (L2 + L3) * drho_m_av__dx4 ...
    +Alpha_L2_av *rho_m_av *U_m_av^2 * (L2 + L3) *dL_r__dx4 ...
    +L_r *rho_m_av *U_m_av^2 * (L2 + L3)*dAlpha_L2__dx4 )/ (4*r2);
dDP_fr__du1 = 0;
dDP_fr__du2 = ( 2*Alpha_L2_av * L_r *rho_m_av *U_m_av * (L2 + L3)*dU_m_av__du2 ...
    +Alpha_L2_av *rho_m_av *U_m_av^2 * (L2 + L3) *dL_r__du2 ) / (4*r2);
dDP_fr__du3 = ( 2*Alpha_L2_av * L_r *rho_m_av *U_m_av * (L2 + L3)*dU_m_av__du3 ...
    +Alpha_L2_av *rho_m_av *U_m_av^2 * (L2 + L3) *dL_r__du3 ) / (4*r2);


%%
DP_G = P1 -DP_fp - P2 - rho_m_av * g * L2 - DP_fr;

dDP_G__dx1 = dP1__dx1;
dDP_G__dx2 = dP1__dx2;
dDP_G__dx3 = - dP2__dx3 - g*L2*drho_m_av__dx3 - dDP_fr__dx3;
dDP_G__dx4 = - dP2__dx4 - g*L2*drho_m_av__dx4 - dDP_fr__dx4;
dDP_G__du1 = 0;
dDP_G__du2 = -dDP_fp__du2  - dDP_fr__du2;
dDP_G__du3 = -dDP_fp__du3  - dDP_fr__du3;


%%
DP_L = P1 -DP_fp +rho_L*g*h1 - P2 -rho_m_av*g *L2 - DP_fr;

dDP_L__dx1 = dP1__dx1;
dDP_L__dx2 = dP1__dx2 + rho_L* g* dh1__dx2;
dDP_L__dx3 = -dP2__dx3 - g* L2 * drho_m_av__dx3 - dDP_fr__dx3;
dDP_L__dx4 = -dP2__dx4 - g* L2 * drho_m_av__dx4 - dDP_fr__dx4;
dDP_L__du1 = 0;
dDP_L__du2 = -dDP_fp__du2 + rho_L*g*dh1__du2 - dDP_fr__du2;
dDP_L__du3 = -dDP_fp__du3 +rho_L*g*dh1__du3 - dDP_fr__du3;


%%
```

```
if h1<hc
    A_G = (A1/hc^2)*(hc - h1)^2;

    dA_G__dx1 = 0;
    dA_G__dx2 = (-2*A1/hc^2)*(hc - h1)*dh1__dx2;
    dA_G__dx3 = 0;
    dA_G__dx4 = 0;
    dA_G__du1 = 0;
    dA_G__du2 = (-2*A1/hc^2)*(hc - h1)*dh1__du2;
    dA_G__du3 = (-2*A1/hc^2)*(hc - h1)*dh1__du3;

else
    A_G=0;

    dA_G__dx1 = 0;
    dA_G__dx2 = 0;
    dA_G__dx3 = 0;
    dA_G__dx4 = 0;
    dA_G__du1 = 0;
    dA_G__du2 = 0;
    dA_G__du3 = 0;

end

%%
A_L = A1 - A_G;

dA_L__dx1 = 0;
dA_L__dx2 = -dA_G__dx2;
dA_L__dx3 = 0;
dA_L__dx4 = 0;
dA_L__du1 = 0;
dA_L__du2 = -dA_G__du2;
dA_L__du3 = -dA_G__du3;

%%
if h1<hc
    if DP_G<0
        disp('The flowdirection is wrong. Check parameters');
        return
    end
    w_G_lp = K_g*A_G*sqrt(rho_G1*DP_G);

    dw_G_lp__dx1 = K_g*A_G*(DP_G*drho_G1__dx1+ rho_G1*dDP_G__dx1)/(2*sqrt(rho_G1*DP_G)
    dw_G_lp__dx2 = K_g*dA_G__dx2*sqrt(rho_G1*DP_G)...
                   + K_g*A_G*(DP_G*drho_G1__dx2 +rho_G1*dDP_G__dx2)/(2*sqrt(rho_G1*DP_G)
    dw_G_lp__dx3 = K_g*A_G*rho_G1*dDP_G__dx3/(2*sqrt(rho_G1*DP_G));
    dw_G_lp__dx4 = K_g*A_G*rho_G1*dDP_G__dx4/(2*sqrt(rho_G1*DP_G));
```

```
    dw_G_lp__du1 = 0;
    dw_G_lp__du2 = K_g*A_G*rho_G1*dDP_G__du2/(2*sqrt(rho_G1*DP_G))...
        +K_g*dA_G__du2*sqrt(rho_G1*DP_G);
    dw_G_lp__du3 = K_g*A_G*rho_G1*dDP_G__du3/(2*sqrt(rho_G1*DP_G))...
        +K_g*dA_G__du3*sqrt(rho_G1*DP_G);
else
    w_G_lp = 0;

    dw_G_lp__dx1 = 0;
    dw_G_lp__dx2 = 0;
    dw_G_lp__dx3 = 0;
    dw_G_lp__dx4 = 0;
    dw_G_lp__du1 = 0;
    dw_G_lp__du2 = 0;
    dw_G_lp__du3 = 0;
end

%%
if DP_L<0
    disp('The flowdirection is wrong. Check parameters 2');
    return
end

w_L_lp = K_L*A_L*sqrt(rho_L*DP_L);

dw_L_lp__dx1 = K_L*A_L*rho_L*dDP_L__dx1/(2*sqrt(rho_L*DP_L));
dw_L_lp__dx2 = K_L*A_L*rho_L*dDP_L__dx2/(2*sqrt(rho_L*DP_L)) ...
    +K_L*dA_L__dx2*sqrt(rho_L*DP_L);
dw_L_lp__dx3 = K_L*A_L*rho_L*dDP_L__dx3/(2*sqrt(rho_L*DP_L));
dw_L_lp__dx4 = K_L*A_L*rho_L*dDP_L__dx4/(2*sqrt(rho_L*DP_L));
dw_L_lp__du1 = 0;
dw_L_lp__du2 = K_L*A_L*rho_L*dDP_L__du2/(2*sqrt(rho_L*DP_L)) ...
    +K_L*dA_L__du2*sqrt(rho_L*DP_L);
dw_L_lp__du3 = K_L*A_L*rho_L*dDP_L__du3/(2*sqrt(rho_L*DP_L)) ...
    +K_L*dA_L__du3*sqrt(rho_L*DP_L);

%%
Alpha_Lt = 2*x4 / (V2*rho_L) - A_L/A1 ;

dAlpha_Lt__dx1 = 0;
dAlpha_Lt__dx2 = -dA_L__dx2/A1;
dAlpha_Lt__dx3 = 0;
dAlpha_Lt__dx4 = 2/(V2*rho_L);
dAlpha_Lt__du1 = 0;
dAlpha_Lt__du2 = -dA_L__du2/A1;
dAlpha_Lt__du3 = -dA_L__du3/A1;

%%
```

```
rho_t=Alpha_Lt*rho_L +(1-Alpha_Lt)*rho_G2;

drho_t__dx1 = 0;
drho_t__dx2 = (rho_L-rho_G2)*dAlpha_Lt__dx2;
drho_t__dx3 = (1-Alpha_Lt)*drho_G2__dx3;
drho_t__dx4 = (rho_L-rho_G2)*dAlpha_Lt__dx4 + (1-Alpha_Lt)*drho_G2__dx4;
drho_t__du1 = 0;
drho_t__du2 = (rho_L-rho_G2)*dAlpha_Lt__du2;
drho_t__du3 = (rho_L-rho_G2)*dAlpha_Lt__du3;

%%
Alpha_Lmt = Alpha_Lt*rho_L/(Alpha_Lt*rho_L + (1-Alpha_Lt)*rho_G2);

dAlpha_Lmt__dx1 = 0;
dAlpha_Lmt__dx2 = (rho_L*dAlpha_Lt__dx2*(Alpha_Lt*rho_L + (1-Alpha_Lt)*rho_G2)...
    - rho_L*Alpha_Lt*dAlpha_Lt__dx2*(rho_L-rho_G2)) ...
    / (Alpha_Lt*rho_L + (1-Alpha_Lt)*rho_G2)^2 ;
dAlpha_Lmt__dx3 = -rho_L*Alpha_Lt*(1-Alpha_Lt)*drho_G2__dx3 /(Alpha_Lt*rho_L + (1-Alph
dAlpha_Lmt__dx4 = (rho_L*dAlpha_Lt__dx4*(Alpha_Lt*rho_L + (1-Alpha_Lt)*rho_G2)...
    - rho_L*Alpha_Lt*dAlpha_Lt__dx4*(rho_L-rho_G2)) ...
    / (Alpha_Lt*rho_L + (1-Alpha_Lt)*rho_G2)^2 ...
    -rho_L*Alpha_Lt*(1-Alpha_Lt)*drho_G2__dx4 ...
    /(Alpha_Lt*rho_L + (1-Alpha_Lt)*rho_G2)^2;
dAlpha__Lmt__du1 = 0;
dAlpha_Lmt__du2 = (rho_L*dAlpha_Lt__du2*(Alpha_Lt*rho_L + (1-Alpha_Lt)*rho_G2)...
    - rho_L*Alpha_Lt*dAlpha_Lt__du2*(rho_L-rho_G2)) ...
    / (Alpha_Lt*rho_L + (1-Alpha_Lt)*rho_G2)^2 ;
dAlpha_Lmt__du3 = (rho_L*dAlpha_Lt__du3*(Alpha_Lt*rho_L + (1-Alpha_Lt)*rho_G2)...
    - rho_L*Alpha_Lt*dAlpha_Lt__du3*(rho_L-rho_G2)) ...
    / (Alpha_Lt*rho_L + (1-Alpha_Lt)*rho_G2)^2 ;

%%
if P2-P0 <0
    disp('The flowdirection is wrong. Check parameters 3');
    return
end
w_mix_out = K_pc*u1*sqrt(rho_t*(P2-P0));

dw_mix__dx1 = 0;
dw_mix__dx2 = K_pc*u1*(drho_t__dx2*(P2-P0))/(2*sqrt(rho_t*(P2-P0)));
dw_mix__dx3 = K_pc*u1*(drho_t__dx3*(P2-P0)+rho_t*dP2__dx3)/(2*sqrt(rho_t*(P2-P0)));
dw_mix__dx4 = K_pc*u1*(drho_t__dx4*(P2-P0)+rho_t*dP2__dx4)/(2*sqrt(rho_t*(P2-P0)));
dw_mix__du1 = K_pc*sqrt(rho_t*(P2-P0));
dw_mix__du2 = K_pc*u1*(drho_t__du2*(P2-P0))/(2*sqrt(rho_t*(P2-P0)));
dw_mix__du3 = K_pc*u1*(drho_t__du3*(P2-P0))/(2*sqrt(rho_t*(P2-P0)));
%%
Q_out = K_pc*u1*sqrt((P2-P0)/rho_t);
```

```matlab
dQ__dx1 = 0;
dQ__dx2 = K_pc*u1*(-drho_t__dx2*(P2-P0))/(2*rho_t*sqrt(rho_t*(P2-P0)));
dQ__dx3 = K_pc*u1*(-drho_t__dx3*(P2-P0)+rho_t*dP2__dx3)/(2*rho_t*sqrt(rho_t*(P2-P0)));
dQ__dx4 = K_pc*u1*(-drho_t__dx4*(P2-P0)+rho_t*dP2__dx4)/(2*rho_t*sqrt(rho_t*(P2-P0)));
dQ__du1 = K_pc*sqrt((P2-P0)/rho_t);
dQ__du2 = K_pc*u1*(-drho_t__du2*(P2-P0))/(2*rho_t*sqrt(rho_t*(P2-P0)));
dQ__du3 = K_pc*u1*(-drho_t__du3*(P2-P0))/(2*rho_t*sqrt(rho_t*(P2-P0)));
%%
w_L_out = Alpha_Lmt*w_mix_out;

dw_L_out__dx1 = 0;
dw_L_out__dx2 = dAlpha_Lmt__dx2*w_mix_out + dw_mix__dx2*Alpha_Lmt;
dw_L_out__dx3 = dAlpha_Lmt__dx3*w_mix_out + dw_mix__dx3*Alpha_Lmt;
dw_L_out__dx4 = dAlpha_Lmt__dx4*w_mix_out + dw_mix__dx4*Alpha_Lmt;
dw_L_out__du1 = dw_mix__du1*Alpha_Lmt;
dw_L_out__du2 = dAlpha_Lmt__du2*w_mix_out + dw_mix__du2*Alpha_Lmt;
dw_L_out__du3 = dAlpha_Lmt__du3*w_mix_out + dw_mix__du3*Alpha_Lmt;
%%
w_G_out = (1 - Alpha_Lmt)*w_mix_out;

dw_G_out__dx1 = 0;
dw_G_out__dx2 = -dAlpha_Lmt__dx2*w_mix_out + dw_mix__dx2*(1-Alpha_Lmt);
dw_G_out__dx3 = -dAlpha_Lmt__dx3*w_mix_out + dw_mix__dx3*(1-Alpha_Lmt);
dw_G_out__dx4 = -dAlpha_Lmt__dx4*w_mix_out + dw_mix__dx4*(1-Alpha_Lmt);
dw_G_out__du1 =  dw_mix__du1*(1-Alpha_Lmt);
dw_G_out__du2 = -dAlpha_Lmt__du2*w_mix_out + dw_mix__du2*(1-Alpha_Lmt);
dw_G_out__du3 = -dAlpha_Lmt__du3*w_mix_out + dw_mix__du3*(1-Alpha_Lmt);
%%
%%%%%%%%%%%%%%%%%%%%%%%%%%%%%%%%%%%%%%%%%%%%%%%%%%%%%%%%%%%%%%%%%%%%%%%%%
%Finished calculating the differensials
%%%%%%%%%%%%%%%%%%%%%%%%%%%%%%%%%%%%%%%%%%%%%%%%%%%%%%%%%%%%%%%%%%%%%%%%%
%%
%%%%%%%%%%%%%%%%%%%%%%%%%%%%%%%%%%%%%%%%%%%%%%%%%%%%%%%%%%%%%%%%%%%%%%%%%
% State equation:
%%%%%%%%%%%%%%%%%%%%%%%%%%%%%%%%%%%%%%%%%%%%%%%%%%%%%%%%%%%%%%%%%%%%%%%%%
%%
dx1 = u2 - w_G_lp;
dx2 = u3 - w_L_lp;
dx3 = w_G_lp - w_G_out;
dx4 = w_L_lp -w_L_out;

% jackobian:
%% For A:
dx1__dx1 = -dw_G_lp__dx1;
dx1__dx2 = -dw_G_lp__dx2;
dx1__dx3 = -dw_G_lp__dx3;
dx1__dx4 = -dw_G_lp__dx4;
```

```
dx2__dx1 = -dw_L_lp__dx1;
dx2__dx2 = -dw_L_lp__dx2;
dx2__dx3 = -dw_L_lp__dx3;
dx2__dx4 = -dw_L_lp__dx4;


dx3__dx1 = dw_G_lp__dx1 - dw_G_out__dx1;
dx3__dx2 = dw_G_lp__dx2 - dw_G_out__dx2;
dx3__dx3 = dw_G_lp__dx3 - dw_G_out__dx3;
dx3__dx4 = dw_G_lp__dx4 - dw_G_out__dx4;


dx4__dx1 = dw_L_lp__dx1 - dw_L_out__dx1;
dx4__dx2 = dw_L_lp__dx2 - dw_L_out__dx2;
dx4__dx3 = dw_L_lp__dx3 - dw_L_out__dx3;
dx4__dx4 = dw_L_lp__dx4 - dw_L_out__dx4;
%% For B:
dx1__du1 = 0;
dx1__du2 = 1 -dw_G_lp__du2; %1
dx1__du3 = -dw_G_lp__du3;


dx2__du1 = 0;
dx2__du2 = -dw_L_lp__du2;
dx2__du3 = 1 -dw_L_lp__du3; %1


dx3__du1 = dw_G_lp__du1 - dw_G_out__du1;
dx3__du2 = dw_G_lp__du2 - dw_G_out__du2;
dx3__du3 = dw_G_lp__du3 - dw_G_out__du3;


dx4__du1 = dw_L_lp__du1 - dw_L_out__du1;
dx4__du2 = dw_L_lp__du2 - dw_L_out__du2;
dx4__du3 = dw_L_lp__du3 - dw_L_out__du3;
%% For C:
% Comments:
%y= [ P1 P2 w_mix_out]
%y(1) = P1(x) all derivatives for P1 done before
%y(2) = P2(x) all derivatives for P2 done before
%y(3) = w_mix_out(x,u) all derivatives done before
%% For D
% Comments:
%only y(3) is a function of u all derivatives done before



%%
%%%%%%%%%%%%%%%%%%%%%%%%%%%%%%%%%%%%%%%%%%%%%%%%%%%%%%%%%%%%%%%%%%%%%%%%%%%%
% Connecting jackobians to form A, B, C and D:
%%%%%%%%%%%%%%%%%%%%%%%%%%%%%%%%%%%%%%%%%%%%%%%%%%%%%%%%%%%%%%%%%%%%%%%%%%%%
A = [ dx1__dx1 dx1__dx2 dx1__dx3 dx1__dx4 ;
      dx2__dx1 dx2__dx2 dx2__dx3 dx2__dx4 ;
      dx3__dx1 dx3__dx2 dx3__dx3 dx3__dx4 ;
```

```
        dx4__dx1 dx4__dx2 dx4__dx3 dx4__dx4 ];


B = [ dx1__du1 dx1__du2 dx1__du3 ;
      dx2__du1 dx2__du2 dx2__du3 ;
      dx3__du1 dx3__du2 dx3__du3 ;
      dx4__du1 dx4__du2 dx4__du3 ];


C = 1e-5.*[ dP1__dx1 dP1__dx2 dP1__dx3 dP1__dx4 ;
            dP2__dx1 dP2__dx2 dP2__dx3 dP2__dx4 ] ; %Pa-> bar
C(3,:) =  1000*[ dQ__dx1 dQ__dx2 dQ__dx3 dQ__dx4 ]; %[L/s]
%C(3,:) =  [ dw_mix__dx1 dw_mix__dx2 dw_mix__dx3 dw_mix__dx4 ]; %[kg/s]


D = zeros(3,3);
D(3,:) = 1000*[ dQ__du1 dQ__du2 dQ__du3 ];
```

E.2   DiMeglio

```
% %%%%%%%%%%%%%%%%%%%%%%%%%%%%%%%%%%%%%%%%%%%%%%%%%%%%%%%%%%%%%%%%%%%%%%%%%%%%%
%
% Linerized model of Di meglio model. Function version.
%
%
% %%%%%%%%%%%%%%%%%%%%%%%%%%%%%%%%%%%%%%%%%%%%%%%%%%%%%%%%%%%%%%%%%%%%%%%%%%%%%
%
% Written by:  Knut Åge Meland
% Date:        5.11.2010
%
% %%%%%%%%%%%%%%%%%%%%%%%%%%%%%%%%%%%%%%%%%%%%%%%%%%%%%%%%%%%%%%%%%%%%%%%%%%%%%

%%
function [A,B,C,D]= linmodfunk(x,y0,u,par)

m_G1 = x(1);
m_G2 = x(2);
m_L2 = x(3);


z = u(1);
w_G_in = u(2);
w_L_in = u(3);

%%
P1 = m_G1*par.R*par.T1/(par.M_G*par.Veb);

dP1__dm_G1 = par.R*par.T1/(par.M_G*par.Veb);
```

70

```
%%
V_G2 = par.V2 - (m_L2+par.m_lstill)/par.rho_L;

dV_G2__dm_L2 = -1/par.rho_L;
%%
P2_t = m_G2*par.R*par.T2/(par.M_G*V_G2);
%P2_t = max(P2_t,par.P0);

dP2_t__dm_G2 = par.R*par.T2/(par.M_G*V_G2);
dP2_t__dm_L2 = -m_G2*par.R*par.T2*dV_G2__dm_L2/(par.M_G*V_G2^2);
%%
P2_b = P2_t + par.g*sin(par.theta2)*(m_L2+par.m_lstill)/par.A2;

dP2_b__dm_G2 = dP2_t__dm_G2;
dP2_b__dm_L2 = dP2_t__dm_L2 + par.g*sin(par.theta2)/par.A2;
%%
w_G1 = par.C_g*max(0,P1-P2_b);

dw_G1__dm_G1 = par.C_g*dP1__dm_G1;
dw_G1__dm_G2 = -par.C_g * dP2_b__dm_G2;
dw_G1__dm_L2 = -par.C_g * dP2_b__dm_L2;
%%
w_out = par.C_c*z*sqrt(max(0,P2_t-par.P0));

dw_out__dm_G1 = 0;
dw_out__dm_G2 = par.C_c*z*dP2_t__dm_G2 / (2* sqrt(P2_t-par.P0) );
dw_out__dm_L2 = par.C_c*z*dP2_t__dm_L2 / (2* sqrt(P2_t-par.P0) );

dw_out__dz = par.C_c*sqrt(max(0,P2_t-par.P0));
%%
w_L_out = (m_L2/(m_L2+m_G2))*w_out;

dw_L_out__dm_G1 = 0;
dw_L_out__dm_G2 = (m_L2/(m_L2+m_G2))*dw_out__dm_G2 + ...
    ( (  - m_L2) / (m_L2+m_G2)^2) * w_out ;
dw_L_out__dm_L2 = (m_L2/(m_L2+m_G2))*dw_out__dm_L2 + ...
    ( ( (m_L2+m_G2)- m_L2) / (m_L2+m_G2)^2) * w_out ;

dw_L_out__dz = (m_L2/(m_L2+m_G2))*dw_out__dz;
%%
w_G_out = (m_G2/(m_L2+m_G2))*w_out;

dw_G_out__dm_G1 = 0;
dw_G_out__dm_G2 = (m_G2/(m_L2+m_G2))*dw_out__dm_G2 + ...
    ( ( (m_L2+m_G2) - m_G2) / (m_L2+m_G2)^2) * w_out ;
dw_G_out__dm_L2 = (m_G2/(m_L2+m_G2))*dw_out__dm_L2 + ...
    ( ( - m_G2) / (m_L2+m_G2)^2) * w_out ;
```

```
dw_G_out__dz = (m_G2/(m_L2+m_G2))*dw_out__dz;

%%
dx1 = (1 - par.ep)*w_G_in - w_G1;
dx2 = par.ep*w_G_in + w_G1 - w_G_out;
dx3 = w_L_in - w_L_out;


%% A,B,C and D:

%A:
dx1__dm_G1 = -dw_G1__dm_G1;
dx1__dm_G2 = -dw_G1__dm_G2;
dx1__dm_L2 = -dw_G1__dm_L2;

dx2__dm_G1 = dw_G1__dm_G1 -dw_G_out__dm_G1;
dx2__dm_G2 = dw_G1__dm_G2 -dw_G_out__dm_G2;
dx2__dm_L2 = dw_G1__dm_L2 -dw_G_out__dm_L2;

dx3__dm_G1 = -dw_L_out__dm_G1;
dx3__dm_G2 = -dw_L_out__dm_G2;
dx3__dm_L2 = -dw_L_out__dm_L2;


%B:
dx1__dz = 0;
dx1__dw_G_in = (1 - par.ep);
dx1__dw_L_in = 0;

dx2__dz = -dw_G_out__dz;
dx2__dw_G_in= par.ep;
dx2__dw_L_in = 0;

dx3__dz = -dw_L_out__dz;
dx3__dw_G_in= 0;
dx3__dw_L_in = 1;

%%
A = [dx1__dm_G1, dx1__dm_G2, dx1__dm_L2 ;
     dx2__dm_G1, dx2__dm_G2, dx2__dm_L2 ;
     dx3__dm_G1, dx3__dm_G2, dx3__dm_L2 ] ;

B = [dx1__dz, dx1__dw_G_in, dx1__dw_L_in ;
     dx2__dz, dx2__dw_G_in, dx2__dw_L_in ;
     dx3__dz, dx3__dw_G_in, dx3__dw_L_in ];

C = 1e-5 .* [dP1__dm_G1, 0,              0 ;
             0,          dP2_t__dm_G2,  dP2_t__dm_L2 ];
```

```
C(3,:) = [dw_out__dm_G1, dw_out__dm_G2, dw_out__dm_L2];

D = zeros(3,3);
D(3,1) = dw_out__dz;
```

Appendix F

Linerized model-Matlab (numerical)

This appendix shows the Matlab code for the linearized models.

F.1   NewModel

```
%%%%%%%%%%%%%%%%%%%%%%%%%%%%%%%%%%%%%%%%%%%%%%%%%%%%%%%%%%%%%%%%%%%%%%%%%%%%%%%
% Function that calculates the jackobians numerically with non constant
% Alpha_L1_av for the new model. Output of the function is the numerical
% linearized state space representation.
%
% A simple first order forward difference is used to approximate the
% derivative. The stepsize are given below.
%
%%%%%%%%%%%%%%%%%%%%%%%%%%%%%%%%%%%%%%%%%%%%%%%%%%%%%%%%%%%%%%%%%%%%%%%%%%%%%%%
%
% Written by:   Knut Åge Meland
% Date:         27.10.2010
%
%%%%%%%%%%%%%%%%%%%%%%%%%%%%%%%%%%%%%%%%%%%%%%%%%%%%%%%%%%%%%%%%%%%%%%%%%%%%%%%


function [A, B, C, D] = nummod(x0,y0,u0,par)

dx_value = 1e-7;
du_value = 1e-7;

A = zeros(4,4);
B = zeros(4,3);
C = zeros(3,4);
D = zeros(3,3);

dx= zeros(4,1);
for i =1:4
    dx(i)=dx_value;
    x = x0 + dx;
```

```
    xdot0=v4_new_4d_model(0,x0,u0,'derivatives',par);
    xdot=v4_new_4d_model(0,x,u0,'derivatives',par);

    y0 = v4_new_4d_model(0,x0,u0,'measurements',par);
    y = v4_new_4d_model(0,x,u0,'measurements',par);

    A(:,i) = (xdot-xdot0)/dx(i);
    C(:,i) = (y-y0)/dx(i);
    dx(i)=0;
end

du=zeros(3,1);
for i =1:3
    du(i)=du_value;
    u = u0 + du;

    xdot0=v4_new_4d_model(0,x0,u0,'derivatives',par);
    xdot=v4_new_4d_model(0,x0,u,'derivatives',par);

    y = v4_new_4d_model(0,x0,u,'measurements',par);

    B(:,i) = (xdot-xdot0)/du(i);
    D(:,i) = (y-y0)/du(i);
    du(i)=0;
end
end
```

F.2   DiMeglio

```
%%%%%%%%%%%%%%%%%%%%%%%%%%%%%%%%%%%%%%%%%%%%%%%%%%%%%%%%%%%%%%%%%%%%%%%%%%
% Function that calculates the jackobians numerically with non constant
% Alpha_L1_av for the new model. Output of the function is the numerical
% linearized state space representation.
%
% A simple first order forward difference is used to approximate the
% derivative. The stepsize are given below.
%
%%%%%%%%%%%%%%%%%%%%%%%%%%%%%%%%%%%%%%%%%%%%%%%%%%%%%%%%%%%%%%%%%%%%%%%%%%
%
% Written by:  Knut Åge Meland
% Date:         6.11.2010
%
%%%%%%%%%%%%%%%%%%%%%%%%%%%%%%%%%%%%%%%%%%%%%%%%%%%%%%%%%%%%%%%%%%%%%%%%%%




function [A, B, C, D] = nummod_DiMeglio(x0,y0,u0,par)
```

```matlab
dx_value = 1e-4;
du_value = 1e-4;

A = zeros(3,3);
B = zeros(3,3);
C = zeros(3,3);
D = zeros(3,3);

dx= zeros(3,1);
for i =1:3
    dx(i)=dx_value;
    x = x0 + dx;
    xdot0=v2_DiMeglio_model(0,x0,u0,'derivatives',par);
    xdot=v2_DiMeglio_model(0,x,u0,'derivatives',par);

    y0 = v2_DiMeglio_model(0,x0,u0,'measurements',par);
    y = v2_DiMeglio_model(0,x,u0,'measurements',par);

    A(:,i) = (xdot-xdot0)/dx(i);
    C(:,i) = (y-y0)/dx(i);
    dx(i)=0;
end

du=zeros(3,1);
for i =1:3
    du(i)=du_value;
    u = u0 + du;

    xdot0=v2_DiMeglio_model(0,x0,u0,'derivatives',par);
    xdot=v2_DiMeglio_model(0,x0,u,'derivatives',par);

    y = v2_DiMeglio_model(0,x0,u,'measurements',par);

    B(:,i) = (xdot-xdot0)/du(i);
    D(:,i) = (y-y0)/du(i);
    du(i)=0;
end
end
```

Appendix G

Simulink model
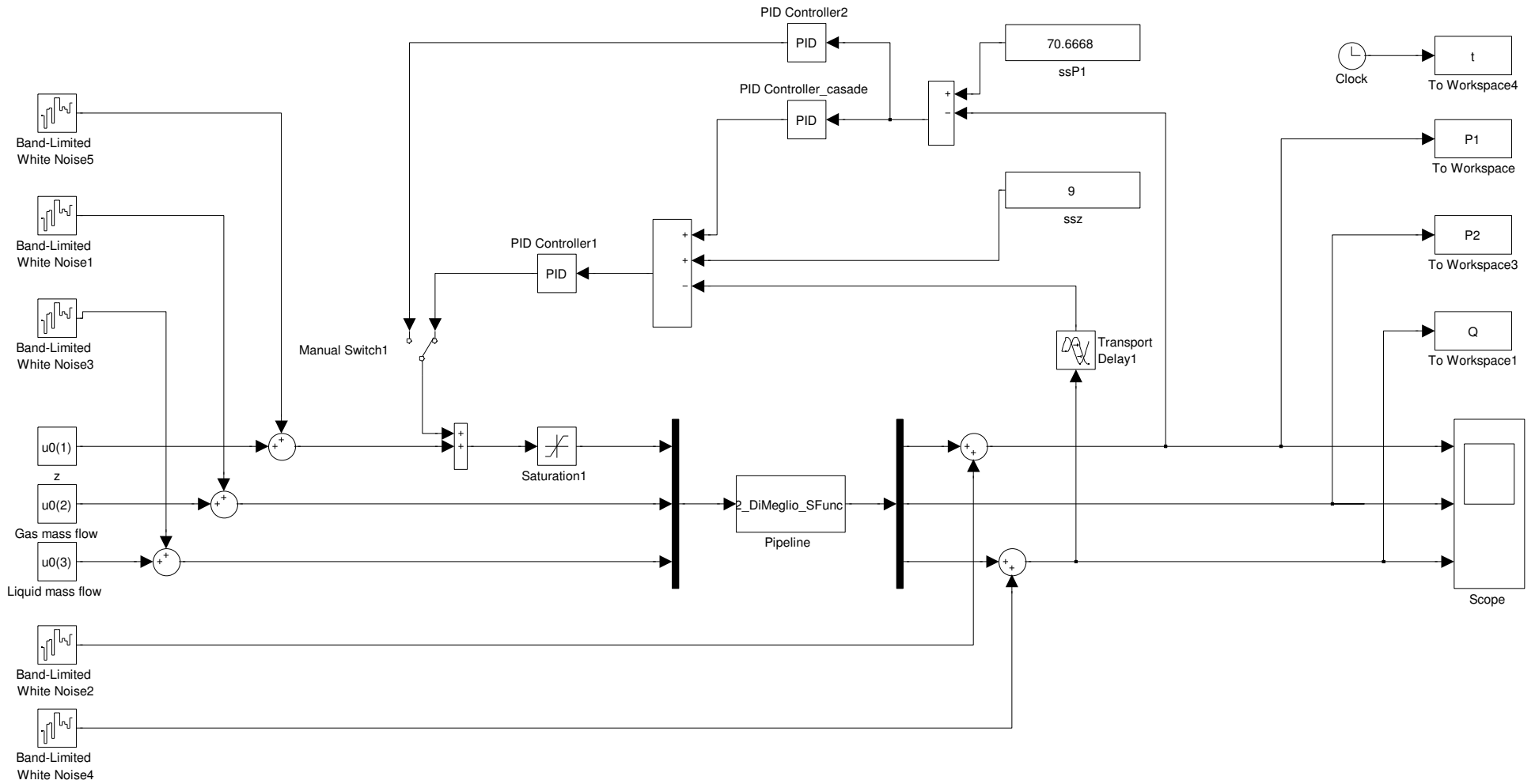
Appendix H

Price of ordered equipment

Riser slugging - mini loop

Siemens project 34056204

Item	Qty	Equipment	Type	Specification I DN/Out Signal/ Range	Specification II Working medium/ Temperature/ Pressure	Status	Check	Net Price	Gross price	Person in charge
1	1 Water flowmeter		Gemü 3021	25mm/4-20mA/ / 0-20L/min	Water/-10--+60°C/(0-10)Bar	received	OK	4900	6125	Claudia
2	1 Air flowmeter		Mass-stream	/ /0-5 V/ 0 to 10 sL/min	Air/10 -50°C/Max Pressure 150psi	received	OK	16601	20751,25	Claudia
3	3 Pressure sensor			/ /0.2-4.5 V/ 0 - 100 kPa		received	OK	2880	3600	Claudia
4	1 Pump		Grundfos Solarpumpe UPS 25-120-180	Max 10bar pressure	Water/-10--+60°C/(0-10)Bar	received	OK	5716	7145	Weiwei
5	1 Compressor		Fini New Airattack 202			received	OK	2850	3562,5	Weiwei
6	1 Control valve		Gemü angle valve			received	OK	2730	3412,5	Claudia
7	1 Amplifier		E3X-DA51-S 2M			received	OK	892,5	1116,63	Weiwei
8	1 Slug sensor		E32-TC200 2M	32 mm ID/1-5 V		received	OK	208	260	Weiwei
9	1 Manual valve - liquid line			DN20/Globe valve	Water	received	OK	164,5	205,63	Claudia
10	1 Manual valve - air line			DN8/Ball valve	Air	received	3/8"	33	41,25	Claudia
11	1 Manual valve - buffer tank drain			DN20/Ball valve	Air	received	OK	60,5	75,63	Claudia
12	1 Manual valve - air line			DN8/Needle valve	Air	received	1/4"	310,1	387,63	Claudia
13	1 Safety valve - buffer tank			DN20	Air	received	OK	1673	2092	Claudia
14	1 Water tank		Mechanic workshop (NTNU)	Plastic		received	OK			Weiwei
15	1 Separator		Mechanic workshop (NTNU)	Plastic		received	OK			Weiwei
16	1 Buffer tank		Mechanic workshop (NTNU)	Plastic		received	OK			Weiwei

					Status	Check			Responsible
17	20m	Flexible tubes		20 mm ID	received	OK	7000	5600,00	Weiwei
18	1	9203 8xAI mA	National Instruments		Not ordered		3419.10		Claudia
19	1	9265 4xAO mA	National Instruments		Not ordered		2474.10		Claudia
20	1	cRIO-9074 8-slot chassis	National Instruments	FP-TB-2	Not ordered		6389.70		Claudia
21	1	Positioner for control valve		DC/DC Select	received	Not correct unit	2380	2975	Claudia
22		Adapters			received	OK			Weiwei
23		Clamps			Received	OK			Weiwei
24		Frames, Boxes	workshop		Received	OK			Weiwei
25	1	Pressure regulator	Rexroth		Recieved	ok	1083.72		Knut Åge
26	2	Adapters for liquid flow meter	Mechanic workshop	Plastic	Recieved	ok			Knut Åge
27	2	Adapters for air flow meter	workshop		Reviewed	ok			Knut Åge
28		Adapters and valves			Recieced	ok			Knut Åge
29		Modules	National Instruments		Ordered				Geir
30		Box for modules			Ordered				Geir
31	1	Valve positioner	JS Cook		Waiting for offer				Knut Åge

Appendix I

Datasheet M+W Instruments air flow meter

MASS-STREAM®

Digital Mass Flow Meters and Controllers for Gases

M+W Instruments

A company of the Bronkhorst group.

M+W Instruments . Your specialists for inline measurement

WORTH KNOWING

M+W Instruments was founded in 1988 and has always specialised in thermal mass flow meters and controllers for gases. Based on our long-lasting experience with the previous and well-established model series D-62xx our new series D-63xx works on the basis of direct through-flow measurement following the constant temperature anemometer principle.

Having benefitted from continuous performance enhancements this through-flow technique can now be applied to lower flow ranges previously only covered by our by-pass technique (series D-51xx).

Our instruments are suitable for use in the chemical and pharmaceutical industries, in mechanical engineering and semi-industrial applications, as well as in gas production, food and beverage industries. We are committed to a long lasting cooperation with our customers and of course we are also your competent contact for special solutions.

You benefit from our well-trained, highly motivated team and our culture of quality. Our standardised product range guarantees short delivery times.

Having joined the Bronkhorst group in 1997 we nowadays cooperate with more than 30 distributors worldwide. Please visit our website www.mw-instruments.com for the contact data of your local distributor.

PRINCIPLE OF THROUGH-FLOW MEASUREMENT

The mass flow meters and controllers consist of a metal body with a straight throughflow path. Two sensors are encased with stainless steel and protrude inside this bore; one is designed as a heater and the other one is designed as a temperature probe. A constant difference in temperature (ΔT) is created between the two sensors. The heater energy required to maintain this ΔT is dependent on the mass flow. The working principle is based on King's law of the ratio between the mass flow and the heater energy. That means the higher the flow, the more energy is required to maintain the chosen ΔT.

MASS-STREAM® . Features and applications
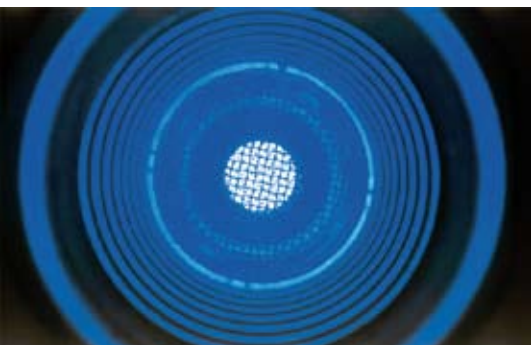
WORTH KNOWING

For the thermal mass flow measurement of gases the new MASS-STREAM® D-63xx series now offers the proven direct inline measurement for an increased measuring range:

Smallest standard range
0.01...0.2 ln/min (Air)
Highest standard range
100...5,000 ln/min (Air)

Within the above mentioned borders intermediate calibrations with a turn-down-ratio up to 1:100 are also possible.

In addition the Bronkhorst group supplies instruments with smaller and higher flow ranges.

FEATURES

- » Direct inline measurement principle
- » Usable for virtually every kind of gas or gas-mix
- » Mass flow measurement and control for a wide scope of applications
- » Digital pc-board with additional interfaces for Flow-Bus, DeviceNet, Profibus-DP, ModBus-RTU
- » Precise control mode and good response times
- » Compact and robust design
- » IP65 for full product range
- » Bodies available in aluminium and stainless steel (AISI 316) for corrosive gases
- » Sensor made of stainless steel
- » Low sensitivity to dirt
- » Low sensitivity to humidity
- » No inlet pipe required
- » Measurement without moving parts
- » Maintenance-free
- » Modern multi-coloured TFT display
  - « IP65 compliant
  - « operator buttons on the instrument
  - « customised adjustable multi-functional display: actual flow, totaliser with memory and reset, alarm, setup and much more

APPLICATIONS

- » Measurement and control technology
- » Analytical instruments
- » Biogas applications
- » Burner controls
- » Coating plants
- » Exhaust gas measurement
- » Gas consumption measurement
- » Gas monitoring systems
- » Mechanical engineering
- » N_2/O_2-generators
- » Paint-spray lines
- » and much more

Mass flow meter (MFM) . D-63x0

Mass flow controller (MFC) . D-63x1, D-63x3

PRINCIPLE OF OPERATION

The digital MASS-STREAM® mass flow meters and controllers are operated with a main-board with all functions for the flow measurement and control. The instruments can be supplied with commonly used digital or analogue input/output signals and when ordering a digital instrument please forward the required presettings. Along with the standard RS232 interface the additional interfaces Profibus-DP, DeviceNet, Flow-Bus and ModBus-RTU are also available.

The digital MASS-STREAM® model series is characterised by a high degree of signal integrity and, as an option, up to 8 calibration curves of different gases can be memorised in the instrument.

To provide adaptability and flexibility for a wide range of different process conditions our customers are offered the possibility to adjust,

to optimise and to evaluate the parameters and control characteristics, even whilst on site. The referring software is a basic part of our scope of supply of digital mass flow meters and controllers, as well as the calibration certificate, the 8-pin DIN connector for the electrical connection and the software and documentation on CD.

The MASS-STREAM® mass flow controllers are delivered as compact control units up to flows of 1,000 ln/min Air-equivalent, with the modular constructed solenoid valve integrated onto the body. The following kv-values are available as a standard: 0.066; 0.17; 1.0.

In addition the control of higher gas flows is possible by using separate valves with the following kv-values: 2.8; 3.4; 4.4. (Further special valves and combinations on request.)

DIMENSIONS M+W D-63xx SERIES (in mm)

Model	A	B	C	D	E	F	G	H	I
D-6310	95	G1/8″	G1/8″	34	15	117			
D-6320	95	G1/8″	G1/8″	34	15	117			
D-6340	95	G1/4″	G1/4″	34	15	114			
D-6360	95	G1/2″	G1/2″	34	16	122			
D-6370	117	G1/2″	G1/2″	58	25	136	95		
D-6380	143	G1″	G1″	83	37,5	164	95		
D-6311	95	G1/8″	G1/8″	34	15	117			
D-6321	95	G1/8″	G1/8″	34	15	117			
D-6341	95	G1/4″	G1/4″	34	15	114			
D-6361	110	G1/2″	G1/2″	34	16	122	95		
D-6371	185	G1/2″	G1/2″	65	25	136	95	36	186

Model	D-6310	D-6320	D-6340	D-6360
	D-6311	D-6321	D-6341	D-6361

Model	D-6370	D-6380

Model	D-6371
	D-6383 dimensions on request
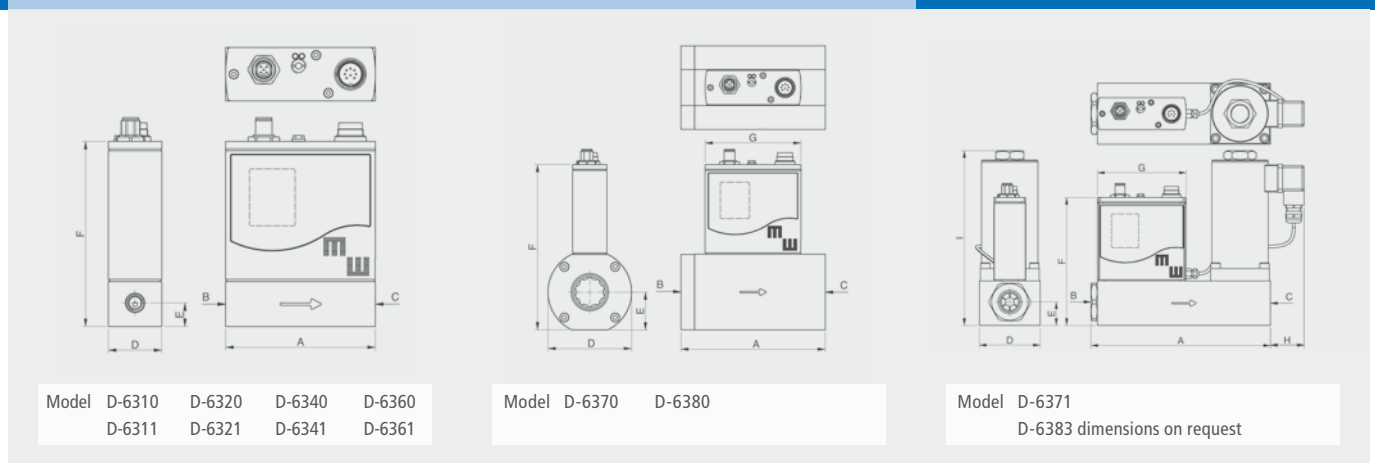
STANDARD MEASUREMENT RANGES

Mass flow meter Model	Flow ranges (Air) intermediate ranges are available
D - 6310 - H♦♦ - AA - ♦♦ - 22 - ♦ - S - D♦	0.01...0.2 ln/min
- 23 -	0.02...2.0 ln/min
D - 6320 - H♦♦ - AA - ♦♦ - 13 - ♦ - S - D♦	0.02...1.0 ln/min
- 53 -	0.05...5.0 ln/min
D - 6340 - H♦♦ - BB - ♦♦ - 53 - ♦ - S - D♦	0.1...5.0 ln/min
- 54 -	0.5...50.0 ln/min
D - 6360 - H♦♦ - CC - ♦♦ - 24 - ♦ - S - D♦	0.4...20.0 ln/min
- 25 -	2.0...200 ln/min
D - 6370 - H♦♦ - CC - ♦♦ - 15 - ♦ - S - D♦	2.0...100 ln/min
- 16 -	10.0...1,000 ln/min
D - 6380 - H♦♦ - DD - ♦♦ - 55 - ♦ - S - D♦	10.0...500 ln/min
- 56 -	50.0...5,000 ln/min

Mass flow controller Model	Flow ranges (Air) intermediate ranges are available
D - 6311 - F♦♦ - AA - ♦♦ - 22 - ♦ - S - D ♦	0.01...0.2 ln/min
- 23 -	0.04...2.0 ln/min
D - 6321 - F♦♦ - AA - ♦♦ - 13 - ♦ - S - D ♦	0.02...1.0 ln/min
- 53 -	0.1...5.0 ln/min
D - 6341 - F♦♦ - BB - ♦♦ - 53 - ♦ - S - D ♦	0.1...5.0 ln/min
- 54 -	1.0...50.0 ln/min
D - 6361 - F♦♦ - CC - ♦♦ - 24 - ♦ - S - D ♦	0.4...20.0 ln/min
- 25 -	4.0...200 ln/min
D - 6371 - F♦♦ - CC - ♦♦ - 15 - ♦ - S - D ♦	2.0...100 ln/min
- 16 -	20.0...1,000 ln/min
D - 6383 - Z♦♦ - DD - ♦♦ - 55 - ♦ - S - D ♦	10.0...500 ln/min
- 56 -	100...5,000 ln/min

Technical changes and alterations in construction are reserved.

MASS-STREAM® . Worth knowing

CONVERSION FACTOR

MASS-STREAM® mass flow meters and controllers are basically calibrated on air. If other gases or gas mixtures are used a conversion factor CF has to be applied. This factor is determined by applying a complex formula. For a number of commonly used gases you will find the value in the adjoining chart.

CONVERSION FACTORS (ln ≙ 1013 mbar and 0 °C air temperature)
– please refer to www.fluidat.com

Gas	CF D-631x and D-632x	CF D-634x up to D-638x	Gas	CF D-631x and D-632x	CF D-634x up to D-638x
Air	1.00	1.00	CO_2	0.86	1.20
Ar	1.50	2.01	HCL	1.12	1.58
CH_4	0.77	0.67	N_2	1.00	1.00
C_2H_2	0.66	0.75	NH_3	0.82	0.80
C_2H_4	0.70	0.89	NO	1.00	1.02
C_2H_6	0.58	0.89	N_2O	0.83	1.15
C_3H_8	0.43	0.63	O_2	0.99	0.98
C_4H_{10}	0.32	0.42	Xe	1.96	6.08
CO	1.01	1.04			Other gases on request.

Above mentioned values are only regarded as an indication. The exact conversion factors are significantly dependent on the process parameters, like media temperature and operating pressure, and on the physical characteristics of the gas. The best accuracy can be obtained by calibrating the instrument under operating conditions. The conversion factor causes an additional error in the absolute accuracy. With a conversion factor ≥1 this error is 2 x CF (in % FS) and with a conversion factor ≤1 this error is 2 / CF (in % FS).

FLOW PROFILE AND SENSITIVITY

In general mass flow measurement is very sensitive to variations of the shape of the flow profile. The MASS-STREAM® instruments are designed for a consistent, fully developed flow profile in the metering section and they are thus less sensitive to changes of the inlet piping conditions. In comparable instruments, which do not consist of such precautions for these effects of inlet piping conditions, some severe variations in the accuracy might occur.

PRESSURE LOSS

The pressure drop over the instrument's D-63xx measurement chamber is almost comparable to a straight run of pipe of the same diameter and is thus almost negligible. However, to make the instruments more insensitive to upstream piping configurations, special mesh screens are required to condition the flow profile. These meshes create a certain pressure drop.

Also the often used compression type connections cause a significant additional pressure loss.

By reducing the number of mesh screens and using an inlet pipe the pressure loss can be minimised as an option. In addition we recommend the use of fittings with maximised internal diameter.

Model number identification . MASS-STREAM®

D N N N N ◆ ◆ ◆ ◆ ◆ ◆ ◆ N N ◆ S D ◆

Base model	Function	Design	Input/Output signal	Supply voltage	Gas connection inlet/outlet	Material	Seals	Flow rate for air	Display	Standard sensor	Communication
D-631 up to 2 ln/min	0 = Meter	F = Controller N/C (Valve normally closed)	A = 0-5 Vdc	A = 15 Vdc	**Internal thread**	A = Aluminium AL50ST/51ST	E = EPDM	12 = 0.1 ln/min	0 = without display		DR = RS232
D-632 up to 5 ln/min	1 = Controller with integrated valve	H = Meter	B = 0-10 Vdc	B = 24 Vdc	AA= G1/8" (= 1/8" BSPP)	S = Stainless steel SS316	K = Kalrez®	22 = 0.2 ln/min	D = with display		DF = Flow-Bus
D-634 up to 50 ln/min		Z = indivual	F = 0-20 mA	D = 15-24 Vdc	BB= G1/4" (= 1/4" BSPP)		V = Viton	52 = 0.5 ln/min			DP = Profibus-DP
D-636 up to 200 ln/min			G = 4-20 mA		CC = G1/2" (= 1/2" BSPP)		Z = individual	13 = 1 ln/min			DN = DeviceNet
D-637 up to 1,000 ln/min	3 = Controller with external valve				DD= G1" (= 1" BSPP)			23 = 2 ln/min			DM= Modbus-RTU
D-638 up to 5,000 ln/min								53 = 5 ln/min			
					Fittings			14 = 10 ln/min			
					11 = 1/8" compression			24 = 20 ln/min			
					22 = 1/4" compression			54 = 50 ln/min			
					33 = 6 mm compression			15 = 100 ln/min			
					44 = 12 mm compression			25 = 200 ln/min			
					55 = 1/2" compression			45 = 400 ln/min			
					66 = 20 mm compression			55 = 500 ln/min			
					88 = 1/4" VCR			16 = 1,000 ln/min			
					99 = individual			26 = 2,000 ln/min			
								36 = 3,000 ln/min			
								46 = 4,000 ln/min			
								56 = 5,000 ln/min			
								99 = other gases/ other flow rates			

ENQUIRY AND ORDER INFORMATION

In order to supply the correct instrument for your application please forward the following data: type of gas, flow range, operating temperature and pressure (for controllers supply and back pressure), electrical connection, desired output signal, type of gas connections (fittings) and seals, analogue or digital presettings.

Based on this information the following calculations and checks will be carried out:
» Conversion of the requested flow to the Air-equivalent flow (the requested flow is divided by the referred conversion factor).

» For mass flow controllers only:
- Check if the differential pressure over the valve (ΔP) is within the allowed limits.
- Check if the calculated kv-value is within the specification.

TECHNICAL SPECIFICATIONS

Measurement system

Accuracy (based on calibration with Air at 5 bar (a) and T = 20 °C)	± 2 % FS including non-linearity* ± 1.5 % FS on request*
Repeatability	< ± 0.2 % FS
Pressure sensitivity	± 0.3 % / bar typical (Air)
Temperature sensitivity	± 0.2 % RD / °C (Air)
Attitude sensitivity	at 90° deviation from horizontal max. error 0,2 % at 1 bar typical N$_2$
Control stability	< 0,2 % FS typical
Leak integrity	< 2 x 10-8 mbar l/s He
Response time sensor (63 %)	τ = 2 seconds
Settling time (controller)	approx. 2 seconds
RFI (radio frequency interference)	according to CE

* The calibration of instruments in the lower measurement range and for some gases could result in a reduced accuracy.

Mechanical parts

Sensor	Stainless steel SS 316 (AISI 316L)
Instrument body	Aluminium AL50ST/51ST (anodised) or stainless steel SS 316
Sieves and rings	Stainless steel SS316
Protection (with and without display)	IP65

Operating limits

Measuring range (turn-down-ratio)	up to 1...100 % (1:100) for meters up to 1...50 % (1:50) for controllers
Type of gases	almost all gases, compatible with chosen materials
Temperature	0…50 °C
Pressure rating	0...10 bar (g), D-6361: 0...7 bar (a), higher on request
Warm-up time	30 minutes for optimum accuracy within 30 seconds for accuracy ± 4 % FS

Electrical properties

Supply voltage	+ 15…24 Vdc ± 10 % active	
Current peak values	Meter	approx. 75 mA at 0 % flow approx. 125 mA at 100 % flow
	Controller	add 250 mA
		add 30 mA for display, if applicable
		add 50 mA for field bus, if applicable
Output signal	0...10 Vdc / 0...5 Vdc active or 0…20 mA / 4…20 mA active	
Connector	8-pol round DIN (male) for analogue and RS232 additional conncetors for interfaces:	
	» 5-pol M12 (male) for Flow-Bus DeviceNet Modbus-RTU	
	» 5-pol M12 (female) for Profibus-DP	

Technical changes and alterations in construction are reserved.

DISTRIBUTOR:

The complete list of all distributors of M+W Instruments GmbH can be found on our website www.mw-instruments.com

M+W Instruments

Appendix J

Datasheet Gemü liquid flow transmitter

Construction

The GEMÜ 3021 intelligent flow transmitter can be used for measuring liquid inert and corrosive* aqueous media. The keypad at the front of the unit enables simple setting of measurement units, required display values etc.

Features

- High-resolution turbine flow measurement
- Medium wetted parts in plastic, sapphire and ceramics
- Totalizer type (flow counter)
    - Frequency/Current output signals
    - Reset input for resetting the accumulated flow rate
- Batch controller type (dosing function)
    - 2x relay outputs
    - 1x binary output for batch end
    - 2x binary inputs for selecting batches
    - 1x binary input as start signal
- Extremely low pressure loss

Advantages

- Easy operation via keypad
- Process adaptable
- Short inlet and outlet distances
- Freely scalable measurement range
- Integrated flow rectifier

*see information on working medium on page 2

| Dimensional drawing - GEMÜ 3021   [mm] |
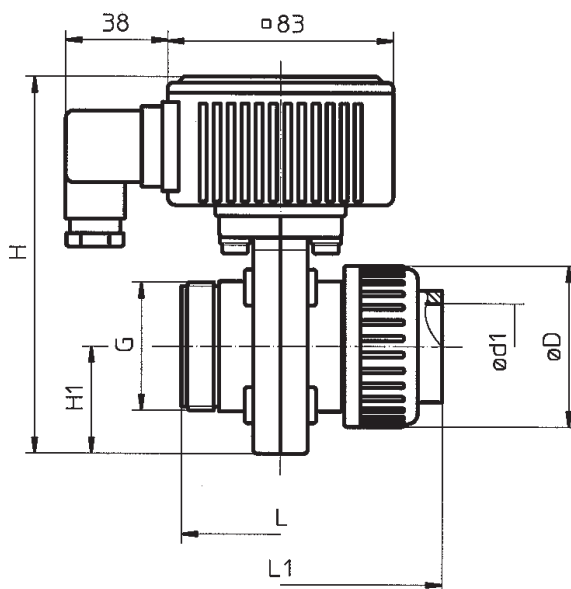
DN	L	L1	H1	ød1	øD	G	H
25	73	123	40	32	60	G 1 1/2	140
50	105	187	63	63	103	G 2 3/4	189

GEMÜ® 3021

Technical data

Working medium

Liquid inert or corrosive aqueous media which have no negative impact on the physical and chemical properties of the body and seal material.

General information

Protection class to EN 60529:	IP 65
Weight:	DN 25: 600 g
	DN 50: 1500 g
Dimensions LxWxH:	see dimensional drawing
Mounting position:	optional
Mounting note:	Inlet/outlet distances 5 x DN
Directives:	CE
EMC	89/336/EEC

Electrical data

Power supply U_V: 18-30 V DC
Power consumption [W]: typ. 1 W
Current consumption [A]: typ. 40 mA
(for current output = 0 mA)

Input signals:
SetBatchNo 1-4, SetBatchQty (Batch Controller)
Total Count reset (Totalizer)
  High-Signal: 14 V DC - 30 V DC
  Low-Signal: 0 V DC - 8 V DC
  Impulse time: ≥ 100 ms
SetQtyFactrTime (Batch Controller)
  High-Signal: 14 V DC - 30 V DC
  Low-Signal: 0 V DC - 8 V DC
  Resolution: 4 ms

Output signals:
Pulse output PNP, $(U_V\text{-}U_{Drop})$
  typ. U_{Drop} 1.7 V at 24 V/ 5 mA
    2.5 V at 24 V / 10 mA
    5.0 V at 24 V / 20 mA
Batch end PNP, $(U_V\text{-}U_{Drop})$
  typ. U_{Drop} 2 V at 24 V DC / 0.7 A

Pulse rate ≤ K-Factor / 2
K-factor adjustable, see enclosed test certificate
Current 0/4 - 20 mA
  Resolution ≤ 23 µA (10 bit)
  Accuracy ±1.5 bit
  Load resistor ≤ 500 Ohm
  Load dependence 0.25%

Relay
Switching voltage / contact ≤ 36 V DC / 30 V AC
Switching current / contact ≤ 1 A
Switch rating / contact ≤ 15 W

Electrical connection:
Plug, type A, DIN EN 175301-803 (Totalizer)
M12x1 5 pin plug (Batch controller)
    Voltage: ≤ 36 V DC/30 V AC
    Current: ≤ 2 A DC
    Rating: ≤ 60 W
Recomm. connection cable; ø: 8-10 mm

Electrical data

Measurement data

Measuring range (adjustable)	DN 25 120 L/h - 7200 L/h
	(factory setting 3600 L/h)
	DN 50 500 L/h - 25000 L/h
	(factory setting 25000 L/h)
Pulse rate (adjustable)	DN 25 max. 256 pulses/L
	(factory setting 1 pulse/L)
	DN 50 max. 25 pulses/L
	(factory setting 1 pulse/L)
Start-up	DN 25 ≤ 80 L/h
	DN 50 ≤ 500 L/h
Pressure loss	DN 25 0.1 bar for 3600 L/h
	DN 50 0.2 bar for 25000 L/h
Accuracy:	±1% FS (FS = full scale)
Repeatability:	±0.5% FS
Optical display:	LC-Display 2 x 16 characters digit height 5.55 mm

Operating conditions

Storage temperature:	-10° to +60°C
Operating temperature:	-20° to +60°C
Medium temperature with body material:	
PVC-U (Code 1)	+10° to +60°C
PVDF (Code 20)	-20° to +80°C
Type of medium	liquid ≤ 120 mm²/s (120cSt)

The permissible operating pressure depends on the working medium temperature, see table below.

Materials

Medium wetted parts	
Inner turbine components:	PVDF
Body:	PVC-U/PVDF
Bearing / shaft:	Sapphire/ Ceramics (Al203)
Seals:	FPM, EPDM
Flow transducer:	
Housing:	PP
Housing cover of measuring device, size B:	PMMA
Housing seal:	NBR
Housing bolt:	1.4303
Plug:	
Plug housing:	PA 6 (Totalizer)
Plug bolt:	PA 66 (Batch controller)
VQSt 36-2-4.8 Profile packing:	NBR
Further housing materials upon request	

Note

Measuring certificate with calibration data is included. Calibration with water 20° C.

To prevent blockage of the rotor due to particles contained in the medium, an upstream dirt filter (mesh width 100 µm) should be installed!

Pressure / temperature correlation for PN 10													
Temperature in °C		-20	-10	±0	5	10	20	25	30	40	50	60	70	80
Body material		permissible operating pressure in bar												
PVC-U, grey	Code 1	-	-	-	-	10.0	10.0	10.0	8.0	6.0	3.5	1.5	-	-
PVDF	Code 20	10.0	10.0	10.0	10.0	10.0	10.0	10.0	9.0	8.0	7.1	6.3	5.4	4.7

GEMÜ®

Q →

Q ↑

Q ←

Q ↓

Code A   **Code B**   **Code C**   **Code D**
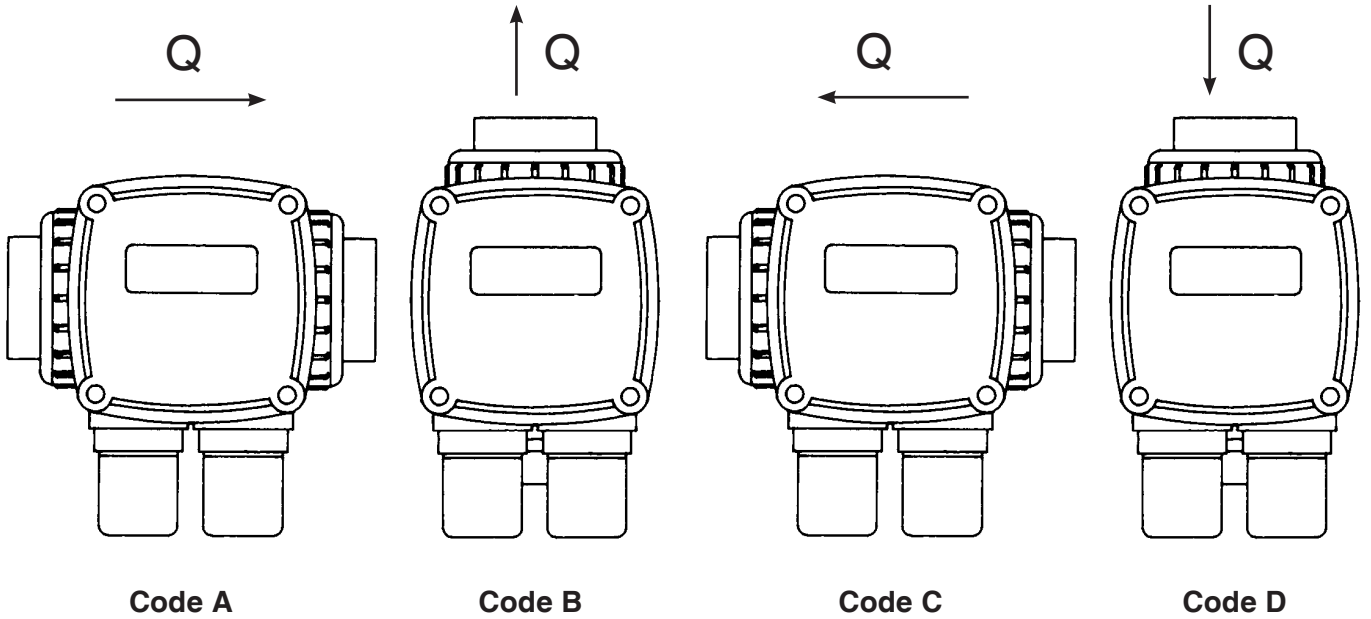
Connection diagram - Totalizer

X1   X2
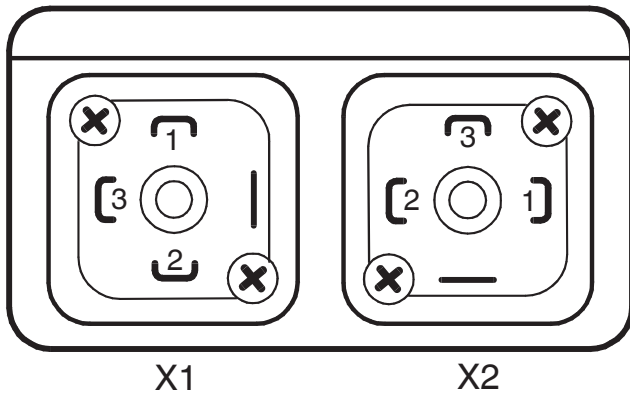
X1	Terminal	Designation
	1	U_v, GND supply voltage
	2	U_v, 24 V DC, supply voltage
	3	Input, 24 V DC, total count reset
	PE	n. c.

X2	Terminal	Designation
	1	I-/f-, GND, signal output
	2	I+, 0/4-20 mA, current output
	3	f+, frequency output
	PE	n. c.

Connection diagram - Batch controller

X1   X2
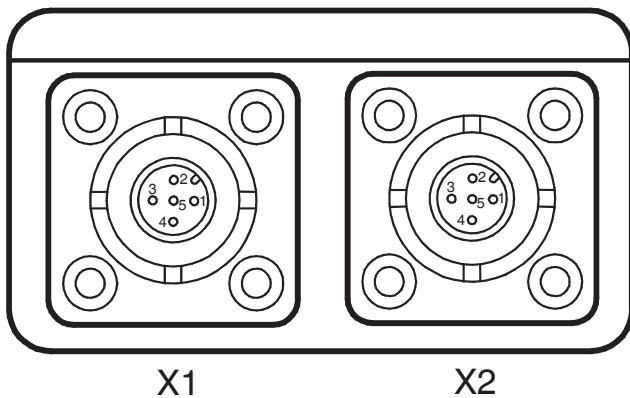
X1	Terminal	Designation
	1	U_v, GND supply voltage
	2	U_v, 24 V DC, supply voltage
	3	U_{input}, relay output
	4	Make contact Batch Qty1, relay output
	5	Make contact Batch Qty2, relay output

X2	Terminal	Designation
	1	GND
	2	Start input Batch/Time basis
	3	Binary code input LSB
	4	Binary code input MSB
	5	Output Batch end

GEMÜ®

3021

Order data

Nominal size	Code
DN 25	25
DN 50	50

Seal material	Code
FPM	4
EPDM	14

Body configuration	Code
2/2-way body	D

Position of display	Code
Display parallel, 0° to flow direction	A
Display vertical, 90° to flow direction	B
Display parallel, 180° to flow direction	C
Display vertical, 270° to flow direction	D
See diagrams on page 3	

Connection	Code
Union ends with DIN insert (socket)	7
Union ends with Inch insert (socket)	33*
Unions ends with DIN insert (IR butt welding)	78
* only body material PVC-U, grey (code 1)	

Function	Code
Totalizer, 0/4-20 mA and pulse output	T41
Batch controller, 2 relays, remote control inputs and time control	BBT

Material	Code
Body PVC-U, grey, inner parts PVDF	1
Body PVDF, inner parts PVDF	20

Voltage / frequency	Code
24 V DC	C1

Order example	3021	25	D	7	1	4	A	T41	C1
Type	3021								
Nominal size (code)		25							
Body configuration (code)			D						
Connection (code)				7					
Material (code)					1				
Seal material (code)						4			
Position of display(code)							A		
Function (code)								T41	
Voltage / frequency (code)									C1

For further products and accessories, please see our Product Range catalogue and Price list. Contact GEMÜ.

DIN EN ISO 9001
Zertifikat: 09 100 4136

GEMÜ® VALVES, MEASUREMENT AND CONTROL SYSTEMS

Appendix K

Datasheet pressure transmitter

SIEMENS

Pressure transmitter
SITRANS P, Z series (7MF1564)

Operating Instructions (Compact)

Product information

Safety notes

This device left the factory in a perfect state with regard to safety. To maintain this status and to ensure safe operation of the device, observe the following notes:

⚠ CAUTION

The device may only be used for the purposes specified in these instructions.

- Observe the test certification, provisions and laws applicable in your country during connection, assembly and operation.
- "Intrinsically-safe" devices lose their certification as soon as they are operated on circuits which do not correspond with the test certification valid in their country.
- The device can be operated both at high pressure and with aggressive and hazardous media. Therefore, improper use of this device may lead to serious injury and or considerable damage to property. Above all, it must be noted when the device was in use and is to be exchanged.
- For this reason, only qualified personnel may set up, install, commission, and operate the product.

Application SITRANS P, Z series (7MF1564)

The pressure transmitter is used for measuring the relative pressure and absolute pressure of gases and liquids in the following industrial areas:

- Mechanical engineering
- Power engineering
- Water supply
- Marine
- Chemicals
- Pharmaceuticals

Hardware configuration

The pressure transmitter consists of a piezoresistive measuring cell with a diaphragm, installed in a stainless steel housing. It can be electrically connected with a plug per EN 175301-803-A (IP65), a round plug M12 (IP67) or a cable (IP68). The output signal is either 4 to 20 mA (device version with or without explosion protection) or 0 to 10 V (device version only without explosion protection)

7MF1564 with plug per EN 175301-803-A
- Type 7MF1564-*****-1**1
- Type 7MF1564-*****-3**1
- Type 7MF1564-*****-4**1

7MF1564 with plug M12x1
- Type 7MF1564-*****-2**1

7MF1564 with cable (2 m)
- Type 7MF1564-*****-6**1

Installation

- The location of the device has no influence on the precision of the measurement.
- Before installation, compare the process data with the data of the rating plate.
- The following operating conditions apply to installation:

Ambient temperature	-20 °C ... +85 °C (-13 °F ... +185 °F)
Process temperature	-30 °C ... +120 °C (-22 °F ... +248 °F)
Storage temperature	-50 °C ... +100 °C (-58 °F ... +212 °F)

© Siemens Ⓟ2008
A5E02059155-01, 02/2008

- The medium being measured must be suitable for the parts of the pressure transmitter in contact with the medium.
- The burst pressure must not be exceeded.
- Attach the devices with fixed cable installation.

Electrical connection

For the device version with plug per EN 175301-803-A and plug M12 x 1 (mating connector as option), we recommend the screened 2- or 3-wire cable (4.5 to 7 mm outside diameter).

The cable is grounded at only one point, e.g. in the switching cabinet.

The grounding connection is conductively bonded to the transmitter housing.

Connecting with current output and plug per EN 175301

| Wiring | 1 (+) 2 (-) |
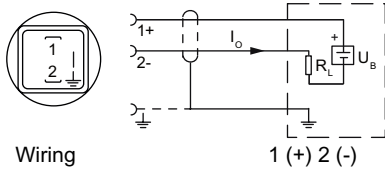
Connecting with current output and plug M12x1
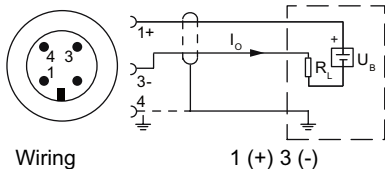
| Wiring | 1 (+) 3 (-) |

Connecting with current output and cable
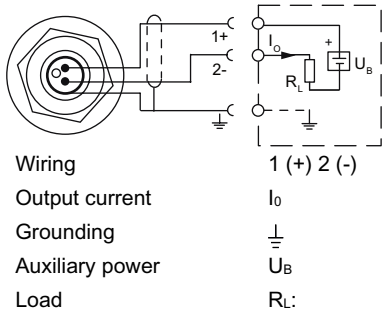
Wiring	1 (+) 2 (-)
Output current	I_0
Grounding	⏚
Auxiliary power	U_B
Load	R_L:

Connecting with voltage output and plug per EN 175301

| Wiring | 1 (+U_B) 2 (-) 3 (+U_0) |
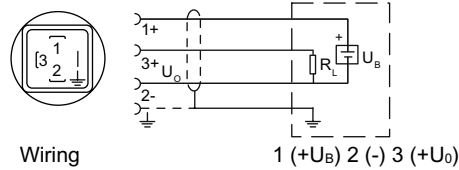
Connecting with voltage output and plug M12x1

| Wiring | 1 (+U_B) 3 (-) 2 (+U_0) |

Connecting with voltage output and cable

Wiring	1 (+U_B) 2 (-) 3 (+U_0)
Output voltage	U_0
Grounding	⏚
Auxiliary power	U_B
Load	R_L:
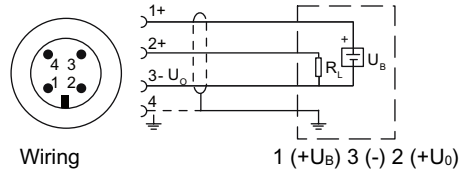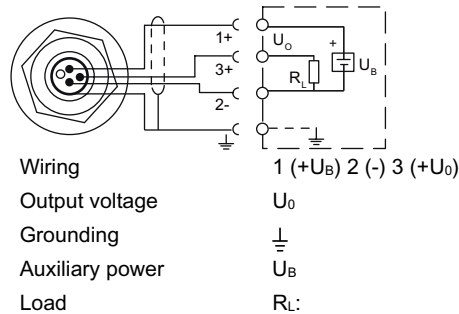
Correction of zero point and span

The transmitter is preset to the respective measuring range at the manufacturer's plant. Additional setting is only possible with the device version with the plug per EN 175301-803-A.

If additional setting is required, connect the transmitter to a suitable pressure source. Remove the upper part with the handle ring of the plug. The output current or output voltage for the lower range value (4 mA or DC 0 V) is set with the potentiometer "Z". The output current or output voltage for the upper range value (20 mA or DC 10 V) is set with the potentiometer "S".

Finally, turn the handle ring closed with $0.8 ^{\pm 0.2}$ Nm.

Maintenance

The transmitter is maintenance-free.

Check the lower range value of the device from time to time.

Technical specifications

Operating principle	
Measuring range < 1 bar	Piezoresistive with stainless steel diaphragm
Measuring range ≥ 1 bar	Piezoresistive with ceramic diaphragm

Input		
Input measured variable	Input relative and absolute pressure	
a) Measuring range for relative pressure	Perm. operating pressure	Burst pressure
0 ... 100 mbar g	-0,6 ... 0.6 bar g	1 bar g
0 ... 160 mbar g	-0,6 ... 0.6 bar g	1 bar g
0 ... 250 mbar g	-1 ... 1 bar g	1.7 bar g
0 ... 400 mbar g	-1 ... 1 bar g	1.7 bar g

Input		
0 ... 600 mbar g	-1 ... 3 bar g	5 bar g
0 ... 1 bar g	-0,4 ... 2 bar g	5 bar g
0 ... 1.6 bar g	-0,4 ... 3.2 bar g	5 bar g
0 ... 2.5 bar g	-0,8 ... 5 bar g	12 bar g
0 ... 4 bar g	-0,8 ... 8 bar g	12 bar g
0 ... 6 bar g	-1 ... 12 bar g	25 bar g
0 ... 10 bar g	-1 ... 20 bar g	50 bar g
0 ... 16 bar g	-1 ... 32 bar g	50 bar g
0 ... 25 bar g	-1 ... 50 bar g	120 bar g
0 ... 40 bar g	-1 ... 80 bar g	120 bar g
0 ... 60 bar g	-1 ... 120 bar g	250 bar g

Input		
• 0 ... 100 bar g	-1 ... 200 bar g	450 bar g
• 0 ... 160 bar g	-1 ... 320 bar g	450 bar g
• 0 ... 250 bar g	-1 ... 500 bar g	650 bar g
• 0 ... 400 bar g	-1 ... 600 bar g	650 bar g
b) Measuring ranges for relative pressure (only for US market)	Perm. operating pressure	Burst pressure
• 0 ... 10 psi g	-3 ... 20 psi g	60 psi g
• 0 ... 15 psi g	-5,8 ... 30 psi g	72 psi g
• 3 ... 15 psi g	-5,8 ... 30 psi g	72 psi g
• 0 ... 20 psi g	-5,8 ... 40 psi g	72 psi g
• 0 ... 30 psi g	-5,8 ... 60 psi g	72 psi g
• 0 ... 60 psi g	-11,5 ... 120 psi g	175 psi g
• 0 ... 100 psi g	-14,5 ... 200 psi g	360 psi g
• 0 ... 150 psi g	-14,5 ... 300 psi g	725 psi g
• 0 ... 200 psi g	-14,5 ... 400 psi g	725 psi g
• 0 ... 300 psi g	-14,5 ... 600 psi g	1750 psi g
• 0 ... 500 psi g	-14,5 ... 1000 psi g	1750 psi g
• 0 ... 750 psi g	-14,5 ... 1500 psi g	3600 psi g
• 0 ... 1000 psi g	-14,5 ... 2000 psi g	3600 psi g
• 0 ... 1500 psi g	-14,5 ... 3000 psi g	6525 psi g
• 0 ... 2000 psi g	-14,5 ... 4000 psi g	6525 psi g
• 0 ... 3000 psi g	-14,5 ... 6000 psi g	9425 psi g
• 0 ... 5000 psi g	-14,5 ... 8700 psi g	9425 psi g
• 0 ... 6000 psi g	-14,5 ... 8700 psi g	9425 psi g
c) Measuring ranges for absolute pressure (only for US market)	Perm. operating pressure	Burst pressure
• 0 ... 10 psi a	0 ... 20 psi a	60 psi a
• 0 ... 15 psi a	0 ... 30 psi a	72 psi a
• 0 ... 20 psi a	0 ... 40 psi a	72 psi a
• 0 ... 30 psi a	0 ... 60 psi a	72 psi a
• 0 ... 60 psi a	0 ... 120 psi a	175 psi a
• 0 ... 100 psi a	0 ... 200 psi a	360 psi a
• 0 ... 150 psi a	0 ... 300 psi a	725 psi a
• 0 ... 200 psi a	0 ... 400 psi a	725 psi a
• 0 ... 300 psi a	0 ... 600 psi a	1750 psi a
d) Measuring range for absolute pressure	Perm. operating pressure	Burst pressure
• 0 ... 600 mbar a	0 ... 3 bar a	5 bar a
• 0 ... 1 bar a	0 ... 2 bar a	5 bar a
• 0 ... 1.6 bar a	0 ... 3.2 bar a	5 bar a
• 0 ... 2.5 bar a	0 ... 5 bar a	12 bar a
• 0 ... 4 bar a	0 ... 8 bar a	12 bar a
• 0 ... 6 bar a	0 ... 12 bar a	25 bar a
• 0 ... 10 bar a	0 ... 20 bar a	50 bar a
• 0 ... 16 bar a	0 ... 32 bar a	50 bar a

Output	
Current signal	4 ... 20 mA
• Load	$(U_H - 10\ V)/0.02\ A$
• Auxiliary power U_H	DC 10 ... 36 V (10 … 30 V for Ex)

Output	
Voltage signal	DC 0 … 10 V
• Load	≥ 10 kΩ
• Auxiliary power U_H	DC 15 ... 36 V
• Power consumption	< 7 mA at 10 kΩ
Characteristic	Linear rising

Measuring accuracy		
Error in measurement at 25 °C (77 °F), including conformity error, hysteresis and repeatability	• Typical: 0.25 % of full scale value • Maximum: 0,5 % of full scale value	
Setting time T_{99}	< 0.1 s	
Long-term drift		
• Lower range value and measuring span	0.25 % of full scale value/year	
Ambient temperature influence		
• Lower range value and measuring span	• 0.25 %/10 K of full scale value • 0.5 %/10 K of full scale value for a measuring range of 100 to 400 mbar	
• Influence of vibration (per IEC 60068-2-6)	0.005 %/g to 500 Hz in all directions	
• Power supply influence	0.005 %/V	
Operating conditions		
• Process temperature	-30 to +120 °C (-22 to +248 °F)	
• Ambient temperature	-25 to +85 °C (-13 to +185 °F)	
• Storage temperature	-50 to +100 °C (-58 to +212 °F)	
• Degree of protection (as per EN 60529)	• IP65 with plug per EN 175301-803-A • IP67 with plug M12 • IP68 with cable	
Electromagnetic compatibility per EN 61326; NAMUR NE 21		
• Measurement error	≤ 1 % of full scale value. Cable screen is not connected to ground connection.	
Design		
Weight	Approx. 0,25 kg (0.55 lb)	
Process connections	Dimension Drawings (Page 4)	
Electrical connections	• Plug per EN 175301-803-A form A with cable inletM16x1.5 or ½-14NPT or Pg 11 • Plug M12 (mating connector as option) • 2- or 3-wire (0.5 mm²) screened lead (∅ 8.3 mm) with vent pipe	
Material of the wetted parts		
• Measuring cell	AI2O3 - 96 % or stainless steel (SST 316 L)	
• Process connection	Stainless steel, mat. no. 1.4571 (SST 316 Ti)	
• Sealing ring	• FPM -15 … +125 °C (+5 … +257 °F) • Neoprene -35 … +100 °C; < 100 bar (-31 … +212 °F; < 1450 psi) • Perbunan -20 … +100 °C (-4 …+212 °F) • EPDM -40 … +145 °C; < 100 bar (-40 … +293 °F; < 1450 psi) usable for drinking water	
Material of parts not in contact with the medium		
• Housing	Stainless steel, mat. no. 1.4571 (SST 316 Ti)	

Measuring accuracy		
• Connector housing	•	Plastic (plug per EN 175301-803-A)
	•	CuZn, nickel-plated (plug M12)
• Cable	•	PE

Certificates and approvals	
Classification according to Pressure Equipment Directive (PED 97/23/EC)	For gases of fluid group 1 and liquids of fluid group 1; fulfills the requirements according to article 3, paragraph 3 (good engineering practice)
Explosion protection	
• Intrinsic safety "i" (with current output only)	Ex II 1/2 G Ex ia IIC T4
• EC type examination certificate	TÜV 02 ATEX 1953 X (E1, E2)
• Connection to certified intrinsically safe circuits with maximum values	U_i = DC 30 DC; I_i = 100 mA; P_i = 0.75 W

Certificates and approvals	
• Effective internal inductance and capacity for versions with plugs per EN 175301-803-A and M12	L_i = 2.2 nH; C_i = 4.9 nF
• Effective internal inductance and capacity for version with cable	L_i = 2.2 nH + 1.5 µH/m; C_i = 4.9 nF + 0.25 nF/m
Lloyds Register of Shipping (LR)	05/20049(E1)
Germanischer Lloyds Register of Shipping (GL)	33 229-06 HH
American Bureau of Shipping (ABS)	06-HG205130-PDA
Bureau Veritas (BV)	19113/A0 BV
Det Norske Veritas (DNV)	A -10351
Drinking water approval (ACS)	07 ACC NY 195

Dimension Drawings

Different electrical connections

M12 x 1

Cable gland with cable

M16x1.5 or ½-14NPT

EN 175301-803-A

SW27

G1/2" EN 837-1

Max. 30 Nm

1) Length for device version with the voltage output 45.5 mm (1.8")

132 (5.2) without Ex protection
141 (5.6) with Ex protection
71 (2.8) without Ex protection 1)
80 (3.2) with Ex protection
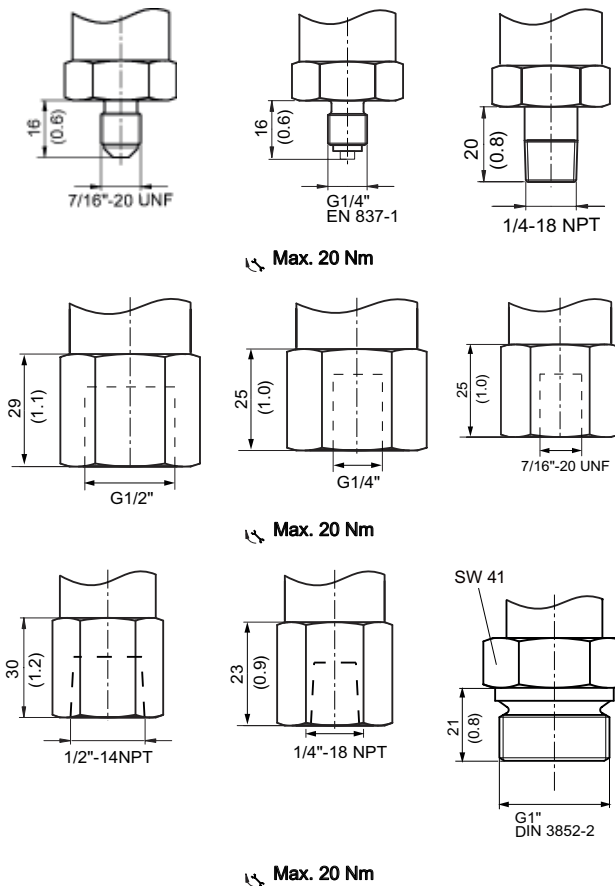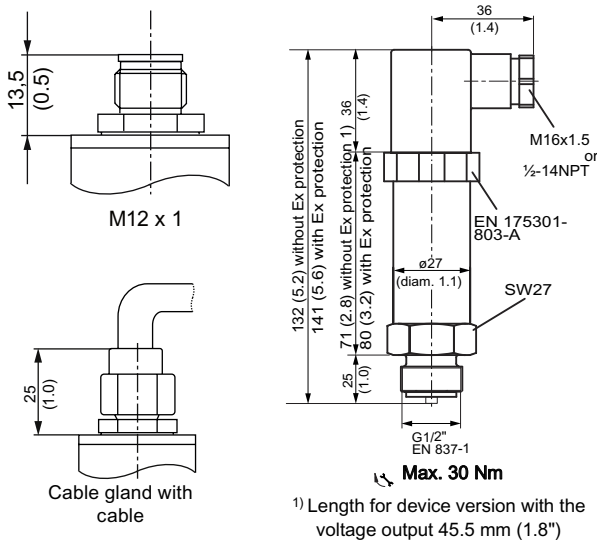
Services & Support
(http://www.siemens.com/automation/service&support)

Different process connections
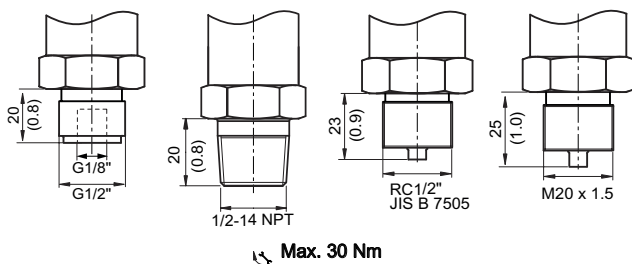
G1/8"
G1/2"

1/2-14 NPT

RC1/2"
JIS B 7505

M20 x 1.5

Max. 30 Nm

7/16"-20 UNF

G1/4"
EN 837-1

1/4-18 NPT

Max. 20 Nm

G1/2"

G1/4"

7/16"-20 UNF

Max. 20 Nm

1/2"-14NPT

1/4"-18 NPT

SW 41

G1"
DIN 3852-2

Max. 20 Nm

Appendix L

Datasheet pressure regulator

Preparation of compressed air → Maintenance units and components

Pressure regulator, Series AS5-RGS
► **G 3/4 - G 1 ► Qn=14500 l/min ► Activation: mechanical ► lockable**

Regulator type	Diaphragm-type pressure regulator, Can be assembled into blocks
Function	with relieving air exhaust
Lock type	with padlock
Installation location	Any
Pressure supply	single
Ambient temperature min./max.	-10°C / +50°C
Medium temperature min./max.	-10°C / +50°C
Working pressure min./max.	See table below
Adjustment range min./max.	See table below
Medium	Compressed air
Max. Internal air consumption	1.5 l/min
Materials:	
Housing	Polyamide
Cover	Acrylonitrile butadiene styrene
Seal	Acrylonitrile Butadiene Rubber

00119787

Technical Remarks
■ The pressure dew point must be at least 15 °C under ambient and medium temperature and may not exceed 3 °C.

		Port	Qn	Working pressure min./max.	Adjustment range min. - max..	Weight	Part No.
			[l/min]	[bar]	[bar]	[kg]	
		G 3/4		0.1 / 16	0.1 - 1		R412009101
		G 3/4		0.1 / 16	0.1 - 2		R412009103
		G 3/4		0.2 / 16	0.2 - 4		**R412009105**
		G 3/4		0.5 / 16	0.5 - 8		**R412009107**
		G 3/4		0.5 / 16	0.5 - 10		**R412009109**
		G 3/4	14500	0.5 / 16	0.5 - 16	0.997	**R412009111**
		G 1		0.1 / 16	0.1 - 1		R412009113
		G 1		0.1 / 16	0.1 - 2		R412009115
		G 1		0.2 / 16	0.2 - 4		R412009117
		G 1		0.5 / 16	0.5 - 8		**R412009119**
		G 1		0.5 / 16	0.5 - 10		**R412009121**
		G 1		0.5 / 16	0.5 - 16		**R412009123**
		G 3/4		0.1 / 16	0.1 - 1		R412009100
		G 3/4		0.1 / 16	0.1 - 2		R412009102
		G 3/4		0.2 / 16	0.2 - 4		R412009104
		G 3/4		0.5 / 16	0.5 - 8		R412009106
		G 3/4		0.5 / 16	0.5 - 10		R412009108
	-	G 3/4	14500	0.5 / 16	0.5 - 16	0.905	R412009110
		G 1		0.1 / 16	0.1 - 1		R412009112
		G 1		0.1 / 16	0.1 - 2		R412009114
		G 1		0.2 / 16	0.2 - 4		R412009116
		G 1		0.5 / 16	0.5 - 8		R412009118
		G 1		0.5 / 16	0.5 - 10		**R412009120**
		G 1		0.5 / 16	0.5 - 16		R412009122

Nominal flow Qn at 6.3 bar and Δp = 1 bar.

Part numbers marked in bold are available from the central warehouse in Germany, see the shopping basket for detailed information
Pneumatics catalog, online PDF, as of 2010-11-02, © Bosch Rexroth AG, subject to change

Preparation of compressed air → Maintenance units and components

Pressure regulator, Series AS5-RGS
▶ **G 3/4 - G 1** ▶ **Qn=14500 l/min** ▶ **Activation: mechanical** ▶ **lockable**

Pressure characteristics curve

$q_n = 20$ l/min

p_2 [bar]

p_1 [bar]

00119826
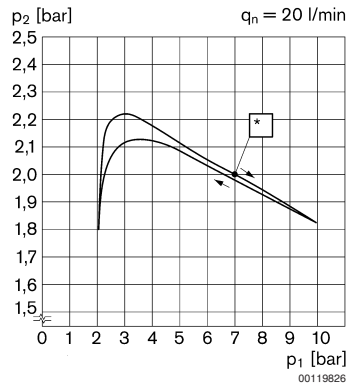
p1 = working pressure
p2 = secondary pressure
qn = nominal flow
* starting point

Flow rate characteristic (setting range p2: 0.5 - 8 bar)

p_2 [bar]

$p_1 = 10$ bar

q_n [l/min]
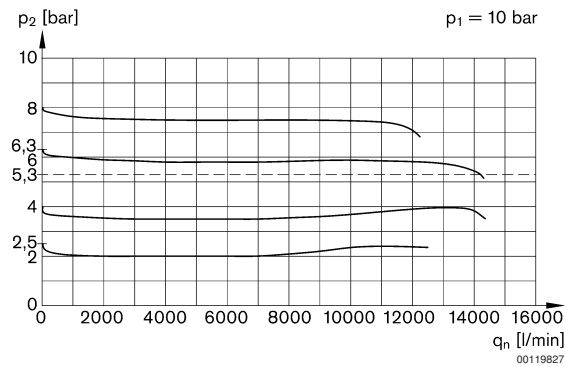
00119827

p1 = working pressure
p2 = secondary pressure
qn = nominal flow

Preparation of compressed air → Maintenance units and components

Pressure regulator, Series AS5-RGS
► G 3/4 - G 1 ► Qn=14500 l/min ► Activation: mechanical ► lockable

Dimensions
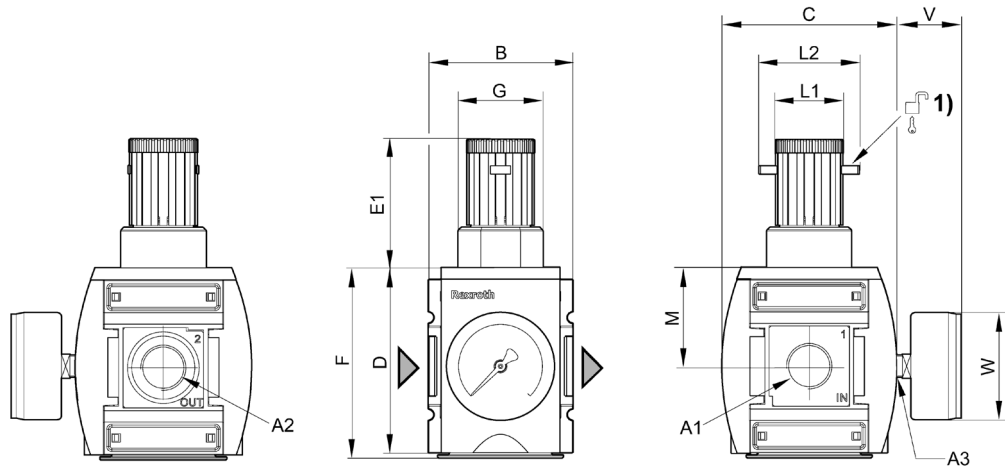
00119833

1) Mounting option for padlocks; max. shackle Ø 8

A1	A2	A3	B	C	D	E1	F	G	L1	L2	M	V
G 3/4	G 3/4	G 1/4	85	103	109	75	112	M50x1,5	41	60	58	38
G 1	G 1	G 1/4	85	103	109	75	112	M50x1,5	41	60	58	38

A1	W											
G 3/4	63											
G 1	63											

Appendix M

Datasheet Gemü 554 20D 195 2 1

Construction

The GEMÜ 554 pneumatically operated 2/2-way angle seat globe valve, which can also be used at relatively high temperatures, has a plastic pneumatic piston actuator and PTFE seat providing reliable operation. The valve spindle is sealed by a self-adjusting gland packing providing low maintenance and reliable valve spindle sealing even after a long service life. The wiper ring fitted in front of the gland packing protects it against contamination and damage.

Features

- Substantially reduced installation dimensions when using the body with male threads which can be installed using union nuts
- When using actuated valves in sizes 0 and 1 the gland packing is not subjected to line pressure as the pressure is sealed by the valve seat when closed
- Materials of all medium wetted parts can be selected to suit relevant applications
- Control valves with control cone available
- Versions according to ATEX on request

Advantages

- Various types of valve body connections:
  Threaded sockets, threaded spigots, butt weld spigots
- Good flow capability
- Extensive range of accessories
- Low weight

Actuator dimensions [mm]			
Actuator size	ø B	M	A2	G
0 + 3	72	M 16x1	70	1/4
1 + 4	96	M 16x1	86	1/4
2	168	M 22x1.5	149	1/4
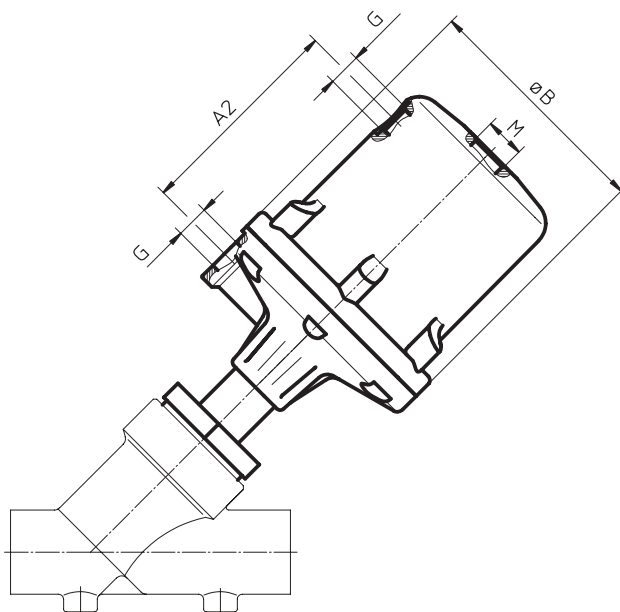
Installation dimensions see page 5.

Technical data

Working medium

Corrosive, inert, gaseous and liquid media which have no negative impact on the physical and chemical properties of the body and seal materials.

Max. perm. pressure of working medium	see table
Medium temperature	-10°C to 180° C
Max. permissible viscosity	600 mm²/s (cSt)
Other versions for higher viscosities on request	

Control medium

Inert gases

Max. perm. temperature of control medium:		60° C
Filling volume	Actuator size 0 and 3:	0.05 dm³
	Actuator size 1 and 4:	0.125 dm³
	Actuator size 2:	0.625 dm³

Ambient conditions

Max. ambient temperature	60° C

Flow direction

See page 4

Nominal size	Max. operating pressure [bar] control function 1*					Min. control pressure [bar] control function 1					Kv value
[mm]	Act. size 0 piston ø 50 mm	Act. size 3 piston ø 50 mm	Act. size 1 piston ø 70 mm	Act. size 4 piston ø 70 mm	Act. size 2 piston ø 120 mm	Actuator size 0	Actuator size 3	Actuator size 1	Actuator size 4	Actuator size 2	[m³/h]
10	12.0	10	25.0	10	-	4.8 - 7.0		5.5 - 7.0		-	4.5
15	12.0	10	25.0	10	-	4.8 - 7.0		5.5 - 7.0		-	5.4
20	6.0	10	20.0	10	25	4.8 - 7.0	min. control pressure see diagram max. control pressure 7 bar	5.5 - 7.0	min. control pressure see diagram max. control pressure 7 bar	4 - 7	10.0
25	2.5	10	10.0	10	25	4.8 - 7.0		5.5 - 7.0		4 - 7	15.2
32	-	-	7.0	10	16	-		5.5 - 7.0		4 - 7	23.0
40	-	-	4.5	10	12	-		5.5 - 7.0		4 - 7	41.0
50	-	-	3.0	10	10	-		5.5 - 7.0		5 - 7	71.0
65	-	-	-	-	7	-		-		5 - 7	108.0
80	-	-	-	-	5	-		-		5 - 7	160.0

* Please note that cast bronze valve bodies, when in pipe systems according to DIN, are only suitable up to PN 16 max., cast stainless steel bodies up to PN 25. All pressures are gauge pressures.
Min. control pressure for actuators 3 and 4 depends on operating pressure.
Kv values determined acc. to IEC 534 standard, body with threaded sockets DIN ISO 228.
The Kv value data refers to control function 1 (NC) and the largest actuator for each nominal size.
Kv values may be different for other combinations. Consult GEMÜ.

Pressure / temperature correlation for angle seat globe valve bodies								
Connection code	Material code	Max. allowable pressure (barg) at temperature °C*						
		RT	50	100	150	200	250	300
1, 31, 3B, 9 (up to DN 50)	9	16.0	16.0	16.0	16.0	13.5	-	-
1, 31, 3B, 9 (from DN 65)	9	10.0	10.0	10.0	10.0	8.5	-	-
1, 9, 17, 60	37	25.0	23.7	21.3	19.2	17.7	16.4	15.4
0, 16, 17, 18, 37, 59, 60	34	25.0	24.2	21.2	19.3	17.9	16.8	15.9
80, 82, 86, 88 (up to DN 65)	34	16.0	16.0	16.0	16.0	-	-	-
80, 82, 86, 88 (DN 80)	34	10.0	10.0	10.0	10.0	-	-	-
31, 3B	C1	25.0	24.2	21.2	19.3	17.9	16.8	15.9
13	34	25.0	24.2	21.2	19.3	17.9	16.8	15.9
47	34	19.0	19.0	16.0	14.8	13.6	12.1	10.2

* The valves can be used down to -10°C   RT = Room Temperature

554

GEMÜ®

Actuator size 0 / Normally open (NO)
Flow direction: under the seat

Min. control pressure dependent on operating pressure
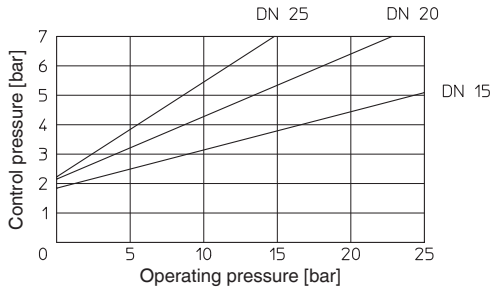
Actuator size 0 / Double acting (DA)
Flow direction: under the seat

Min. control pressure dependent on operating pressure
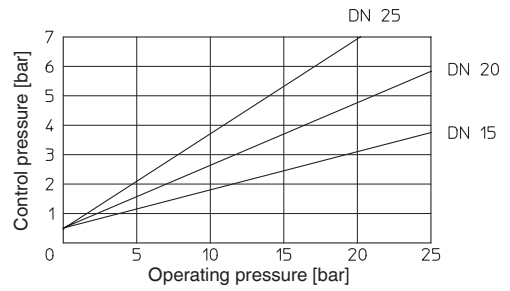
Actuator size 1 / Normally open (NO)
Flow direction: under the seat

Min. control pressure dependent on operating pressure
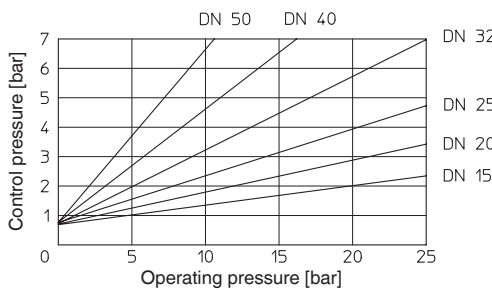
Actuator size 1 / Double acting (DA)
Flow direction: under the seat

Min. control pressure dependent on operating pressure
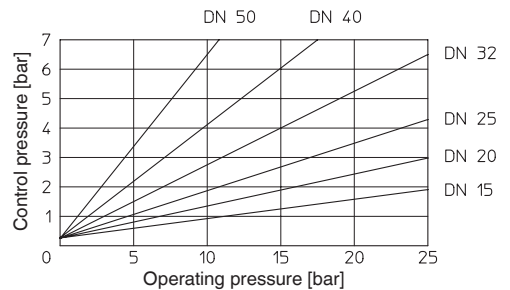
Actuator size 2 / Normally open (NO)
Flow direction: under the seat

Min. control pressure dependent on operating pressure
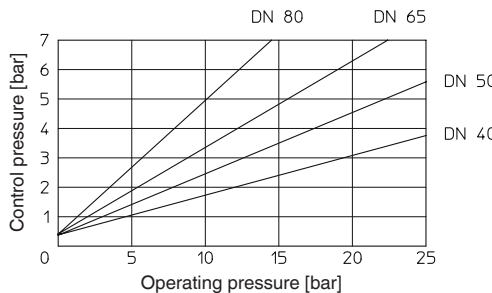
Actuator size 2 / Double acting (DA)
Flow direction: under the seat

Min. control pressure dependent on operating pressure

Actuator size 3 / Normally closed (NC)
Flow direction: over the seat

Min. control pressure dependent on operating pressure

Actuator size 4 / Normally closed (NC)
Flow direction: over the seat

Min. control pressure dependent on operating pressure

554
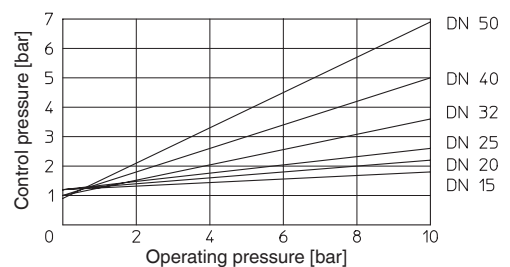
Order data

Body configuration	Code
2/2-way body	D

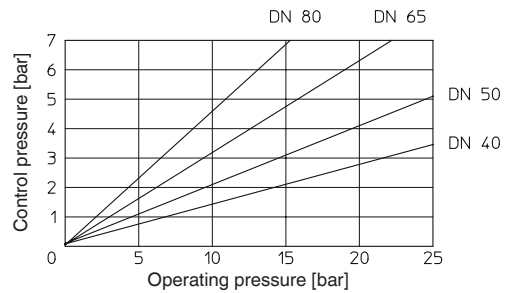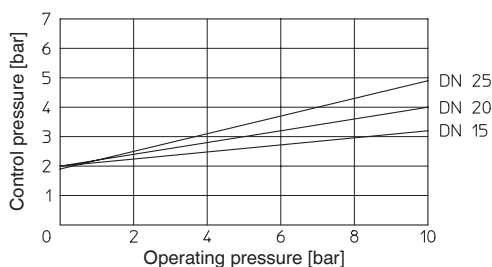| Connection	Code
Butt weld spigots	
Spigots DIN	0
Spigots DIN 11850, series 1	16
Spigots DIN 11850, series 2	17
Spigots DIN 11850, series 3	18
Spigots SMS 3008	37
Spigots ASME BPE	59
Spigots EN ISO 1127	60
Threaded connections	
Threaded sockets DIN ISO 228	1
Threaded sockets BS 21 Rc	3B
Threaded spigots DIN ISO 228	9
Threaded sockets NPT	31
Flanges	
Flanges EN 1092 / PN25 /form B length see body dimensions	13
Flanges ANSI class 125/150 RF length see body dimensions	47
Clamp connections	
Clamps ASME BPE for pipe ASME BPE, short design	80
Clamps DIN 32676 series B for pipe EN ISO 1127, length EN 558, series 1	82
Clamps DIN 32676 series A for pipe DIN 11850, length EN 558, series 1	86
Clamps ASME BPE for pipe ASME BPE, length EN 558, series 1	88

Valve body material	Code
Rg 5, cast bronze	9
1.4435 (ASTM A 351 CF3M ≙ 316L), investment casting	34
1.4408, cast stainless steel	37
ASTM A 351 CF3M, investment casting*	C1
* Material equivalency 316L	

Seat seal	Code
PTFE	5
PTFE, glass reinforced	5G
Other seat seals on request	

Control function		Code
Normally closed	(NC)	1
Normally open	(NO)	2
Double acting	(DA)	3

Actuator size	Flow	Code
Actuator 0 piston ø 50 mm	under the seat	0*
Actuator 1 piston ø 70 mm	under the seat	1*
Actuator 2 piston ø 120 mm	under the seat	2*
Actuator 3 piston ø 50 mm	over the seat	3**
Actuator 4 piston ø 70 mm	over the seat	4**
* Preferred flow direction with incompressible liquid media to avoid "water hammer"		
** only control function NC		

GEMÜ 554
Actuators 0, 1, 2

Flow
under the seat

GEMÜ 554
Actuators 3, 4

Flow
over the seat

Order example	554	15	D	1	9	5	1	1
Type	554							
Nominal size		15						
Body configuration (code)			D					
Connection (code)				1				
Valve body material (code)					9			
Seat seal (code)						5		
Control function (code)							1	
Actuator size (code)								1

GEMÜ®

Installation dimensions [mm] / Weight [kg]							
		Actuator size 0 and 3		Actuator size 1 and 4		Actuator size 2	
DN	Wrench size SW1	H/LA	Weight	H/LA	Weight	H/LA	Weight
10	36	152	0.9	179	1.4	-	-
15	36	155	0.9	182	1.4	-	-
20	41	165	1.1	192	1.6	279	-
25	46	165	1.3	192	1.8	279	-
32	55	-	-	200	2.4	287	5.1
40	60	-	-	206	2.7	293	6.0
50	75	-	-	214	3.4	301	6.9
65	75	-	-	-	-	313	8.5
80	75	-	-	-	-	330	10.1

Body dimensions [mm]

Butt weld spigots, connection code 0, 16, 17, 18, 37, 59, 60 Valve body material: 1.4435 (code 34), 1.4408 (code 37)																		
				Connection code														
	Material code 34		Material code 37		0		16		17		18		37		59		60	
DN	L	LB	L	LB	ø d	s	ø d	s	ø d	s	ø d	s	ø d	s	ø d	s	ø d	s
10	105	35.5	-	-	-	-	12	1.0	13	1.5	14	2.0	-	-	-	-	17.2	1.6
15	105	35.5	100	33	18	1.5	18	1.0	19	1.5	20	2.0	-	-	12.70	1.65	21.3	1.6
20	120	39.0	108	33	22	1.5	22	1.0	23	1.5	24	2.0	-	-	19.05	1.65	26.9	1.6
25	125	38.5	112	32	28	1.5	28	1.0	29	1.5	30	2.0	25.0	1.2	25.40	1.65	33.7	2.0
32	155	48.0	137	39	-	-	34	1.0	35	1.5	36	2.0	-	-	-	-	42.4	2.0
40	160	47.0	146	40	40	1.5	40	1.0	41	1.5	42	2.0	38.0	1.2	38.10	1.65	48.3	2.0
50	180	48.0	160	38	52	1.5	52	1.0	53	1.5	54	2.0	51.0	1.2	50.80	1.65	60.3	2.0
65	-	-	290	96	-	-	-	-	70	2.0	-	-	63.5	1.6	63.50	1.65	76.1	2.0
80	-	-	310	95	-	-	-	-	85	2.0	-	-	76.1	1.6	76.20	1.65	88.9	2.3

For materials see overview on last page
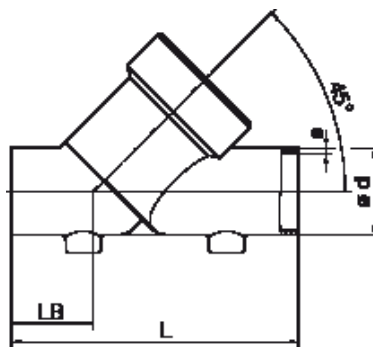
Body dimensions [mm]

Threaded sockets DIN, connection code 1
Valve body material: Cast bronze (code 9), 1.4408 (code 37)

DN	L	LB	G	Material code 9			Material code 37		
				t	SW2		t	SW2	
10	65	16.5	G 3/8	-	-	-	9	27	hexagonal
15	65	17.0	G 1/2	15.0	27	hexagonal	9	25	hexagonal
20	75	18.0	G 3/4	16.3	32	hexagonal	11	31	hexagonal
25	90	24.0	G 1	19.0	41	hexagonal	12	39	hexagonal
32	110	33.0	G 1 1/4	21.4	50	octagonal	14	48	octagonal
40	120	30.0	G 1 1/2	21.4	55	octagonal	14	55	octagonal
50	150	40.0	G 2	25.7	70	octagonal	15	66	octagonal
65	190	46.0	G 2 1/2	24.0	85	octagonal	22	85	octagonal
80	220	50.0	G 3	27.0	100	octagonal	25	100	octagonal

For materials see overview on last page.

Threaded sockets NPT. BS 21 Rc. connection code 31. 3B
Valve body material: Cast bronze (code 9), 316L (code C1)

DN	L	LB	SW2		Connection code			
					31		3B	
					G	t	G	t
15	81	24.5	27	6	1/2" NPT	13.6	Rc 1/2	15.0
20	87	24.0	32	6	3/4" NPT	14.0	Rc 3/4	16.3
25	104	31.0	41	6	1" NPT	16.8	Rc 1	19.0
32	122	39.0	50	8	1 1/4" NPT	17.3	Rc 1 1/4	21.4
40	136	38.0	55	8	1 1/2" NPT	17.3	Rc 1 1/2	21.4
50	165	47.5	70	8	2" NPT	17.7	Rc 2	25.7
65	212	57.0	85	8	2 1/2" NPT	23.7	Rc 2 1/2	30.2
80	242	61.0	100	8	3" NPT	25.9	Rc 3	33.3

For materials see overview on last page.

GEMÜ®
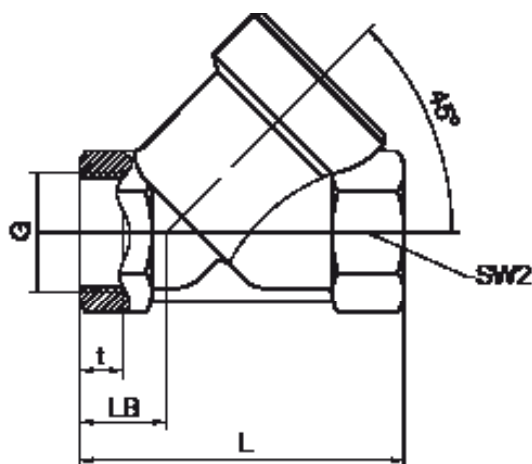
Body dimensions [mm]

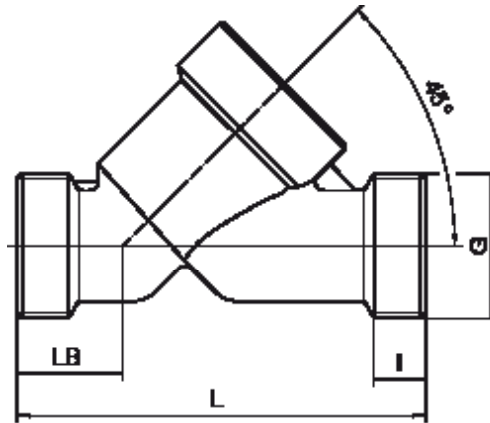| Threaded spigots, connection code 9 |
|---|
| Valve body material: Cast bronze (code 9), investment casting (code 37) |

DN	L	LB	I	G
15	90	25	12	G 3/4
20	110	30	15	G 1
25	118	30	15	G 1 1/4
32	130	38	13	G 1 1/2
40	140	35	13	G 1 3/4
50	175	50	15	G 2 3/8
65	216	52	15	G 3
80	254	64	18	G 3 1/2

For materials see overview on last page.

Flanges, connection code 13, 47										
Valve body material: 1.4435 (code 34)										
			Connection code 13				Connection code 47			
DN	FTF	LB	ø D	ø L	ø k	Number of bolt	ø D	ø L	ø k	Number of bolt
15	210	72	95	14	65	4	89.0	15.7	60.5	4
20	280	78	105	14	75	4	98.6	15.7	69.8	4
25	280	77	115	14	85	4	108.0	15.7	79.2	4
32	310	89	140	18	100	4	117.3	15.7	88.9	4
40	320	91	150	18	110	4	127.0	15.7	98.6	4
50	333	95	165	18	125	4	152.4	19.1	120.7	4
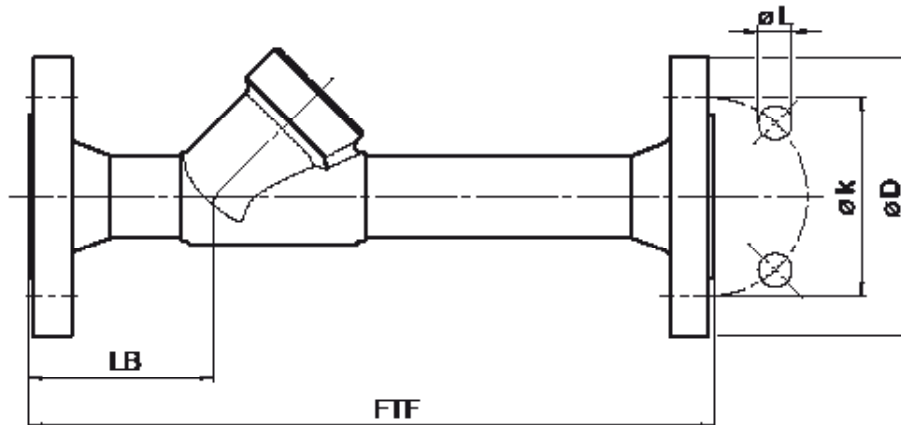
Body dimensions [mm]

Clamp connections, connection code 80, 82, 86, 88
Valve body material: 1.4435 (code 34)

DN	NPS	LB	LC	82		86		88		80			
				ø d1	ø d3	ø d1	ø d3	ø d1	ø d3	LB	LC	ø d1	ø d3
15	1/2"	35.5	130	18.1	50.5	16	34.0	9.40	25.0	33.5	101.60	9.40	25.0
20	3/4"	39,0	150	23.7	50.5	20	34.0	15.75	25.0	30.0	101.60	15.75	25.0
25	1"	38,5	160	29.7	50.5	26	50.5	22.10	50.5	33.0	114.30	22.10	50.5
32	1 1/4"	48,0	180	38.4	64.0	32	50.5	-	-	-	-	-	-
40	1 1/2"	47,0	200	44.3	64.0	38	50.5	34.80	50.5	37.0	139.70	34.80	50.5
50	2"	48,0	230	56.3	77.5	50	64.0	47.50	64.0	36.5	158.75	47.50	64.0
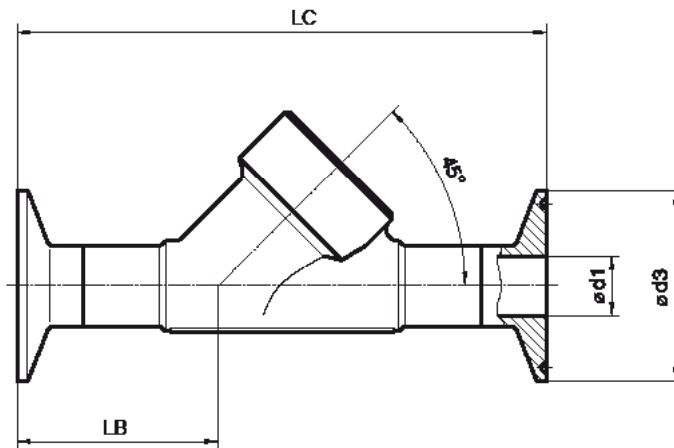
Overview of metal bodies for GEMÜ 554

Connection code	1		3B		9		31		13	47	0	16	17		18	37		59		60		80	82	86	88
Material code	9	37	9	C1	9	37	9	C1	34	34	34	34	34	37	34	34	37	34	37	34	37	34	34	34	34
DN 10	-	X	-	-	-	-	-	-	-	-	X	X	-	X	-	-	-	-	X	-	-	-	-	-	-
DN 15	X	X	X	X	X	X	X	X	X	X	X	X	X	X	-	-	X	-	X	X	X	X	X	X	X
DN 20	X	X	X	X	X	X	X	X	X	X	X	X	X	X	-	-	X	-	X	X	X	X	X	X	X
DN 25	X	X	X	X	X	X	X	X	X	X	X	X	X	X	X	-	X	-	X	X	X	X	X	X	X
DN 32	X	X	X	-	-	X	X	-	X	X	-	X	X	X	-	-	-	-	X	X	-	X	X	-
DN 40	X	X	X	X	X	X	X	X	X	X	X	X	X	X	X	-	X	-	X	X	X	X	X	X	X
DN 50	X	X	X	X	X	X	X	X	X	X	X	X	X	X	X	-	X	-	X	X	X	X	X	X	X
DN 65	X	X	X	-	X	X	X	-	-	-	-	-	-	X	-	-	X	-	X	-	X	-	-	-	-
DN 80	X	X	X	-	X	X	X	-	-	-	-	-	-	X	-	-	X	-	X	-	X	-	-	-	-

For further globe valves, accessories and other products please see our Product Range catalogue and Price List.
Contact GEMÜ

GEMÜ ® VALVES, MEASUREMENT AND CONTROL SYSTEMS